To the Graduate Council:

I am submitting herewith a thesis written by David Reed Oglesby entitled "A Digital Simulation of a Dual-Duct Air Handling System." I recommend that it be accepted in partial fulfillment of the requirements for Master of Science, with a major in Electrical Engineering.

Walter L. Green

Walter L. Green, Major Professor

We have read this thesis
and recommend its acceptance:

J. Vaughn Blalock

J M Bailey

C F. Moss

Accepted for the Council:

L Evans Roth

Vice Chancellor
Graduate Studies and Research

Thesis
'77
.O353
cop.2

A DIGITAL SIMULATION OF A DUAL-DUCT AIR HANDLING SYSTEM

A Thesis

Presented for the

Master of Science

Degree

The University of Tennessee, Knoxville

David Reed Oglesby

August 1977

1328495

ACKNOWLEDGEMENTS

The author wishes to sincerely thank Dr. Walter Green for his friendship and encouragement and for the fine example that he has set both in and out of the classroom.

This thesis is dedicated to the author's parents, Homer and Beulah, his brother and his sister-in-law, Alex and Libby, and especially to his wife, Stephanie. Without their love, patience, faith, and understanding, this thesis would not have been written.

The author would like to thank Ms. Jane Davis and Ms. Susan Emery for the enthusiasm, diligence, and care that they exhibited in typing this manuscript.

Special thanks also go to Mr. Enzo Romita, Mr. Carl Moore, and Mr. Cleon Robinson and his co-workers at the IBM facility in Kingston, New York. All provided indispensable assistance and guidance in conducting the research necessary for this project.

ABSTRACT

This thesis presents a method for developing a dynamic digital simulation of a dual-duct air handling system. The individual control loops and system components of the dual-duct system which was studied are explained in detail. The testing and data recording devices used in the investigation are described. An appropriate model for the system transfer functions is presented and an effective computer-aided method of fitting test data to this model is discussed. A detailed development of the resulting FORTRAN simulation program is given. Finally, two simulation examples are illustrated and their results are compared.

TABLE OF CONTENTS

CHAPTER		PAGE
1.	INTRODUCTION	1
2.	THE DUAL-DUCT AIR HANDLING SYSTEM	3
	General System Description	3
	System Control Loops	8
	Hot duct temperature control	8
	Cold duct temperature control	9
	Supply air temperature control	9
	Zone control	10
	Catastrophic Event Sensors	10
	Existing Control Hardware	11
	Justification for Digital Control	11
3.	SYSTEM TESTING AND MODELING PROCEDURES	14
	Test Apparatus	14
	Cold Duct Tests	18
	Hot Duct Tests	24
	Damper Tests	24
	Zone Tests	31
4.	THE DUAL-DUCT SYSTEM SIMULATION	33
	Basics of the Computer Simulation	33
	The Simulation Program	36
	The main program	36
	Subroutine CLIMAT	39

CHAPTER PAGE

Subroutine WWRTN 39
Subroutine TTRTN 40
Subroutine DAMPER 41
Subroutines XLEFT and RIGHT 43
Subroutine COLD 46
Subroutine FLOWS 49
Subroutine PSYSUN 49
Subroutine HOT 51
Subroutine ZFEED 53
Subroutine ZONE 54
Verification of Simulation Accuracy 58
5. SIMULATION RESULTS 61
Operating Strategies 61
Simulation Results and Discussion 62
Simulation of winter operation 63
Simulation of spring operation 80
Simulation of summer operation 80
Simulation of fall operation 99
Summary 117
6. CONCLUSIONS 129
LIST OF REFERENCES 132
APPENDIX 135
VITA 163

LIST OF TABLES

TABLE		PAGE
4.1.	Zone Characteristics	57
5.1.	Responses for the Original System in Winter	76
5.2.	Responses for the Modified System in Winter	77
5.3.	Zone Responses for the Original System in Winter	78
5.4.	Zone Responses for the Modified System in Winter	79
5.5.	Responses for the Original System in Spring	92
5.6.	Responses for the Modified System in Spring	93
5.7.	Zone Responses for the Original System in Spring	94
5.8.	Zone Responses for the Modified System in Spring	95
5.9.	Responses for the Original System in Summer	108
5.10.	Responses for the Modified System in Summer	109
5.11.	Zone Responses for the Original System in Summer	110
5.12.	Zone Responses for the Modified System in Summer	111
5.13.	Responses for the Original System in Fall	124
5.14.	Responses for the Modified System in Fall	125
5.15.	Zone Responses for the Original System in Fall	126
5.16.	Zone Responses for the Modified System in Fall	127

LIST OF FIGURES

FIGURE		PAGE
2.1.	General Dual-duct System	4
2.2.	Dual-duct System Which Was Investigated	7
3.1.	Test Module for Dual-duct Tests	15
3.2.	General Program Using PATERN	19
3.3.	General Cold Duct Temperature Control Loop	21
3.4.	Cold Duct Responses to Positive Inputs	22
3.5.	Cold Duct Responses to Negative Inputs	23
3.6.	General Hot Duct Temperature Control Loop	25
3.7.	Hot Duct Responses to Positive Inputs	26
3.8.	Hot Duct Responses to Negative Inputs	27
3.9.	General Supply Air Temperature Control Loop	29
3.10.	Steady-state Damper Performance	30
4.1.	Main Program Flowchart	37
4.2.	Supply Air Temperature Control Loop	44
4.3.	Damper Hysteresis Flowchart	45
4.4.	Cold Duct Temperature Control Loop	50
4.5.	Hot Duct Temperature Control Loop	52
4.6.	Block Diagram of Subroutine ZFEED	55
4.7.	Zone Temperature Control Loop	59
5.1.	Approximate Outside Air Conditions in Winter	64
5.2.	Upstream Temperatures for the Original System in Winter.	65
5.3.	Upstream Temperatures for the Modified System in Winter.	66

FIGURE PAGE

5.4. Air Flows for the Original System in Winter 67
5.5. Air Flows for the Modified System in Winter 68
5.6. Midstream Temperatures for the Original System in Winter 70
5.7. Midstream Temperatures for the Modified System in Winter 71
5.8. Downstream Temperatures for the Original System in Winter 72
5.9. Downstream Temperatures for the Modified System in Winter 73
5.10. Energy Use for the Original System in Winter 74
5.11. Energy Use for the Modified System in Winter 75
5.12. Approximate Outside Air Conditions in Spring 81
5.13. Upstream Temperatures for the Original System in Spring . 82
5.14. Upstream Temperatures for the Modified System in Spring . 83
5.15. Air Flows for the Original System in Spring 84
5.16. Air Flows for the Modified System in Spring 85
5.17. Midstream Temperatures for the Original System in Spring. 86
5.18. Midstream Temperatures for the Modified System in Spring. 87
5.19. Downstream Temperatures for the Original System in Spring 88
5.20. Downstream Temperatures for the Modified System in Spring 89
5.21. Energy Use for the Original System in Spring 90
5.22. Energy Use for the Modified System in Spring 96

FIGURE PAGE

5.23. Approximate Outside Air Conditions in Summer 96

5.24. Upstream Temperatures for the Original System 97

A.1. Main Program 136

A.2. Subroutine CLIMATE 140

A.3. Subroutine WWRTN 141

A.4. Subroutine TTRTN 142

A.5. Subroutine DAMPER 143

A.6. Subroutine XLEFT 146

A.7. Subroutine RIGHT 147

A.8. Subroutine COLD 148

A.9. Subroutine FLOWS 154

A.10. Subroutine PSYSUN 155

A.11. Subroutine HOT 158

A.12. Subroutine ZFEED 160

A.13. Subroutine ZONE 161

FIGURE PAGE

5.25. Upstream Temperatures for the Modified System in Summer 98

5.26. Air Flows for the Original System in Summer 100

5.27. Air Flows for the Modified System in Summer 101

5.28. Midstream Temperatures for the Original System in Summer 102

5.29. Midstream Temperatures for the Modified System in Summer 103

5.30. Downstream Temperatures for the Original System in Summer 104

5.31. Downstream Temperatures for the Modified System in Summer 105

5.32. Energy Use for the Original System in Summer 106

5.33. Energy Use for the Modified System in Summer 107

5.34. Approximate Outside Air Conditions in Fall 112

5.35. Upstream Temperatures for the Original System in Fall 113

5.36. Upstream Temperatures for the Modified System in Fall. . 114

5.37. Air Flows for the Original System in Fall 115

5.38. Air Flows for the Modified System in Fall 116

5.39. Midstream Temperatures for the Original System in Fall 118

5.40. Midstream Temperatures for the Modified System in Fall 119

5.41. Downstream Temperatures for the Original System in Fall 120

FIGURE PAGE

5.42. Downstream Temperatures for the Modified System in Fall 121

5.43. Energy Use for the Original System in Fall 122

5.44. Energy Use for the Modified System in Fall 123

CHAPTER 1

INTRODUCTION

Energy conservation techniques are particularly applicable to buildings constructed prior to the energy crisis of the early 1970's. These techniques can vary widely in complexity and scope. In some buildings, an expedient means of significantly reducing energy consumption can be as simple as reducing the interior lighting levels. In other buildings where more complex conservation practices have been in use for several years, the entire building may need to be renovated in order to accomplish noticeable energy savings. Such a renovation may include installation of additional insulation, creation of a centralized computer control system for energy usage, and a complete rework of the mechanical system to increase efficiency and to reclaim as much energy as possible.

Few building supervisors would rely only on the simple scheme of reducing lighting levels to conserve energy. On the other hand, the expense of completely renovating a building for energy conservation purposes is extreme. Fortunately, many conservation schemes lying within these two bounds are reasonable in cost yet effective in decreasing building energy consumption.

This thesis deals with developing extended energy reduction techniques in a building where conservation practices were already in effect. The conservation measures had combined common sense tactics with a simplified, centralized computer control scheme. For example, lighting levels had already been reduced and thermostat setpoints had

been adjusted to minimize energy usage. Machinery which was not in current use had been turned off. The minimum fresh air ventilation had been lowered, yet was still within state regulations. Lights and the heating, ventilating, and air conditioning (HVAC) system were automatically cycled off at the end of the workday. HVAC maintenance procedures had been upgraded as well.

The HVAC system maintains the desired environmental conditions inside the building and may consist of several subsystems. Each subsystem does not necessarily employ the same methods to achieve the correct heating, cooling, and ventilation desired. One particular subsystem where studies indicated considerable energy reduction could be realized was the dual-duct air handling units (hereafter referred to as the dual-duct system).

Specifically, this thesis focuses on the development of a digital simulation for use in testing control strategies for the energy optimization of the dual-duct system. Chapter 2 presents a detailed description of the dual-duct system which was studied. Chapter 3 discusses the system testing and modeling required for the simulation. Chapter 4 describes the simulation program in detail. Chapter 5 presents the results of simulating two different control strategies for the dual-duct system. Chapter 6 describes conclusions drawn from the study and areas for future work.

CHAPTER 2

THE DUAL-DUCT AIR HANDLING SYSTEM

This chapter presents both a general description of a typical dual-duct system and a specific description of the commercial dual-duct system which was tested, modeled and simulated. Individual system components and control loops are identified and discussed. The suitability of the existing analog controls is analyzed and the justification for a changeover to direct digital control is set forth.

General System Description

The dual-duct air handling system is one of several standard heating, ventilating, and air conditioning systems employed in relatively large office buildings, factories and department stores. This system relies on individual ducts to distribute heated air and cooled air to the load areas (zones). Figure 2.1 illustrates a general dual-duct system. External air, pulled through the outside air damper by the supply fan, is mixed with return air from the zones in the correct proportion to produce a controlled constant dry bulb temperature supply air flow (unless noted, all following references to temperature signify dry bulb temperature). Before reaching the supply fan this airstream is filtered and then possibly humidified. After passing through the supply fan the airstream divides according to the zones' hot and cold demands and passes over the heating and cooling coils. The hot duct air flow

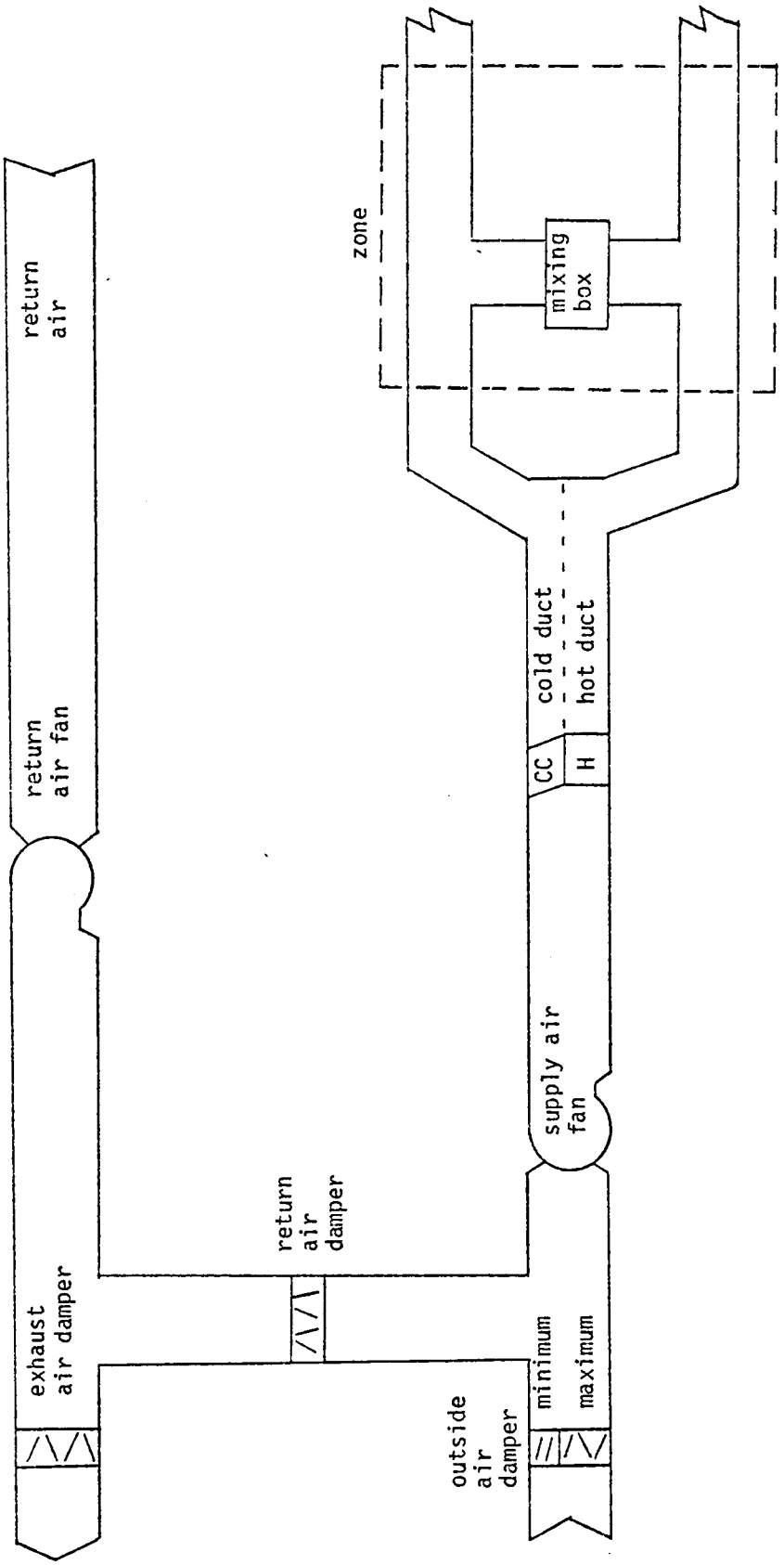


Figure 2.1. General dual-duct system.

undergoes sensible heating to a controlled constant temperature determined by the external air temperature. The cold duct air flow undergoes sensible cooling to a controlled constant temperature and, depending upon the thermodynamic properties of the supply air, possibly undergoes latent cooling. For example, if the supply air is cooled below its dewpoint, water vapor must condense, changing state and thereby releasing heat. The cooling coils thus offer the ability to dehumidify at least a portion of the air supplied to the zones.

At an individual zone, the hot and cold ducts feed a mixing box controlled by the zone thermostat. Proportional mixing of the two air streams produces the desired zone temperature. Diffusers attached to the exit duct of the mixing box then disperse the air flow throughout the zone.

Air is extracted from the zones by the return air fan and is conveyed toward the exhaust and return dampers by a common return air duct. The exhaust damper determines the amount of air flow rejected to the external environment while the return air damper determines the amount of air flow to be recycled and mixed with the incoming outside air.

The actual air handling unit studied is one of nine dual-duct systems utilized in a large four-story commercial building. One dual-duct unit of smaller capacity and of considerably more complexity than the others serves in a special application. As a result, one of the remaining eight essentially identical air

handling units was chosen for investigation since a typical representative was desired. All eight have a design cooling capacity of 2,000,000 BTU/HR and a design heating capacity of approximately 800,000 BTU/HR. The total system air flow is 38,660 ft^3/minute (CFM).

Although originally planned to handle heavy industrial heating and cooling demands, the entire system is now subjected to lighter loads due to the conversion of the building to office areas. Since many offices are not enclosed from floor to ceiling, zones tend to be ill-defined and hence show temperature interaction with adjacent load areas.

Figure 2.2 shows a detailed schematic of the dual-duct air handling unit which was studied. Chilled water serves as the refrigerant in the cooling coil, while low pressure steam serves as the heating fluid in the heating coil. Conditioned air is supplied to 15-20 zones distributed throughout the four floors in quantities of one to five zones per floor. Air flow capacity is not constant, but varies from zone to zone.

The hot and cold ducts share a larger air duct in distributing air to the various load areas. Cold duct insulation reduces ambient heating of the cold air flow and prevents condensation of moisture on the outer surface of the cold duct. Each zone contains 3 to 6 air diffusers which feed rooms ranging in size from 15 x 15 x 8 ft to 30 x 30 x 8 ft. The supply and return fans operate at constant RPM to maintain a constant volume air exchange.

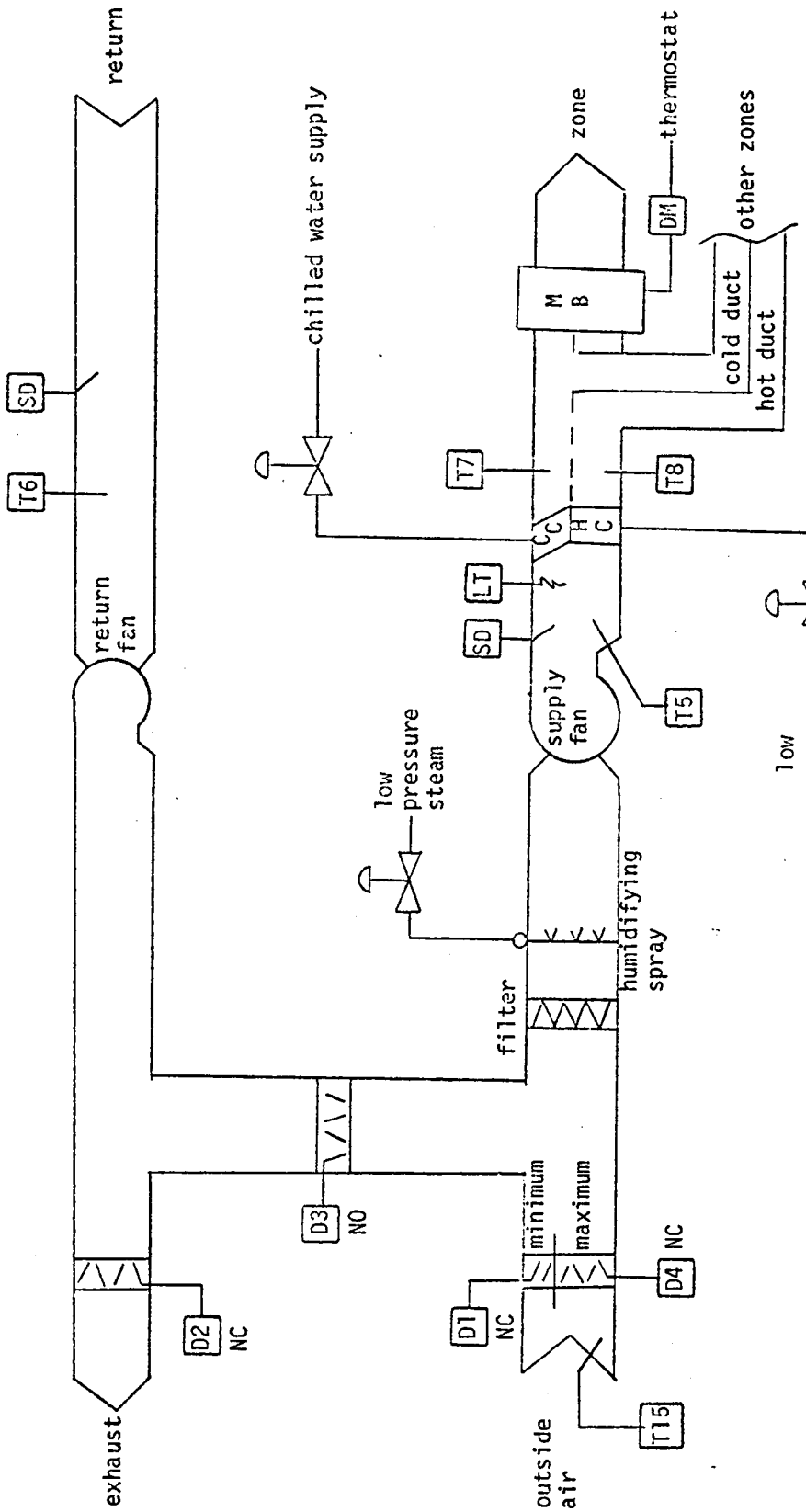


Figure 2.2. Dual-duct system which was investigated.

Since the individual air handling units service zones on all four floors, the plenum return air is a mixture from several zones and dual-duct systems.

System Control Loops

Four types of closed loop control exist, each of which is implemented with commercially available analog pneumatic equipment: hot duct temperature control, cold duct temperature control, supply air temperature control, and individual zone temperature control. No closed loop controls are operational unless power is applied to the return and supply fans.

Hot Duct Temperature Control. The hot duct temperature controller provides a corrective pressure signal to the low-pressure steam valve proportional to the hot duct error. This error is defined as the difference between the submaster hot duct setpoint and the hot duct temperature. Since the building heating load is dependent on the external air condition, the sub-master setpoint is determined by the following relationships, where T_{out} is the outside air temperature:

$$\text{Setpoint} = 90F, \; T_{out} < 0F \tag{2.1a}$$

$$\text{Setpoint} = -0.25T_{out} + 90F, \; 0F \leq T_{out} \leq 60F \tag{2.1b}$$

$$\text{Setpoint} = 75F, \; T_{out} > 60F. \tag{2.1c}$$

The low pressure steam valve, which is normally open with no air pressure signal present, begins closing at a 3 psi controller signal level and is completely closed at a 15 psi signal level.

Cold Duct Temperature Control. The cold duct temperature controller transmits a corrective pressure signal to the chilled water valve proportional to the cold duct error. Unlike the hot duct error, the cold duct error depends on the difference between the constant cold duct master setpoint of 53F and the cold duct temperature. Normally closed with no controller signal present, the chilled water valve begins opening at the 3 psi actuation level and is completely open at the 15 psi level.

Supply Air Temperature Control. Supply air temperature control is effected by manipulating the position of outside, exhaust, and return air dampers with piston-like damper operators. This control system operates in either one of three modes: (a) summer, (b) winter, or (c) automatic. The mode is set by a manual switch. Regardless of which mode this control system is in, the minimum outside air damper is open to provide adequate ventilation to occupants of the building. In the summer mode the exhaust and maximum outside air dampers are closed. The return air damper is fully opened and recirculates the return air to be combined with the minimum outside air flow. In the winter mode, the supply air temperature controller modulates the exhaust air, outside air, and return air damper positions to maintain a constant air temperature at the output of the supply air fan. The modulation signal, common to all three damper operators, is proportional to the difference between the 55F supply air temperature setpoint and the measured supply air temperature. This signal is effective in damper

movement only over the 5-10 psi operating range of the damper operators. In the automatic mode, the air handling system is switched to winter operation when the outside air temperature falls below 60F. Above 62F, the system automatically resets to summer operation.

Zone Control. Thermostats serve as the control mechanism in the individual zones. The mixing box regulating signal insures the correct mixture of the hot and cold airstreams necessary to reduce the zone temperature error. This regulating signal is proportional to the difference between measured zone temperature and zone temperature setpoint.

Catastrophic Event Sensors

Extreme condition sensors monitoring the return and supply air flows safeguard against damage to the air handling system, the building, or the building's occupants. Fire, smoke, and subnormal temperatures represent the major hazards. A smoke detector and a high-level thermostat for detecting supernormal temperatures are present in the return air duct. These devices signal that a fire hazard exists in the zones or in the return duct. In addition, a smoke detector and a low-level thermostat for sensing subnormal temperatures monitor the supply air duct. The smoke detector signals that a fire is present in the supply air duct or that smoke is entering through the outside air dampers. The low-level thermostat warns of subnormal temperatures which

could cause the heating and cooling coils to freeze. Normally, none of these sensors affects any dual-duct function.

Existing Control Hardware

The majority of dual-duct systems in use today operate with analog pneumatic controls. These controls are functionally reliable and particularly useful in industrial environments where electrical or electronic systems fail due to excessive heat, radiated electromagnetic interference, or power line noise. However, analog systems in general suffer from a lack of flexibility. Any change in the analog control of a given dual-duct system will generally be time and cost prohibitive. Furthermore, modification of the system control strategy will require modification of the analog hardware.[1]

Justification for Digital Control

Because of their inflexibility, analog systems in the past have not been used extensively to minimize energy usage in dual-duct systems. Rapidly increasing energy costs since 1973 now make optimum energy usage extremely desirable, however. The dual-duct system studied was economical in terms of initial outlay for the equipment and remained economical throughout the years of cheap energy costs in the 1960's. The system does make some use of free cooling from the environment but currently relies on operator judgement as to when to enter the energy saving winter mode.

On the whole, this analog control system cannot be deemed optimal. Even if operating in the automatic mode, the system essentially ignores the possibility of free external cooling if the outside temperature is greater than 62F. Above this temperature, the system transfers to the summer mode and intakes no outside air. The cold duct setpoint is fixed so that the cold duct is capable of satisfying the maximum cooling load demanded by the zones. Whenever maximum cooling is not required, the setpoint is unnecessarily low. Under this condition the zones' temperature requirements can be satisfied only by mixing additional hot air with the overcooled air. Morever, the determination of the hot duct setpoint depends only on the external air temperture. Free heating from lights, occupants, and machinery does not directly affect this setpoint value.

In an attempt to gain greater control flexibility for energy minimization, direct digital control was chosen to replace the analog controllers. Digital computers offer several important advantages over analog control. One of the most appealing is their ability to continuously analyze system performance, compare the performance with an ideal standard and make adjustments to approach this standard.[2] Control strategies may be varied by simply rewriting the computer's software. This adaptability enables the user to quickly find an optimum control strategy.

Rather than install a digital controller on the existing air handling unit and use trial and error methods to obtain an

optimum strategy, dynamic testing was initiated to obtain valid subsystem models. Upon completion, a system simulation was developed and various control configurations were then attempted to obtain an optimum control strategy for system energy minimization.

The following chapter discusses the modeling of the system components. A description of the test equipment utilized and examples of the test results are included.

CHAPTER 3

SYSTEM TESTING AND MODELING PROCEDURES

Developement of the dynamic and steady-state simulation model for the dual-duct air handling system required detailed testing of subsystem components followed by computer-aided system identification and modeling. This chapter describes the test apparatus, test procedures, test results, modeling philosophy, and proposed subsystem models.

Test Apparatus

Of prime importance in testing the dual-duct system was the capability to apply air pressure input signals independently to the various pneumatically driven actuators. Of equal importance was the ability to monitor and record the resultant outputs from the components under test. The test module designed to meet those requirements is illustrated in Figure 3.1.

A current-to-pressure (I/P) transducer driven by an independent current source produced an output pressure ranging from 3-15 psi. Solenoid valves SV1 and SV2 were installed to maintain steady-state equilibrium during the changeover from system device control to test module control. Prior to changeover, the device controller output was routed through the normally open port of SV2. At this point the test module had no effect, simply passing the control signal on since the I/P transducer output was fed to the normally closed port of SV1. The current source was adjusted until

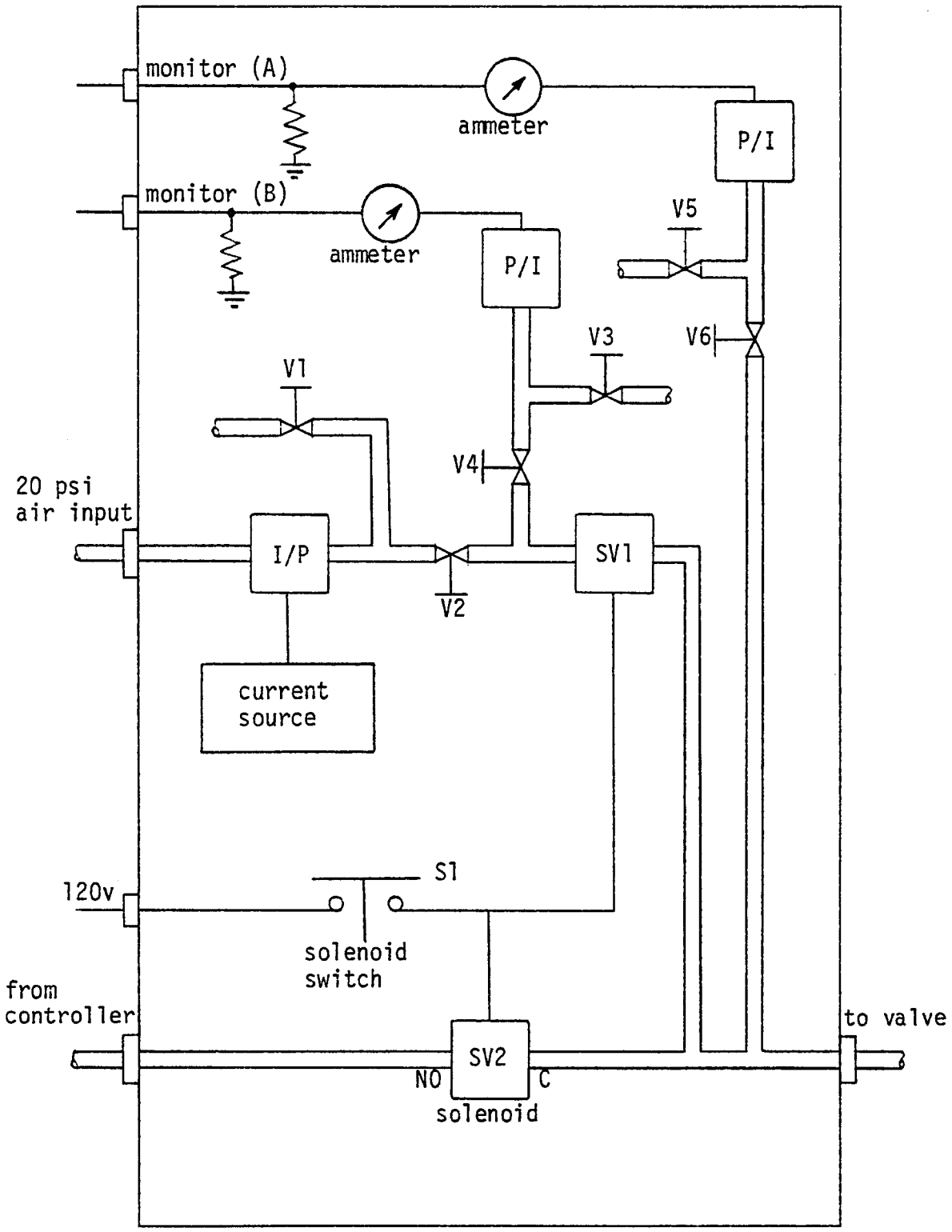


Figure 3.1. Test module for dual-duct tests.

the device controller (monitor point A) and the I/P transducer output (monitor point B) agreed. Closing switch S1 then provided a bumpless transfer by simultaneously shutting off the device controller signal from solenoid SV2 and passing the I/P transducer signal through SV1 to the control valve. Step input pressure signals from the test module could then be applied to the device under test.

Specific pneumatic signals from the physical system were monitored by two pressure-to-current (P/I) transducers in the test module. Each current was monitored by an ammeter, thereby giving a rough indication of the pressure level sensed. For increased accuracy in measurement, a precision resistor placed in each current path applied voltage signals (directly proportional to the pressure sensed) to a two-channel strip chart recorder. An increase in the number of pneumatic sensors utilized later dictated the installation of four additional P/I transducers. To facilitate data logging, all six P/I transducers were then connected to a a digital computer by an analog-to-digital interface.

Only a limited number of system temperature measurements were available from the existing instrumentation in the form of pneumatic signals. As a result, a ten-channel thermocouple input discrete data logger with a sampling time of six seconds was employed. Air flow values in ft^3/minute (CFM) were derived from hand-held air velocity meter measurements and knowledge of the duct cross-sectional area. The chilled water flow was measured by placing an annubar in the chilled water supply line. Pneumatic relative humidity transducers

installed in the cold duct sensed humidity changes across the cooling coil.

Steady-state as well as dynamic tests were conducted on the dual-duct system. Steady-state tests were undertaken to verify manufacturers' design data and to determine the flow versus valve position profiles for the chilled water valve. Experiments were also performed to calculate the overall heat transfer coefficient of the cooling coil as a function of air flow, water flow, and incoming air temperature and humidity.

The objective of the dynamic tests was to determine transfer functions which would describe the operation of the cooling and heating coils, the damper operators, and the mixing boxes. Input and output data were available by measurement but a relatively simple mathematical means of relating the two sets was desired for simulation purposes. Since many physical phenomena, especially those involving heat transfer, may be described by a first-order lag plus deadtime model, primary emphasis was placed on curve fitting the data to an equation of the form

$$G(s) = \frac{Ke^{-\Theta s}}{1+\tau s} \tag{3.1}$$

where Θ is the deadtime, K is the steady-state gain, and τ is the time constant. Assuming a unit step input, the output response from such a system is described as

$$C(s) = R(s)G(s) = \frac{Ke^{-\Theta s}}{s(1+\tau s)} \tag{3.2}$$

In the time domain, Eq. (3.2) would be represented as

$$c(t) = K(1-e^{-t/\tau})u(t-\Theta). \qquad (3.3)$$

Curve fitting proceeded with the use of PATERN, a nonlinear regression program shown in the generalized block diagram of Figure 3.2. Iterative search procedures in this program optimize parameters K, τ, and Θ so as to minimize the integral of the absolute error, where error is defined as the difference between the model output data and the measured output data. The process model, written in the form of a difference equation, must be supplied by the user in subroutine PROC. This model may be of other forms than Eq. (3.1). Constraints on the process parameters are defined in subroutine BOUNDS, also user supplied.[3]

Data points from the discrete data logger, taken at a maximum sample time of six seconds, were time coordinated with other recording device data and plotted by hand. Since two seconds was the largest sample time which would adequately represent the fastest dynamic system response, points at this sample interval were then interpolated and recorded to conform to the general system rate.

Cold Duct Tests

Initial tests were performed on the cold duct cooling coil to establish a mathematical relationship between the pressure signal to the chilled water valve and the temperature of the air exiting the coil. A block diagram of the control loop involved is shown in

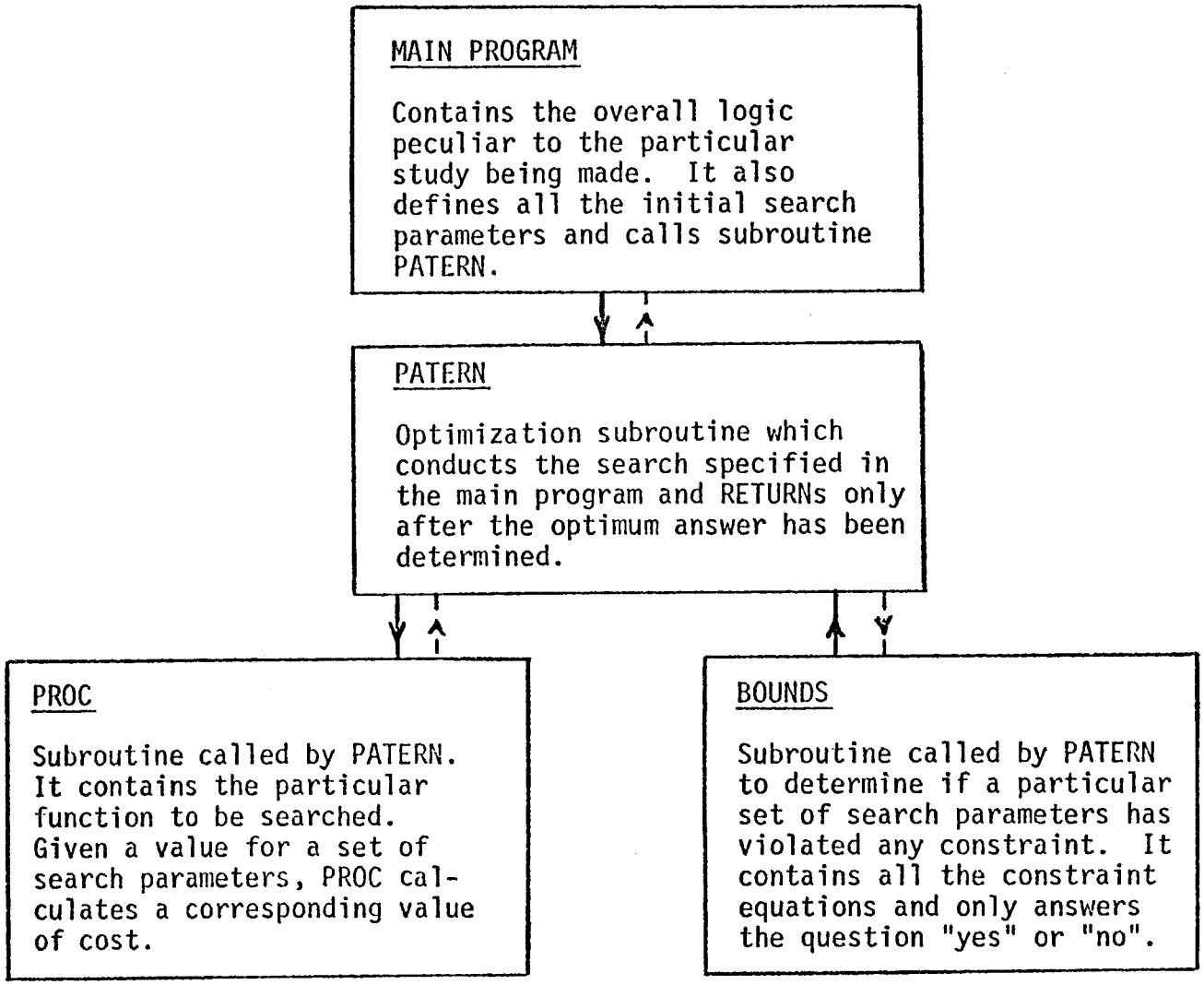


Figure 3.2. General program using PATERN.

Figure 3.3. The cold duct setpoint controller was disconnected and a series of positive and negative step current inputs were applied to the I/P transducer. The system was operating in the summer mode so that the air entering the cooling coil was approximately 72F. The corresponding input pressure to the chilled water valve and the output temperature for the coil are shown in Figures 3.4 and 3.5. Since air is a compressible fluid, neither the pressure signal to the valve from the test module nor the controller signal was observed to be a step input.

Model parameters K, τ, and Θ are also indicated in Figures 3.4 and 3.5. Values of K for the temperature response are representative of normal valve operation but will not hold for all valve pressure inputs since cooling coil efficiency is dependent upon water flow as well as other variables. At low water flow rates, laminar water flow prevails and less heat transfer occurs in the cooling coil. At high water flow rates, turbulent flow is in effect and heat transfer is increased significantly, thereby increasing K.

The steady-state controller gain for the above tests was negative. This indicates that a negative error signal (implying that the cold duct temperature is above the setpoint value) produces a positive controller pressure signal to the chilled water valve. An increase in valve pressure opens the normally closed valve further and thus increases the chilled water flow through the cooling coil while reducing the exit air temperature.

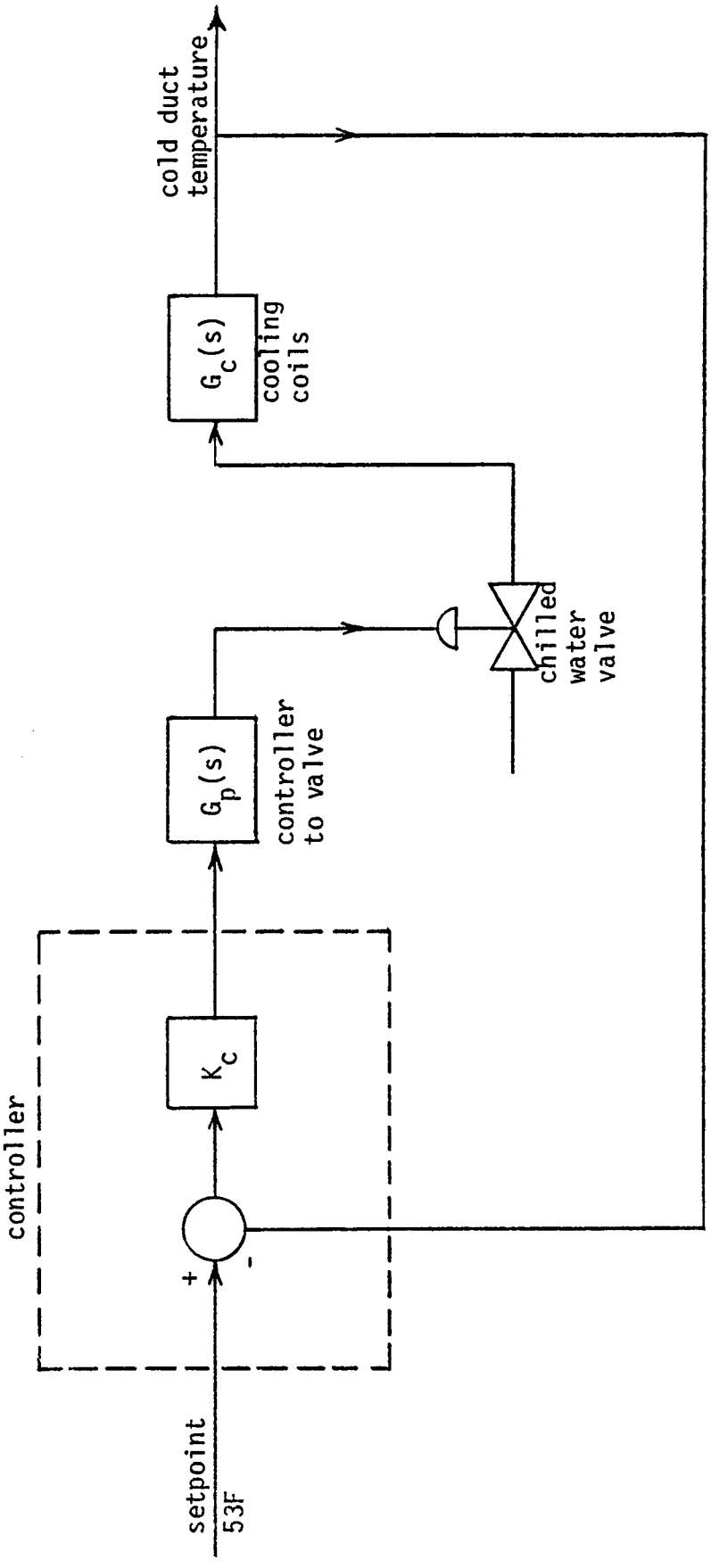


Figure 3.3. General cold duct temperature control loop.

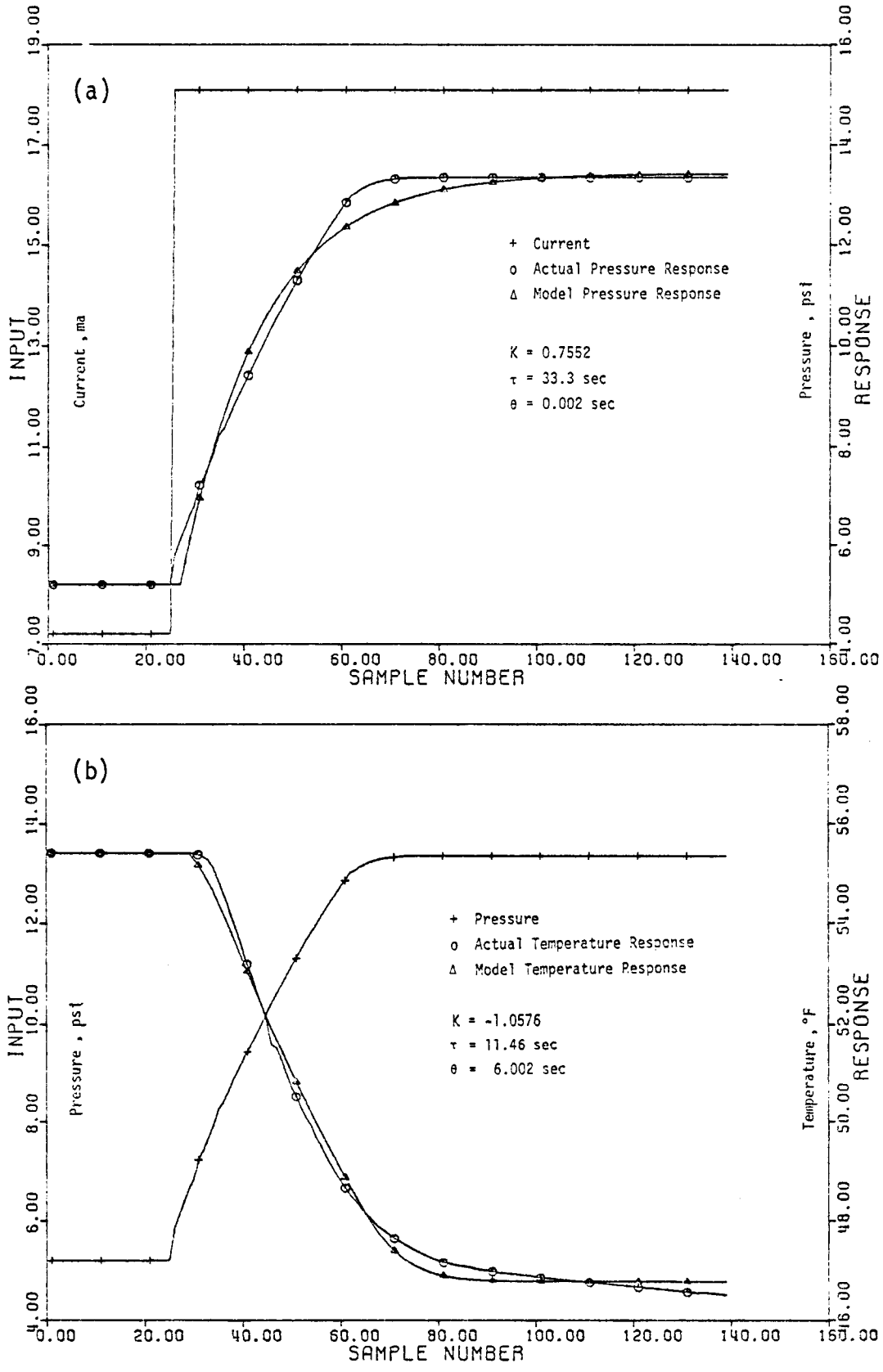


Figure 3.4. Cold duct responses to positive inputs.

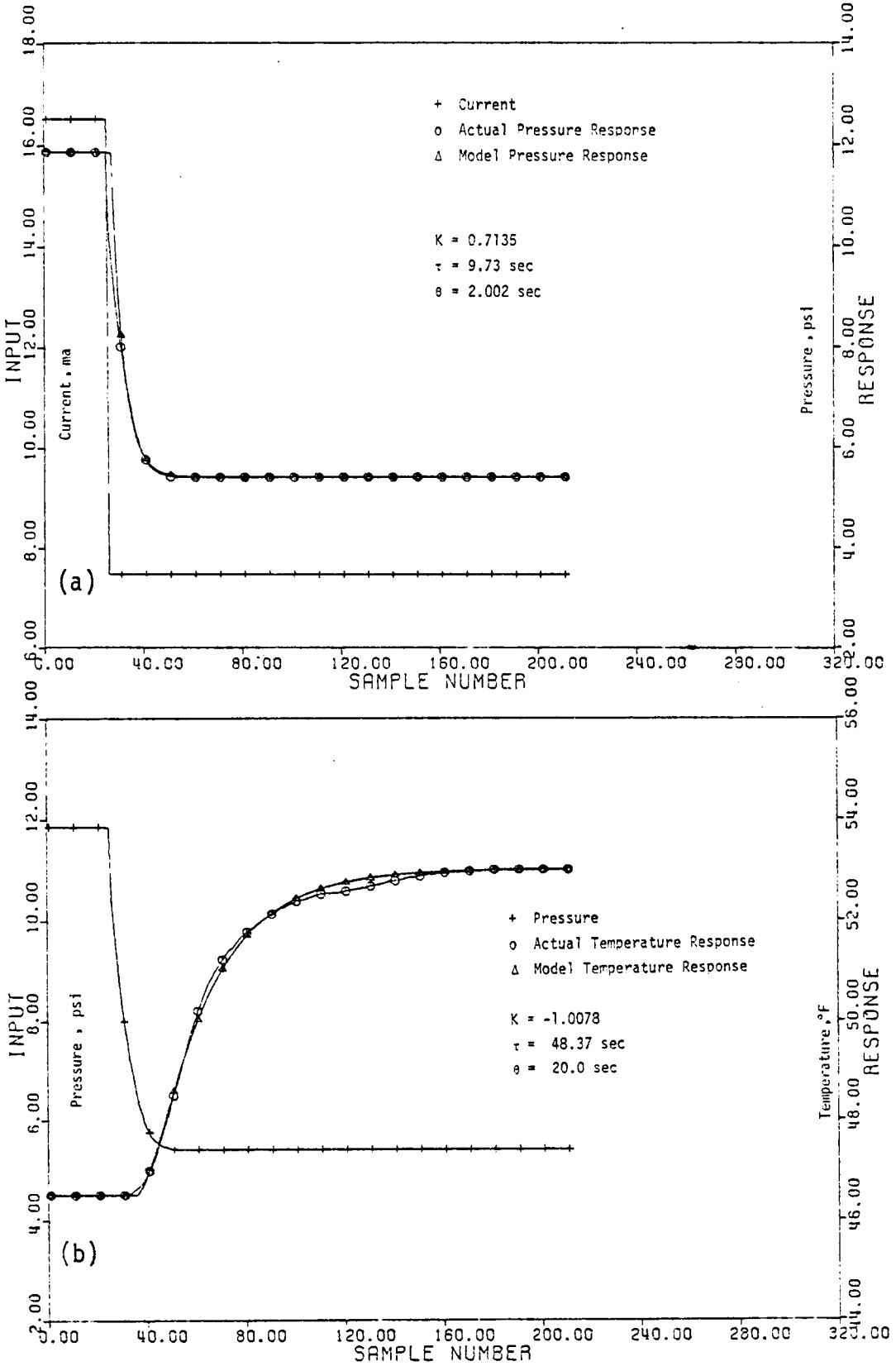


Figure 3.5. Cold duct responses to negative inputs.

The results of the dynamic tests of the cooling coils are incorporated in the final system model. These results do not include transfer function gains.

Hot Duct Tests

The hot duct control loop discussed in this section is given in Figure 3.6. Hot duct tests proceeded in a manner analogous to the cold duct tests. Disconnection of the hot duct controller placed the low pressure steam valve under open-loop control from the test module. A transfer function was desired for relating heating coil outlet air temperature and steam valve pressure. Negative and positive step current inputs to the I/P transducer produced the valve pressure and temperature responses shown in Figures 3.7 and 3.8. Indicated model parameters K, τ, and θ in Figures 3.7(b) and 3.8(b) are not constants but depend upon air flow, steam flow, incoming air temperature, and humidity. However, they are representative of the heating coil under average conditions.

In both the cold duct and hot duct tests, parameter values depend upon the direction of the current step to the I/P transducer. Some error in K, as indicated by comparing values in Figures 3.7(a) and 3.8(a), was expected since the I/P transducer was not truly linear. In addition, the valves responded more rapidly to a decreasing pressure signal than to an increasing signal. As a result, values for τ and θ were not symmetrical.

Damper Tests

Damper tests were designed to develop a dynamic relationship

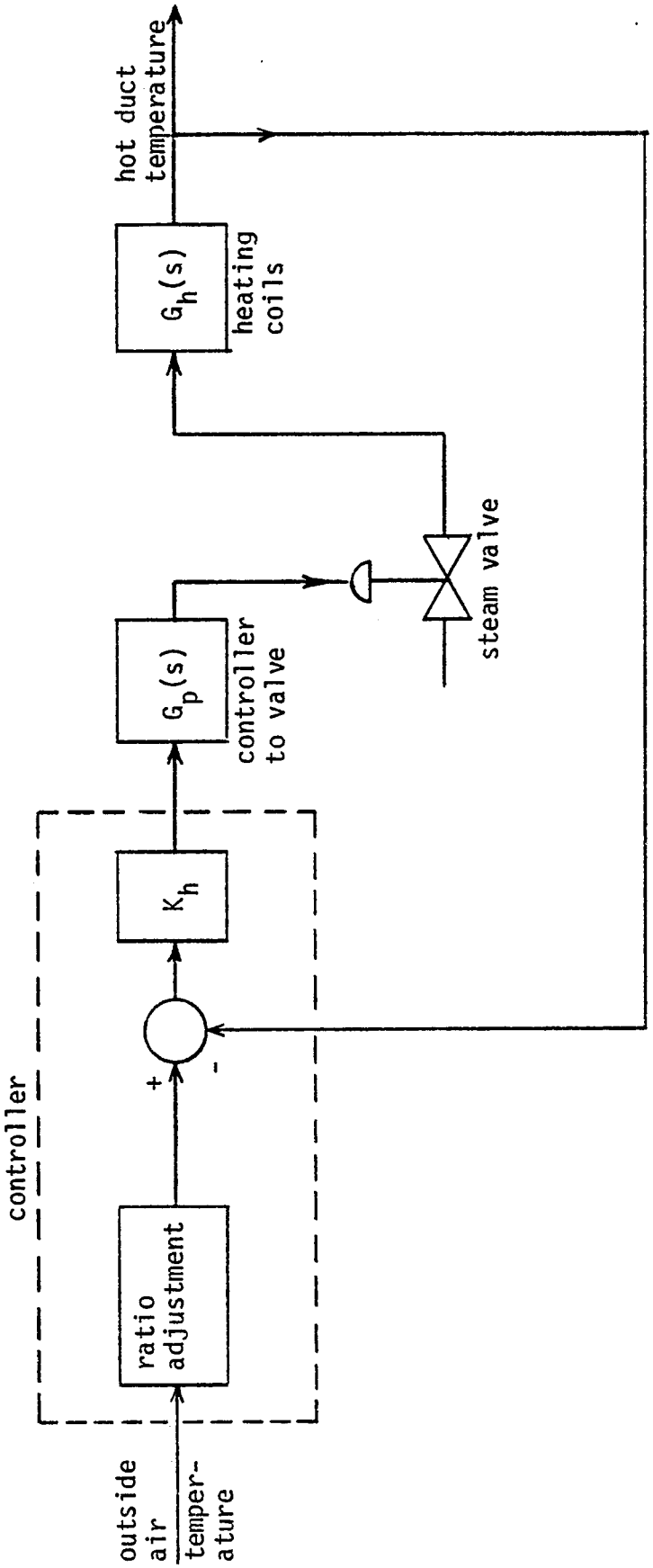


Figure 3.6. General hot duct temperature control loop.

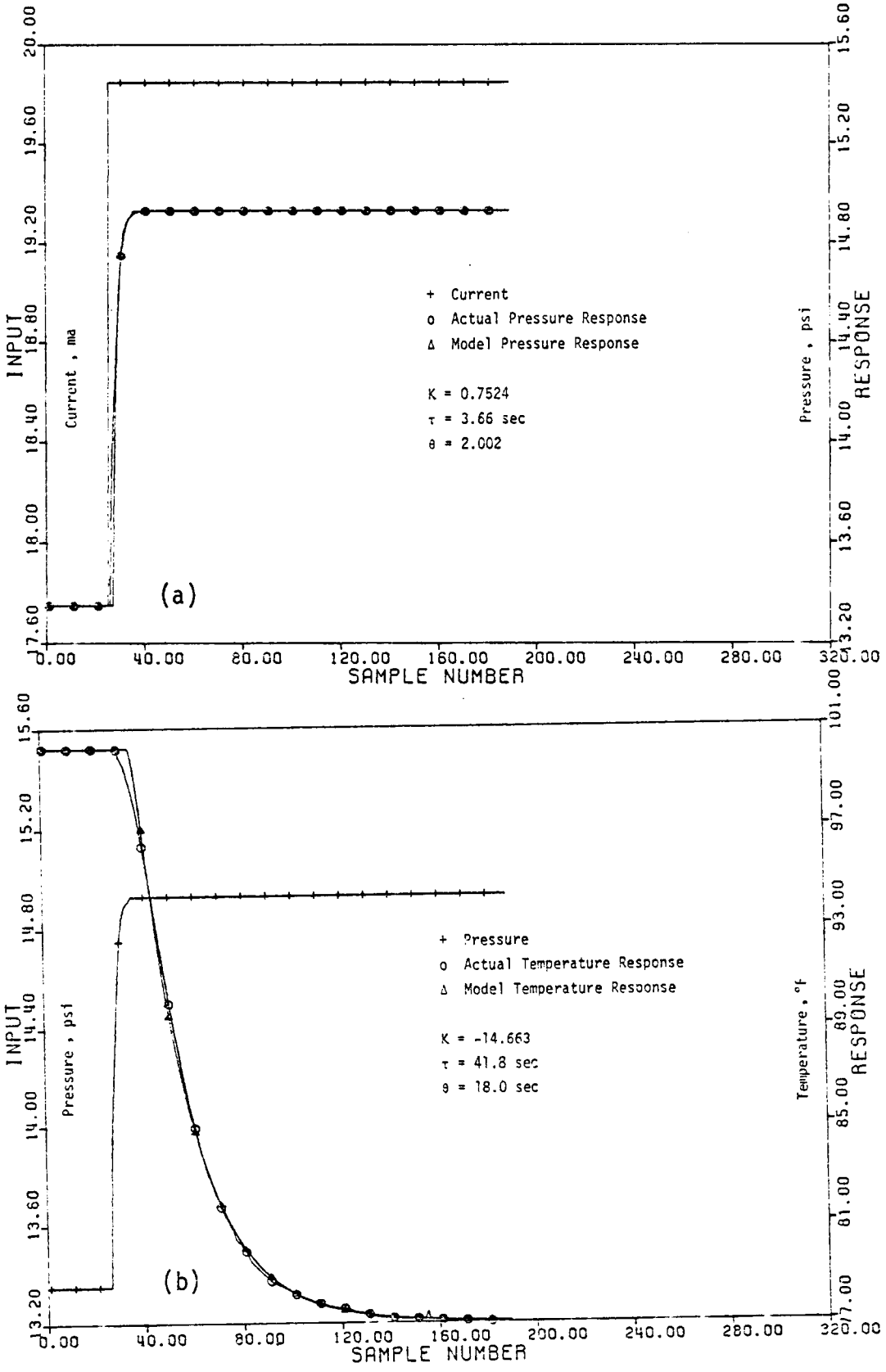


Figure 3.7. Hot duct responses to positive inputs.

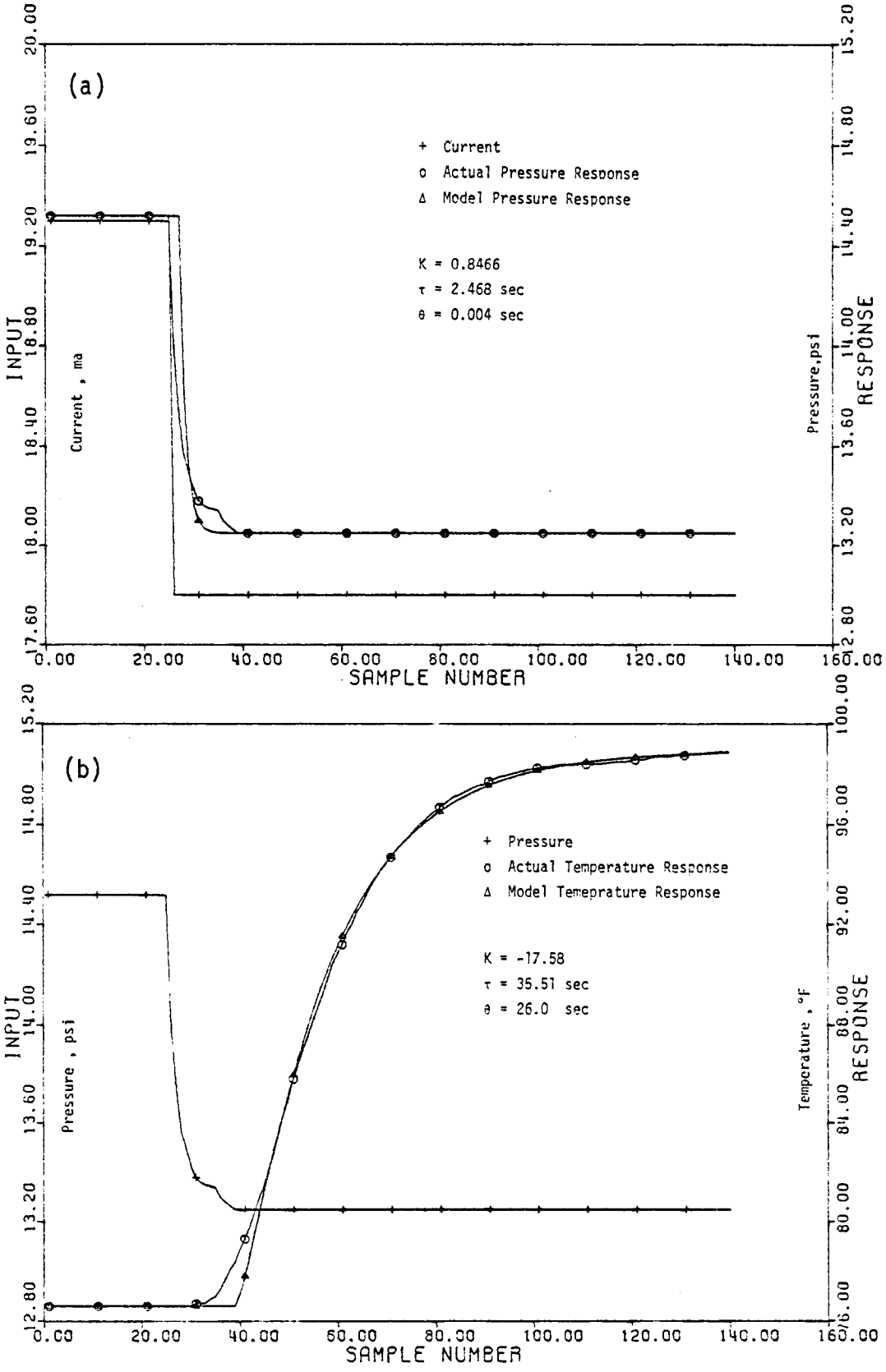


Figure 3.8. Hot duct responses to negative inputs.

between pressure to the air dampers and the resultant supply air temperature. Figure 3.9 illustrates the control loop involved. Recorded variables included air temperature entering and leaving the return air fan, air temperature entering and leaving the supply fan, cold duct temperature, hot duct temperature, outside air temperature, pressure signal to the damper operators, and exhaust air flow. Each series of tests was conducted both with the minimum outside air damper opened and closed. In one series of tests, positive current corresponding to pressure signals of 1.5 psi were applied to the I/P transducer. The outside and exhaust dampers were gradually moved from fully closed to fully opened as the return air damper simultaneously moved from fully opened to fully closed. The test was then repeated in reverse order with decreasing current steps until the dampers were returned to their original position. In a second series of tests, a current step large enough to move the outside and exhaust dampers fully open from their closed position and to move the return air damper fully closed was issued. The procedure was then reversed using a single negative current step. Transfer functions were developed for both series of tests.

The steady-state performance of the damper, as obtained during the above tests, is given in Figure 3.10. This performance clearly indicates a hysteresis effect most likely due to flexure of the mechanical linkage.

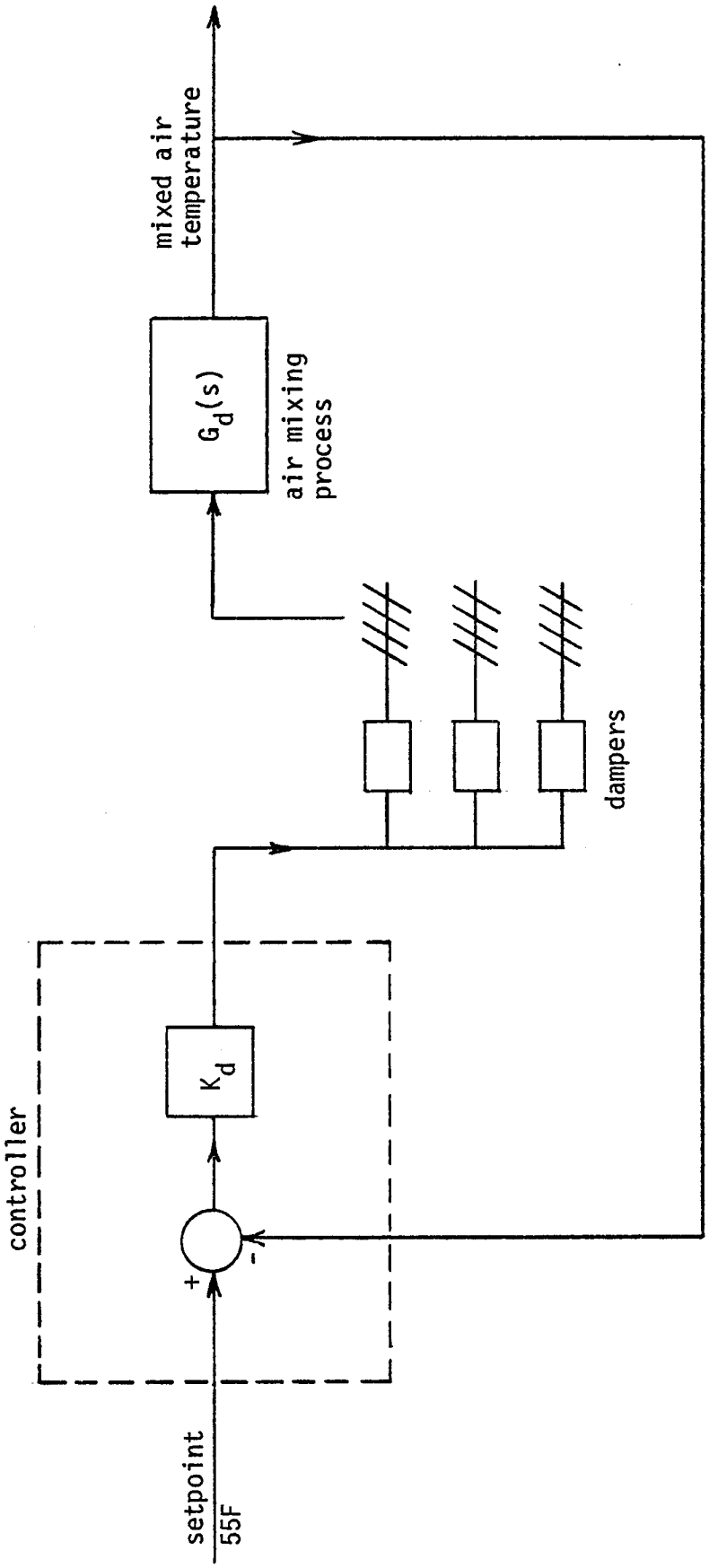


Figure 3.9. General supply air temperature control loop.

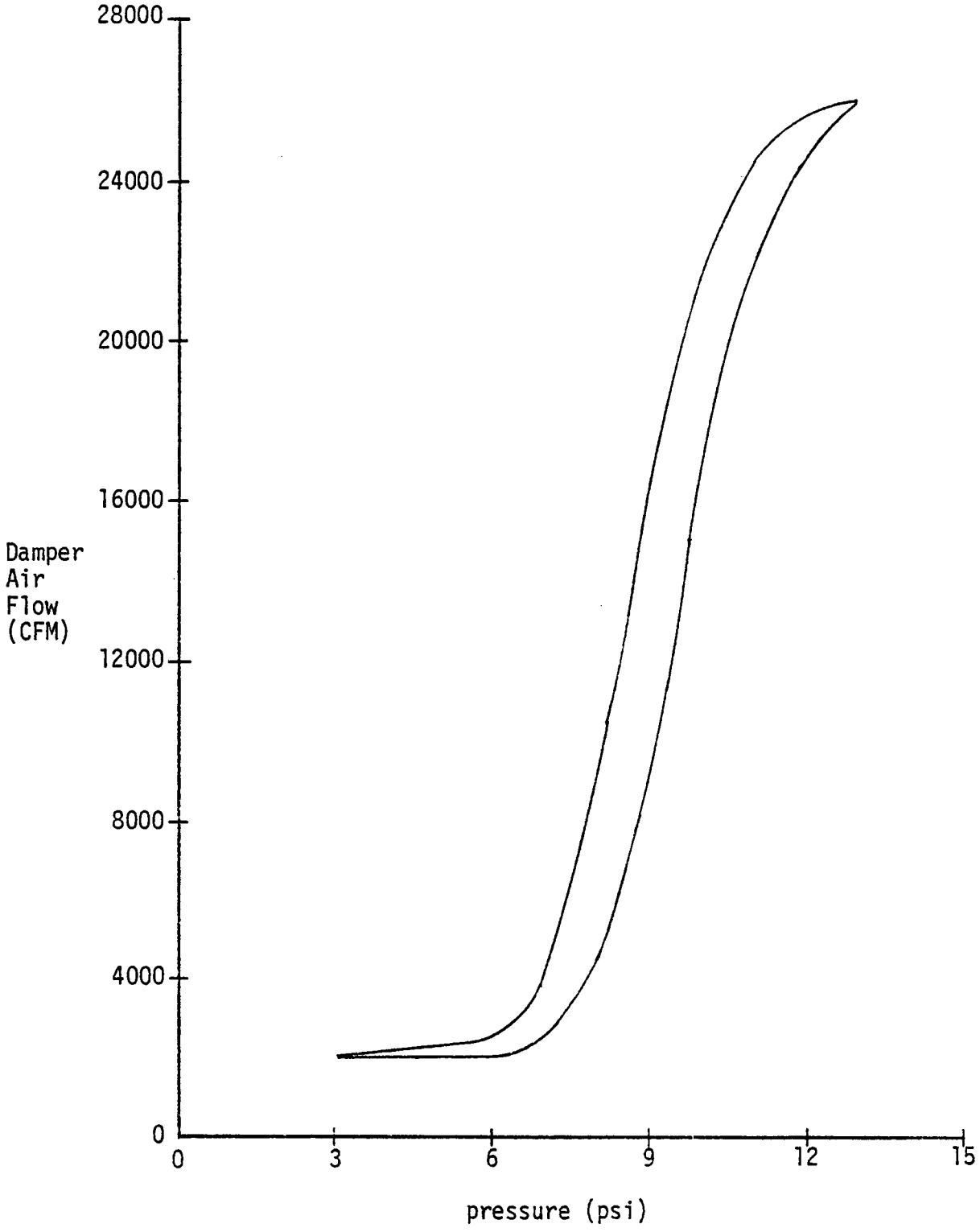


Figure 3.10. Steady-state damper performance.

Zone Tests

Four tests were performed in order to determine zone response characteristics due to temperature changes of the air from the hot and cold ducts. The first two tests consisted of both raising and lowering the cold duct temperature by manipulation of the chilled water valve while maintaining a constant hot duct temperature. The mixing box was fixed in its mid-position so that equal amounts of hot air and cold air would flow to the diffuser. Variables recorded were:

(a) The pressure signals to the chilled water and steam valves.

(b) The hot duct and the cold duct temperature leaving the heating and cooling coils, respectively.

(c) The hot and cold duct temperature entering the mixing box.

(d) The hot and cold duct air flow entering the mixing box.

(e) The air temperature leaving the diffuser.

(f) The zone temperature.

Specific transfer functions of interest were derived. Transfer functions involving zone temperatures were difficult to obtain since temperature changes in the zone under test were insignificant. Lack of isolation from adjacent zones and time constants on the order of several hundred seconds precluded the development of any reasonable measured results for transfer functions including this

variable. However, analytical methods (as presented in Chapter 4) were used to determine zone time constants.

The following chapter discusses the compilation of test data, manufacturer design data, theory, and knowledge of component operation necessary to implement the system simulation.

CHAPTER 4

THE DUAL-DUCT SYSTEM SIMULATION

The development of a digital computer simulation for the dual-duct air handling system is presented in this chapter. The test data, manufacturers' design data, knowledge of component operation, and theory, as combined to form the system simulation, is discussed in detail.

Basics of the Computer Simulation

Normal operation of the dual-duct air handling unit is between 7:00 am and 5:30 pm, a time span of 10.5 hours (37,800 seconds). Both analog and digital computers are capable of running a simulation program of this length. However, large digital computers offer a much greater capacity in terms of the number of variables available to the user. As a result, the dual-duct system simulation was designed for implementation on a digital computer.

One of the most obvious tools for modeling a physical system on a digital computer is the Continuous System Modeling Program (CSMP). This program is specifically designed to allow users to simulate many types of physical systems with a minimum of programming difficulty. FORTAN, a powerful and flexible scientific programming language, is utilized as the source language. CSMP contains many user-oriented statements for formulating numerically complicated mathematical operations which are not available to the FORTRAN user.[4]

Like many higher level languages, CSMP exchanges programming

ease for increased central processing unit (CPU) time. Initial attempts at developing the dual-duct system simulation indicated that large scale simulations using CSMP often require so much CPU time that they become impractical to run. Both the monetary costs and the time between program submission and return become prohibitive. Consequently, the widely used FORTRAN was chosen as the appropriate programming language for the dual-duct simulation.

The system components were modeled by an equation of the form

$$G(s) = \frac{C(s)}{R(s)} = \frac{Ke^{-\theta s}}{1+\tau s} . \tag{4.1}$$

The gain factor, K, was obviously easy to implement in FORTRAN. The time delay, $e^{-\theta s}$, was represented by a one-dimensional array utilized as a shift register. The lag factor, $\frac{1}{1+\tau s}$, was described using the Tustin approximation,

$$s = \frac{2}{T}\frac{z-1}{z+1} , \tag{4.2}$$

where T is defined as the sample interval.[5] Substituting Eq. (4.2) into a simplified version of Eq. (4.1) with K = 1 and θ = 0 yields

$$\frac{C}{R} = \frac{1}{1 + \tau(\frac{2}{T}\frac{z-1}{z+1})} . \tag{4.3}$$

Rearranging produces

$$\frac{C}{R} = \frac{A(1+z^{-1})}{1+Bz^{-1}} , \tag{4.4}$$

where

$$A = \frac{T}{T+2\tau} \tag{4.5}$$

and

$$B = \frac{T-2\tau}{T+2\tau} . \tag{4.6}$$

Expanding Eq. (4.4) results in

$$C(z) = AR(z) + Az^{-1}R(z) - Bz^{-1} C(z) \tag{4.7}$$

Application of the inverse Z - transform

$$Z^{-1} [z^{-m}F(z)] = f[(nT-mT)] \tag{4.8}$$

gives

$$C(nT) = AR(nT) + AR[(n-1)] - BC[(n-1)T] \tag{4.9}$$

where n is the n^{th} discrete instant.

As commonly used, C(nT) and R(nT) represent the current values of the output and input, respectively. R[(n-1)T] and C[(n-1)T] indicate the first past values of the input and output. The current value of the output is therefore dependent on the current input value, the last input value, and the last output value. Equation (4.9) is easily described in FORTRAN.

The successful use of the Tustin approximation in the lag factor term $\frac{1}{1+\tau s}$ depends on the relative sizes of T and τ. For $\frac{\tau}{T} = 3$, the error between the ideal exponential time response

$$c(t) = (1-e^{-\frac{t}{\tau}})u(t) \tag{4.10}$$

and the Tustin method response given by Eq. (4.9) is less than 11% at the sample time nT = one time constant.

The Simulation Program

The dual-duct system simulation program consists of a main program and 12 subroutines. This modular design was adopted to maintain clarity and to increase program execution efficiency. The following sections discuss each program segment in detail.

The Main Program. This portion of the simulation functions as an executive program. Here, data input and output is controlled and initial conditions for the simulation are defined. Most importantly, the main program controls the subroutine calling sequences and timing information necessary for overall operation of the system simulation.

Figure 4.1 details in flowchart form the significant characteristics of the main program. Output is requested from subroutines DAMPER, HOT, and COLD at one second intervals. Physical responses represented by output variables from subroutines ZFEED and ZONE vary less rapidly with time than those from DAMPER, HOT, and COLD. Consequently, ZFEED and ZONE are called at five second intervals. Subroutines CLIMATE, WWRTN, and TTRTN are called at 30 second intervals since they model functions with slow time responses.

The four remaining subroutines are XLEFT, RIGHT, FLOWS and PSYSUN. Subroutines XLEFT and RIGHT are called by subroutine DAMPER, while subroutines FLOWS and PSYSUN are called by subroutine COLD.

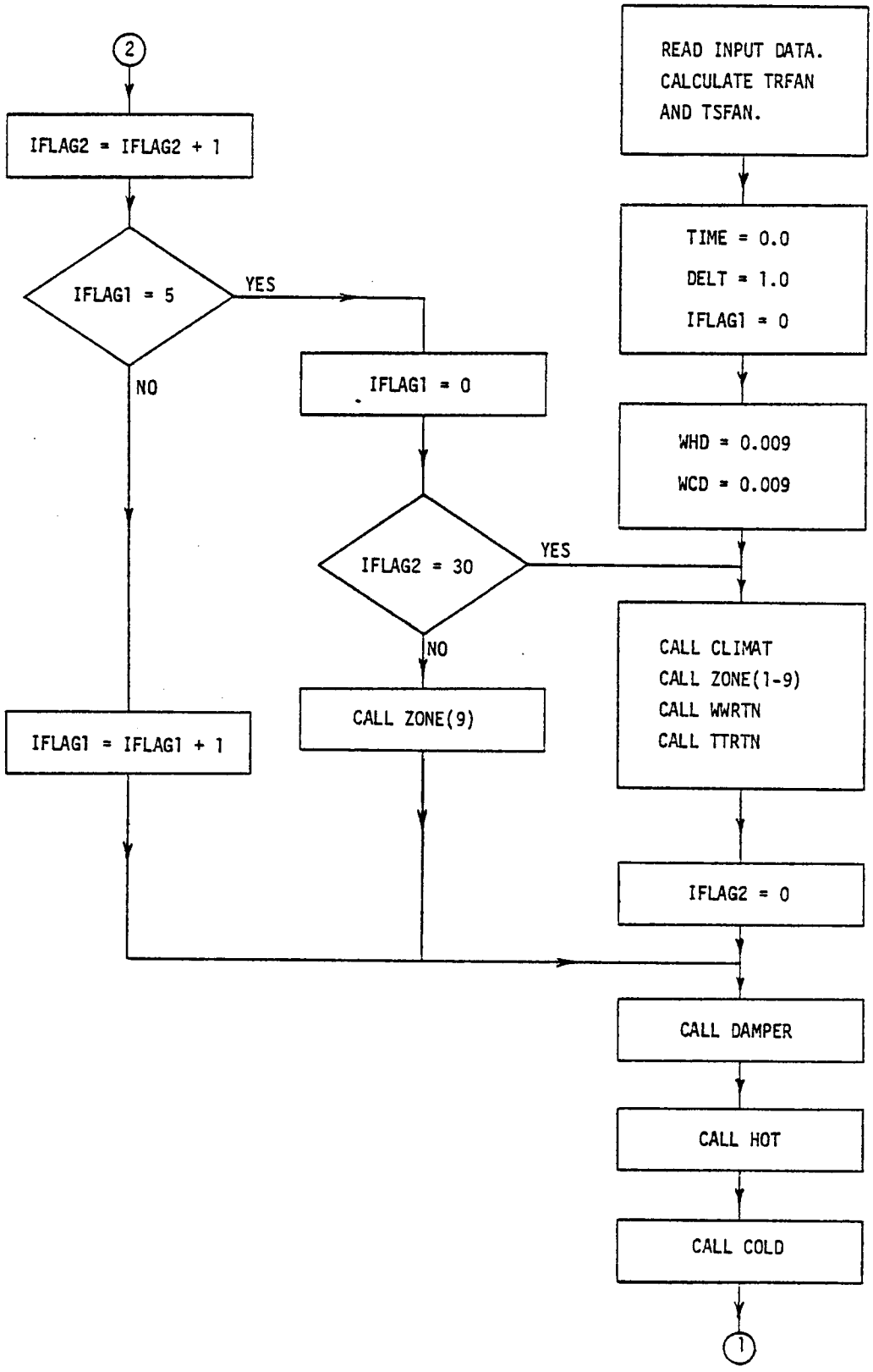


Figure 4.1. Main program flowchart.

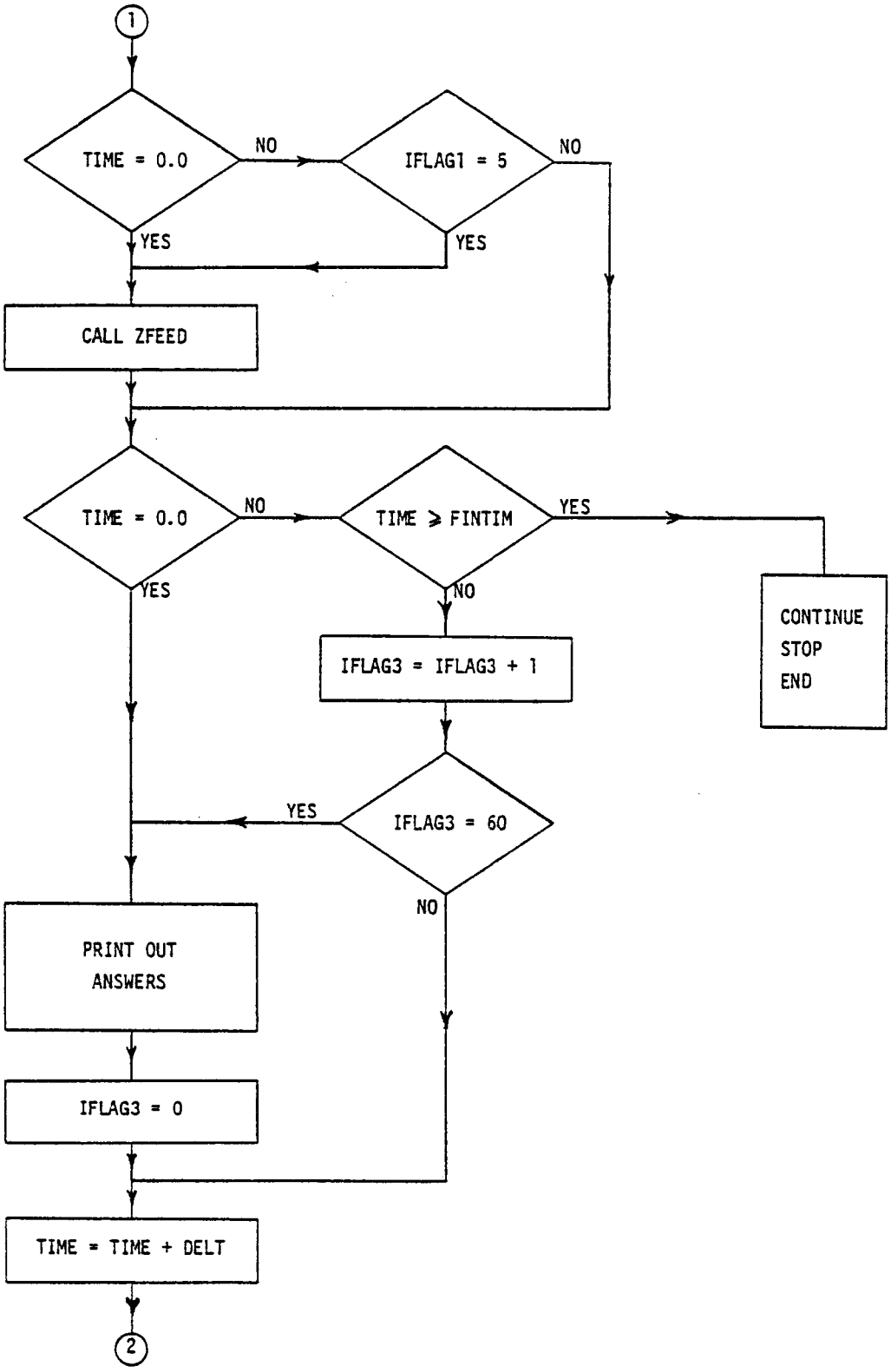


Figure 4.1. (Continued)

Subroutine CLIMAT. This subroutine gives the outside air temperature and humidity ratio as a function of the time of day and the season. User supplied input is an integer from one to four which specifies the desired season.

The 1970 meteorological data for Albany, New York produced values for the average daily temperature and relative humidity versus the time of day.[6] A psychrometric chart was used to convert the relative humidity readings to humidity ratios. This temperature and humidity ratio data was plotted for the months of January, April, July, and October. Straight line approximations of the resultant curves were then made so that the two variables could be expressed easily in equation form. If desired, a user could employ more exact data obtainable from weather data tapes.

Subroutine WWRTN. This subroutine calculates the return air humidity ratio as determined by the humidity ratios and air flows of the nine zones. Assuming steady-state flows, the return air mass flow rate equation for moisture is given by:

$$\dot{M}_{ret} = \dot{M}_1 + \dot{M}_2 + \ldots + \dot{M}_9 \tag{4.11}$$

where

$$\dot{M} = 60\rho FW. \tag{4.12}$$

In Eq. (4.12), $\dot{M}$ indicates mass flow rate in pounds-mass per hour (lbm/hr). The variable ρ represents density in pounds-mass of dry air per cubic foot of moist air (lbm/ft^3). F indicates volumetric air flow in CFM, and W represents the humidity ratio in pounds-mass of moisture per pound-mass of dry air (lbm/lbm).

Therefore,

$$\rho_{ret}F_{ret}W_{ret} = \rho_1F_1W_1 + \rho_2F_2W_2 +\ldots+ \rho_9F_9W_9. \qquad (4.13)$$

Air density varies little over the range of temperatures and humidity ratios commonly encountered in dual-duct systems. Because of the individual zone thermostats, the zone air temperatures remain near 75F. At this temperature, the density of dry air and moist air differ at most by 2.9%. Even a dry air temperature change from 60F to 80F involves a density increase of only 3.8%[7]. As a reasonable approximation, all density terms in Eq. (4.13) can therefore be set equal. The resulting expression for the return air humidity ratio is

$$W_{ret} = \frac{\sum_{n=1}^{9} F_nW_n}{F_{ret}}, \qquad (4.14)$$

where F_n is the volumetric air flow returning from the n^{th} zone and W_n is the humidity ratio from the n^{th} zone.

Subroutine TTRTN. In this subroutine, the return air temperature is calculated from the temperatures and air flows of the nine zones. The calculation is based on a heat transfer balance which assumes steady-state air flows:

$$\dot{Q}_{ret} = \dot{Q}_1 + \dot{Q}_2 +\ldots+ \dot{Q}_9 \qquad (4.15)$$

where

$$\dot{Q} = 60\rho FCp(T-T_{ref}). \qquad (4.16)$$

Therefore,

$$\rho_{ret}F_{ret}C_{p,ret}(T_{ret}-T_{ref}) = \rho_1F_1C_{p,1}(T_1-T_{ref}) + \rho_2F_2C_{p,2}(T_2-T_{ref}) + \ldots + \rho_9F_9C_{p,9}(T_9-T_{ref}). \quad (4.17)$$

The heat transfer rate $\dot{Q}$ has units of BTU/hr and the specific heat has units of BTU/lbm-F. Temperature is specified in degrees Farenheit(F).

The variables ρ and C are not strong functions of temperature and humidity ratio over the system's operating range. The products of ρ and C_p for each term in Eq. (4.17) can thus be considered equal constants. T_{ref} is an arbitrary temperature reference. With these conditions, Eq. (4.17) can be solved for the return air temperature T_{ret}:

$$T_{ret} = \frac{\sum_{n=1}^{9} F_nT_n}{F_{ret}}. \quad (4.18)$$

Temperature increases due to air passing through the return air fan (10 HP) is added to T_{ret} in the subroutine.

Subroutine DAMPER. This subroutine simulates the supply air temperature control loop. Since the maximum outside air and exhaust air dampers are similar in construction and are driven by the same pressure signal, their flows are set equal:

$$F_{exh} = F_{max}. \quad (4.19)$$

The minimum outside air flow, F_{min}, is set by system hardware to approximately 9,000 CFM. Observations of the physical system indicate

that this amount of air is exfiltrated in the zones. Otherwise, the total air mass in the building would steadily increase and would produce increasing positive pressures in the zones. The supply air flow to the zones, F_{sup}, is 38,660 CFM. The return air flow, F_{ret}, is thus

$$F_{ret} = F_{sup} - F_{min}. \tag{4.20}$$

That part of the return air flow which is not exhausted flows through the return air dampers and contributes to the supply air flow. Writing F_{sup} in terms of the other flow variables,

$$F_{sup} = F_{min} + F_{max} + (F_{ret} - F_{exh}). \tag{4.21}$$

Equation (4.21) reduces to Eq. (4.20) upon substitution of Eq. (4.19).

Just before entering the supply air fan, the air flow is a mixture of: (a) return air which has not been exhausted, (b) minimum outside air, and (c) air from the maximum outside air damper. Equations of the form of (4.18) and (4.14) are used to determine the temperature and humidity ratio of this air flow. The supply fan performs maximum sensible heating described by

$$\Delta T = \frac{\left(\frac{\text{Fan HP}}{0.85}\right)\left(\frac{2545 \text{ BTU/hr}}{1 \text{ HP}}\right)}{(\text{CFM})\left(1.086 \frac{\text{BTU-min}}{\text{hr-ft}^3\text{-}^\circ\text{F}}\right)}. \tag{4.22}$$

The maximum total applied power to the fan is calculated by dividing the fan horsepower rating by an 85% efficiency factor.[8] Total applied power is used in Eq. (4.22) because the supply fan is completely inside the air flow. Air heating normally occurs because the fan shaft

power (85% of the total applied power) adds kinetic energy to the air flow. Fan power losses due to bearing friction or winding resistance (15% of the total applied power) contribute to the air heating effect as well.

Figure 4.2 illustrates the supply air temperature control loop with the variable names used in the subroutine. As indicated, the outputs of subroutine DAMPER are the exhaust flow, the supply air temperature, and the supply air humidity.

Relatively complex logic is required in a digital simulation to adequately represent all of the responses characteristic of systems exhibiting hysteresis. Figure 4.3 indicates, in flowchart form, the portion of subroutine DAMPER which models the exhaust damper hysteresis. Two additional subroutines, XLEFT and RIGHT, are called from this program segment.

Subroutines XLEFT and RIGHT. These subroutines represent a piecewise linear approximation of the exhaust damper hysteresis curve shown on page 30. Subroutine DAMPER calls either subroutine XLEFT or RIGHT depending on where the exhaust damper operating point was located at the last iteration.

Subroutine XLEFT describes the left portion of the hysteresis curve while subroutine RIGHT describes the right portion. The input variable to subroutine XLEFT or RIGHT is the pressure applied to the damper operator. The output variable returned by the two subroutines is the exhaust damper air flow. This part of the damper hysteresis program development is general and can be applied to a number of hysteresis characteristics derived from other systems.

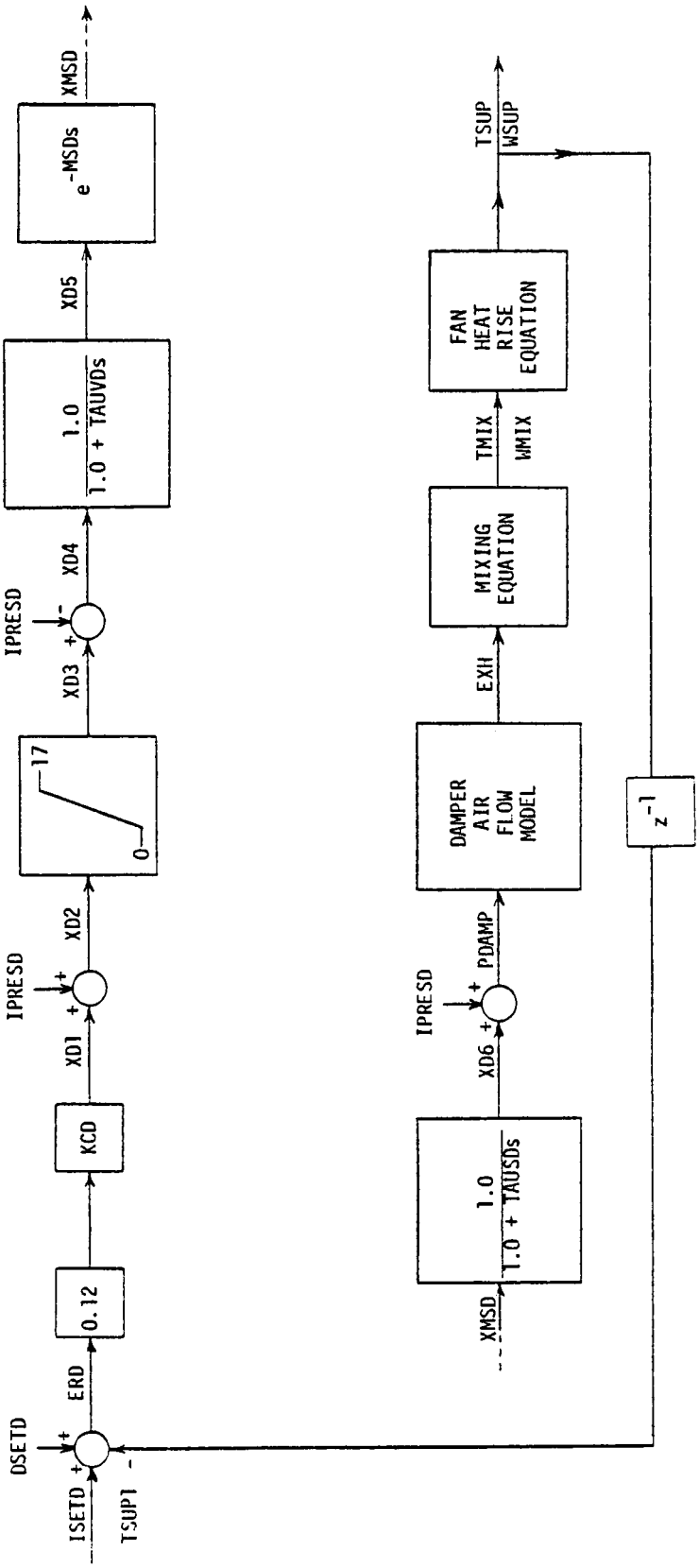


Figure 4.2. Supply air temperature control loop.

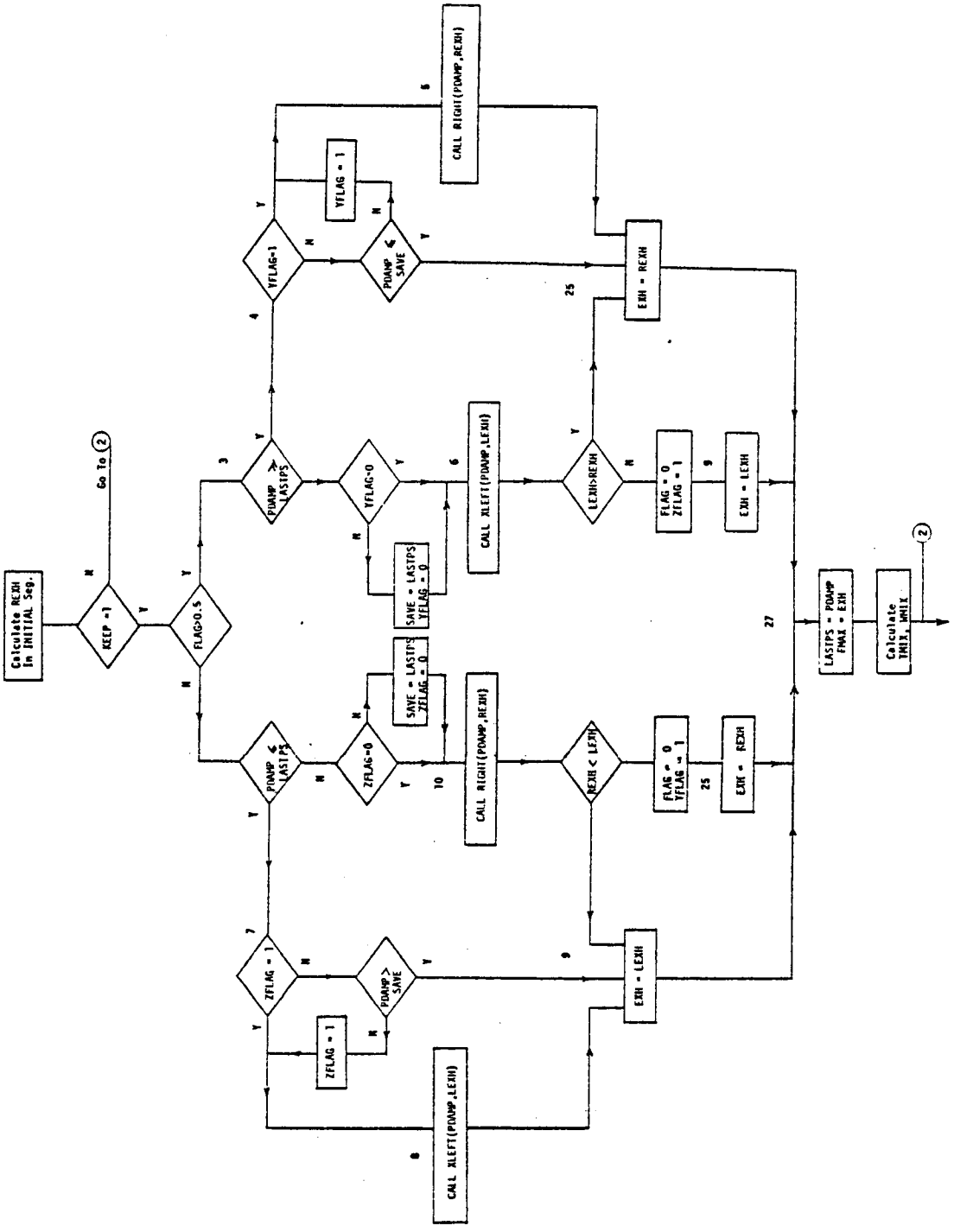


Figure 4.3. Damper hysteresis flowchart.

Subroutine COLD. This simulation models the cold duct temperature control loop. The major portion of this subroutine is dedicated to the representation of the psychrometric changes experienced by air passing over the cold duct cooling coil.

Many variables affect the outlet air condition of a cooling coil. Some of these variables which are the most readily identificable are:

(a) The inlet air temperature, humidity ratio, and pressure.

(b) The air flow across the coils.

(c) The inlet cooling water temperature.

(d) The cooling water flow.

(e) The geometry of the cooling coils.

(f) The materials from which the coils are manufactured.

A steady state energy balance is performed to calculate the state of the air exiting the coil. The energy loss of the air is expressed by:

$$Q_a = 60 \rho_a F_a (C_s (T_{a,1} - T_{a,2}) + \lambda (W_1 - W_2)). \qquad (4.23)$$

Q_a is the heat flow from the air in BTU/hr. C_s is the humid heat of air given by:

$$C_s = 0.24 + 0.46\ W_1. \qquad (4.24)$$

W_1 is the cooling coil inlet air humidity ratio and W_2 is the outlet humidity ratio. $T_{a,1}$ and $T_{a,2}$ represent the inlet air and outlet air temperatures, respectively. The constant, λ, is the latent heat of fusion for water and is equal to 1050 BTU/lbm.

The energy gained by the water is equal to that lost by the air:

$$Q_w = 500\ G_w C_p (T_{w,2} - T_{w,1}) = Q_a \qquad (4.25)$$

G_w indicates the water flow in gallons per minute (GPM). $T_{w,1}$ is the inlet water temperature and $T_{w,2}$ is the outlet water temperature. Equation (4.25) is easily solved for $T_{w,2}$, the only unknown.

A third energy equation must be utilized to find the cooling coil outlet air conditions. The manufacturer's data sheets give the design heat flow absorbed by the water in the cooling coil as:[9]

$$Q_d = KAR\ \Delta T_m. \qquad (4.26)$$

Q_d should agree with the value of Q_w and Q_a. K is an overall heat transfer coefficient with units of BTU per hour per foot squared per Farenheit degree per row ($\frac{BTU}{hr\text{-}ft^2\text{-}F\text{-}row}$). A is the face area of the coil in square feet (ft^2) while R is the number of rows of cooling tubes in the coil. The variable ΔT_m is the coil logarithmic mean temperature difference defined by:

$$\Delta T_m = \frac{\Delta T_g - \Delta T_1}{\ln_e (\frac{\Delta T_g}{\Delta T_1})} \quad . \qquad (4.27)$$

The greatest temperature difference, ΔT_g, is

$$\Delta T_g = T_{a,1} - T_{w,2} \ . \qquad (4.28)$$

The least temperature difference, ΔT_1, is[2]

$$\Delta T_1 = T_{a,2} - T_{w,1} \ . \qquad (4.29)$$

K is a complex function of air and water flows. However, the range of water flows found in this cooling coil permit the use of a piecewise linear approximation for K. As a result, ΔT_m is the only unknown in Eq. (4.26).

The determination of the correct value for $T_{a,2}$ and W_2 requires an iterative process. An estimate is first made of the dry bulb temperature $T_{a,2}$. If this estimate is below the dewpoint of the inlet air to the coil, condensation (latent cooling) is indicated and the humidity ratio is decreased. If the estimate of $T_{a,2}$ is not below the dewpoint of the inlet air, sensible cooling is simulated and the humidity ratio remains constant. Q_a is calculated and the value of $T_{w,2}$ is then found from Eq. (4.25). Equations (4.26) through (4.29) are utilized to find the design heat flow, Q_d. If Q_d and Q_w differ by more than 7.5%, the product of a proportional gain constant and the error is used as a correction factor for the estimate of $T_{a,2}$. Iterations continue until the error condition is met or until an iteration counter exceeds a user-set limit.

Examination of catalog data from cooling coil manufacturers shows that when condensation occurs, the relative humidity of the outlet air may be as high as 98%. Relative humidity is defined as the ratio of the vapor pressure of the air under study to the saturation pressure of pure water at the same temperature.[10] This high value of relative humidity occurs when a deep coil (10 rows, for example) with a low air face velocity (330 feet per minute, or fpm) cools high humidity ratio air. A shallow coil (3 rows) with a high

face velocity (600 fpm) has outlet air relative humidities of approximately 85%.[11] The first example closely resembles the dual duct cooling coil, which is 8 rows deep and has a normal face velocity of approximately 150 fpm. Consequently, if any latent cooling occurs in the simulation the outlet air is estimated to be saturated (100% relative humidity).

Figure 4.4 details the cold duct temperature control loop. Both subroutine FLOWS and subroutine PSYSUN are necessary for the operation of this simulation segment.

Subroutine FLOWS. This subroutine is a piecewise linear approximation of the chilled water flow through the cooling coil as a function of the pressure signal to the chilled water valve. The input to the subroutine is the simulated cold duct temperature controller pressure output. The output from FLOWS is the chilled water flow in GPM.

Subroutine PSYSUN. Subroutine PSYSUN is a compact FORTRAN subroutine developed to solve psychrometric problems in practical applications. Basically, the subroutine uses the algorithms developed by the American Society of Heating, Refrigerating, and Air-Conditioning Engineers (ASHRAE) Task Group for Energy Requirements, Heating and Cooling Load Calculation Subcommittee.[12]

This psychrometric subroutine contains six variables; (a) dry bulb temperature in degrees F (b) wet bulb temperature in degrees F (c) relative humidity in percent, (d) humidity ratio in lbm water/lbm air, (e) enthalpy in BTU/lbm air, and (f) dewpoint in

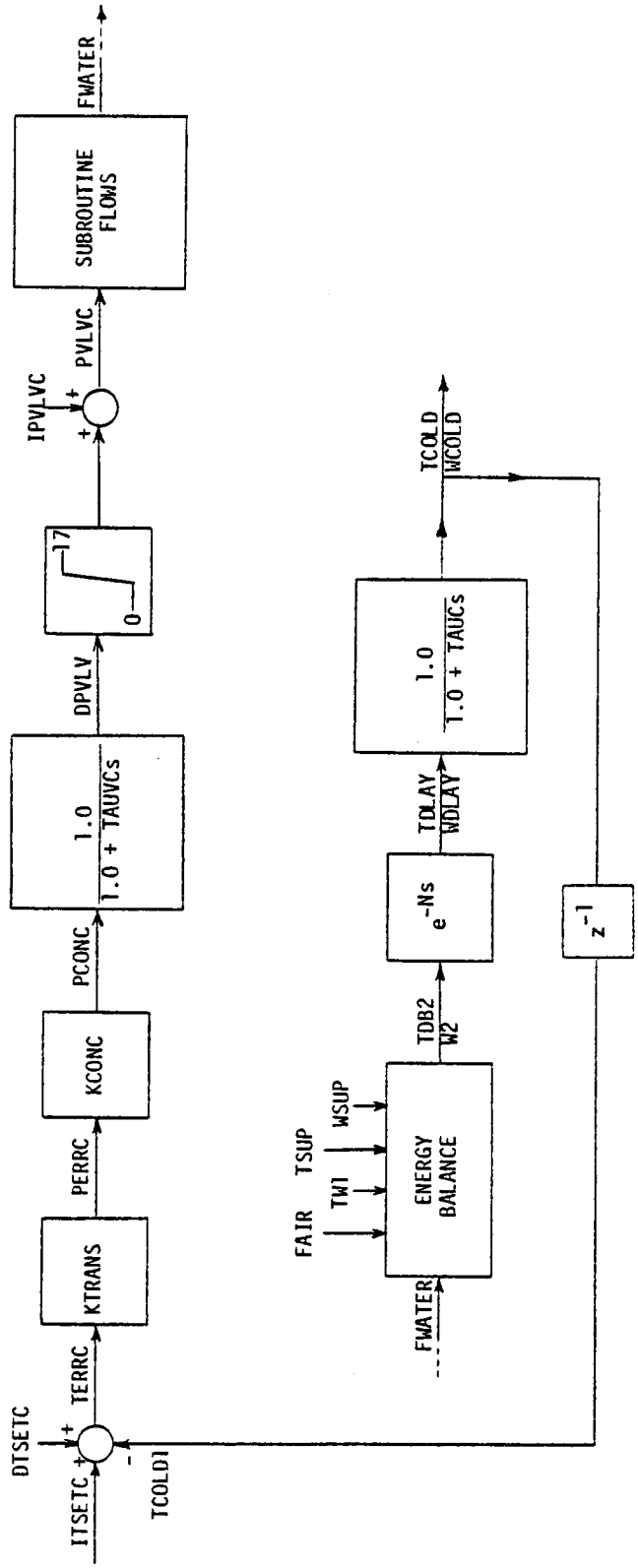


Figure 4.4. Cold duct temperature control loop.

degrees F. The air-water vapor mixture is assumed to be at standard atmospheric pressure. Definition of any two of the listed properties of the mixture variables describes a unique thermodynamic state. The remaining state properties of the mixture can immediately be found.

For this subroutine, one of the defined input variables must be the dry bulb temperature. Any one of the other five psychrometric parameters may be specified as the remaining input. The four associated psychrometric parameters are then calculated and passed back to subroutine COLD.

Subroutine HOT. This segment models the hot duct temperature control loop. Figure 4.5 indicates the control loop and the variable names employed in the subroutine. In practice, this dual-duct system rarely demands the use of the heating coil. Occupants, lights and office machinery serve very effectively as internal heat sources. In fact, these serve so well that the low pressure steam is manually blocked from the heating coil unless the outside air temperature falls below -10F. Since the heating coil performs only sensible heating, the outlet air humidity ratio is identical to the supply air humidity ratio. As a result, the hot duct model is less complex than the cold duct model. The single output variable, T_{hot}, can be calculated at each sample time without an iterative procedure. The variation of T_{hot} with changes in the supply air temperature is described by a gain factor and a lag term. Similarly, the dependence of T_{hot} on the air flow is reflected by a change in temperature that is inversely proportional to air flow. This is an empirical relationship that is

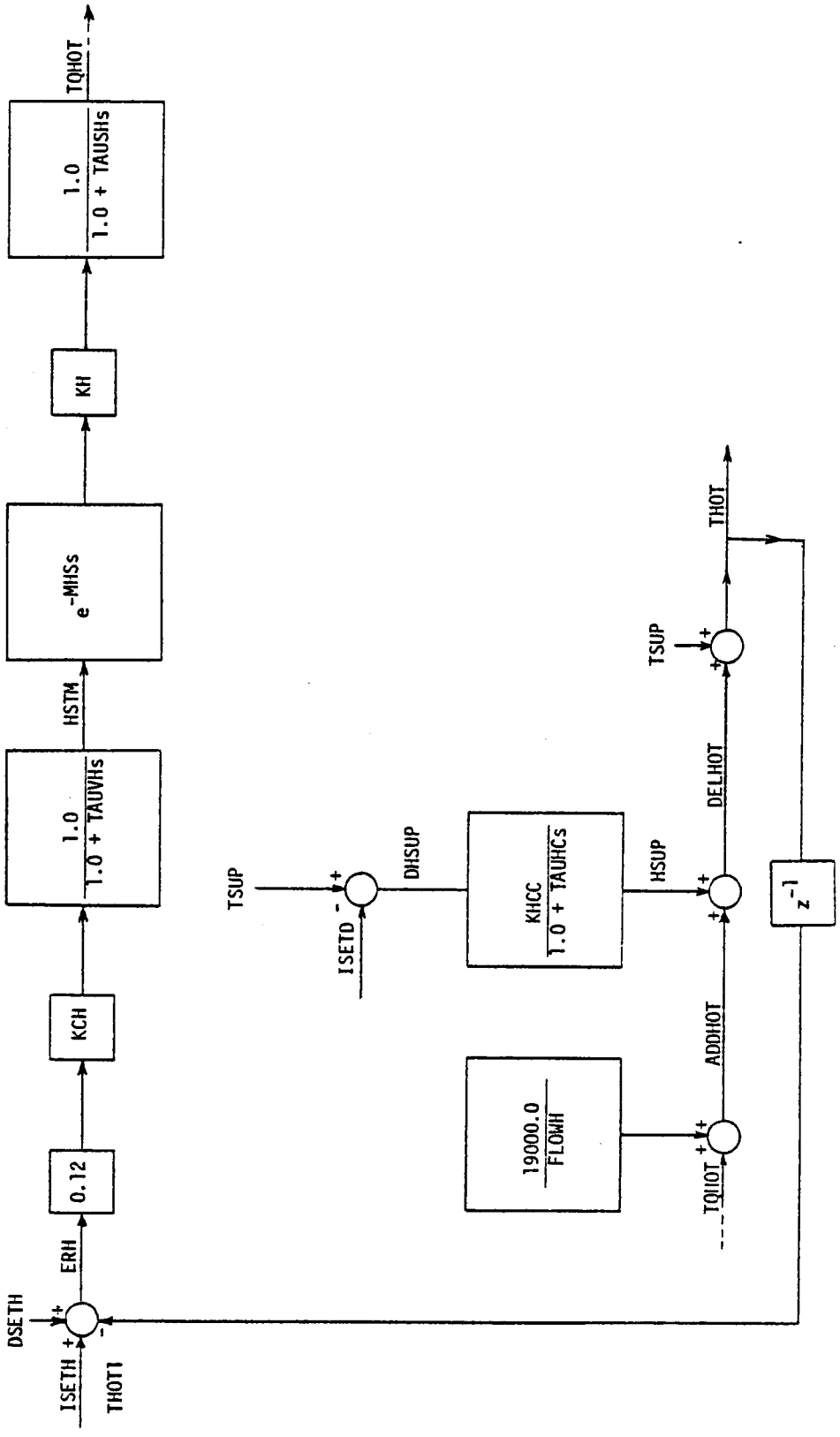


Figure 4.5. Hot duct temperature control loop.

justified on the basis of results which reasonably agree with actual system performance.

Subroutine ZFEED. The temperature of air moving down a duct is affected by the temperature of the ambient air, T_{amb}. This subroutine describes the temperature change experienced by air traveling from the heating and cooling coils to the individual zone mixing boxes.

In steady-state, the duct outlet air temperature is expressed as

$$T_{out} = T_{amb} + (T_{in} - T_{amb})e^{-\frac{UA}{\dot{M}C_p}} \tag{4.30}$$

where T_{in} is the inlet air temperature.[13] U is an overall heat transfer coefficient and A is the duct cross-sectional area in square feet. Rather than attempt to determine U and A (which vary all along the duct) the exponential term $\frac{UA}{\dot{M}C_p}$ in Eq. (4.30) was found for one zone by inserting steady-state values of T_{out} and T_{in}. Both the hot and cold ducts are routed through the return air plenum, so T_{amb} is approximately 75F. For the hot duct the resulting form of Eq. (4.30) is

$$T_{out} = 0.36\ T_{amb} + 0.64\ T_{in}. \tag{4.31}$$

For the cold duct,

$$T_{out} = 0.16\ T_{amb} + 0.84\ T_{in}. \tag{4.32}$$

Dynamic tests indicated that the time response of the air temperature in the hot and cold ducts could be modeled by a simple lag term. Steady-state and dynamic testing of all zones was not possible. Therefore, these dynamic results and Eqs. (4.31) and (4.32) were utilized as a rough approximation of the duct temperature

variation for each zone. Fig. 4.6 illustrates the basic concept of subroutine ZFEED.

Subroutine ZONE. Subroutine ZONE simulates the individual zone cooling loads as well as the individual zone temperature control loops.

This particular dual-duct system, AC-1, serves 20 zones. The constant air flow capacities for mixing boxes in each zone were obtained from architectural specifications. Data concerning the total area serviced by AC-1 on each floor was also provided. Ceiling height was known to be ten feet. On a particular floor, then, the volume served by an individual AC-1 zone was calculated as

$$V_{zone} = \frac{(F_{zone})(V_{total})}{F_{total}} . \qquad (4.33)$$

F_{zone} is the individual zone air flow and F_{total} is the total air flow from AC-1 to the floor. V_{total} is the total volume on the floor serviced by AC-1 in cubic feet.

Assuming perfect mixing in the zones, the relationship between the zone temperature and the inlet air temperature from the diffuser can be described in the s-domain as $\frac{1}{1+\tau s}$. The constant τ is equal to the volume of the zone divided by the air flow rate.[14]

In order to reduce the computer simulation time, zones with similar placements on a given floor were grouped together. For example, three zones on the first floor which all touch the same external wall were combined into one large zone in the subroutine. Further groupings reduced the total number of simulated zones to nine.

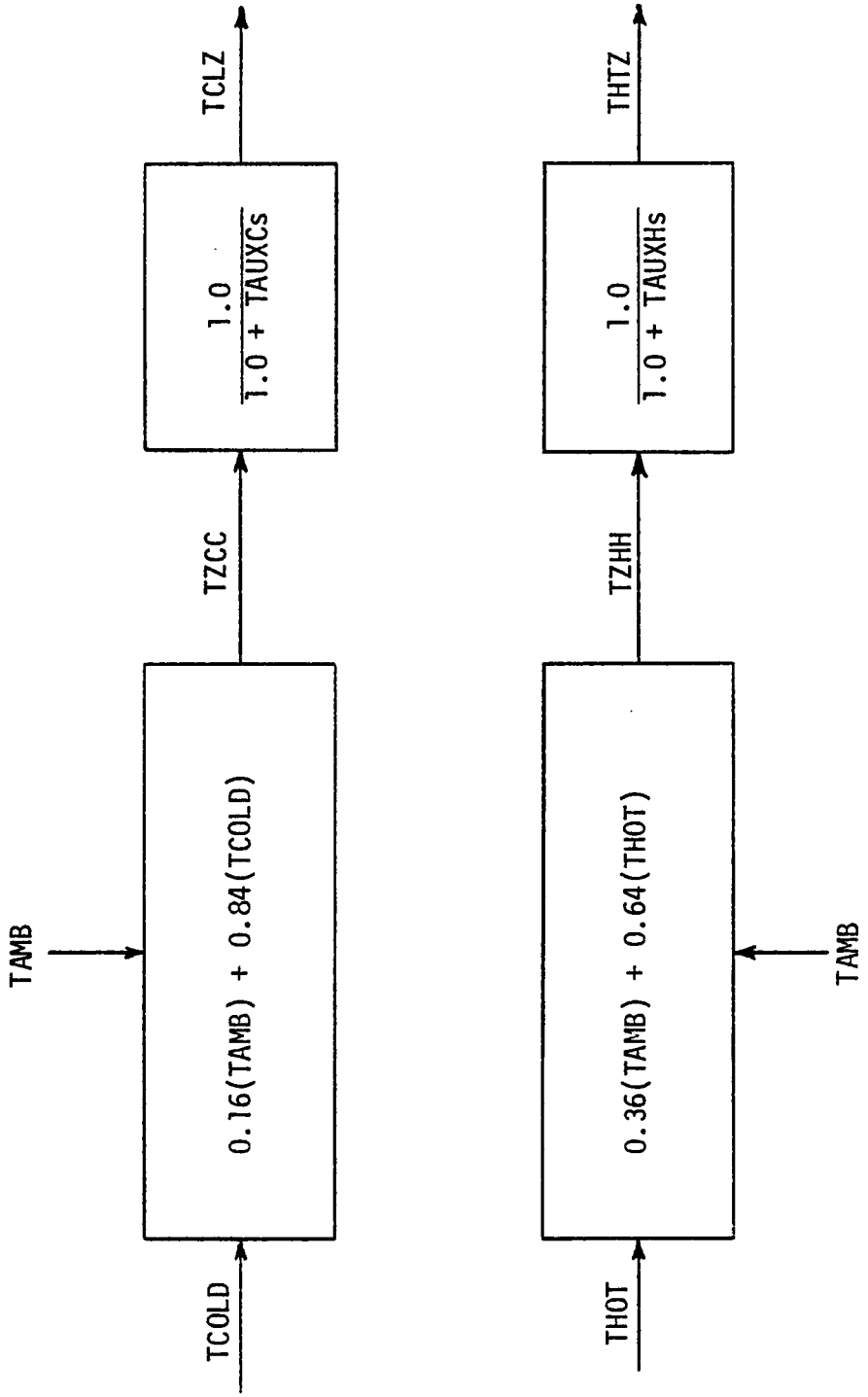


Figure 4.6. Block diagram of subroutine ZFEED.

Both sensible and latent heat loads appear in the zones. Relatively constant sensible heat contributions from lights and occupants were investigated. Normal office building specifications call for eight to fifteen watts of lighting per square foot. Conservation practices have reduced lighting levels, so a figure of 3 watts/ft^2 (10.2 BTU/hr-ft^2) was chosen. Heating effects are calculated using this same figure.[8] An individual sitting at a desk normally releases sensible heat at the rate of 250 BTU/hr-person. The latent heat, dependent on both the activity level of the individual and the room temperature, is taken to be 250 BTU/hr-person. The building occupant density was estimated at 1 person/150 ft^2.

Sensible heat gains are also produced by solar radiation and air infiltration. Lack of information precluded the simulation of these highly variable gains. In addition, sensible heat gains and losses occur because of thermal conduction through the building walls and glass. A perimeter wall heating system prevents heat loss from the zones if the outside air temperature falls greatly below 70F. If the outside temperature rises above 70F, heat is transferred to the perimeter zones at the rate

$$\dot{Q} = UA(T_{out} - T_{zone}). \qquad (4.34)$$

With an overall building heat transfer coefficient, U, of 0.3 BTU/ft^2-hr-F, heat gains are significant only when the outside temperature is 90F. Conduction heat gains are therefore ignored. In summary, the parameters used to characterize the nine zones are shown in Table 4.1.

Table 4.1. Zone characteristics.

Zone No.	Zone Area (ft^2)	Zone CFM (CFM)	Zone Time Constant (sec	Sensible Heating (BTU/hr)	Latent Heating (BTU/hr)
1.1	5612	5740	587	66800	9350
1.2	4888	5000	587	58100	8150
2.1	4634	5740	484	55100	7720
2.2	2906	3600	484	34600	4840
2.3	2260	2800	484	26900	3770
3.1	1940	1940	60	23100	3230
4.1	3976	7100	336	47300	6630
4.2	2637	4710	336	31400	4400
4.3	1138	2030	336	13500	1900

Figure 4.7 illustrates the simulation strategy for the zone temperature control loops. The mixing algorithm calculates the temperature of air leaving the diffuser and the zone humidity ratio. The temperature calculation is of the form of Eq. (4.18) where the mixed air streams are from the hot and cold ducts. The humidity ratio calculation is similar to Eq. (4.14) except that the moisture increases due to the latent heat load must be included.

Verification of Simulation Accuracy

An ideal simulation of a physical system responds exactly as the system does. Unfortunately, pneumatic air handling systems can rarely be tested so extensively that the resulting simulation is ideal. Manufacturer's device data may be misleading. Most transducers and controllers are accurate at best within 10% of their full scale range, nor are they perfectly linear. Additional factors which make precisely accurate simulations improbable are duct leakage, varying hysteresis effects in mechanical operators, unknown heat transfer coefficients and capacitance effects, and the presence of such a great number of input variables. Measurements for highly accurate simulations can only be obtained with inordinate expense and effort over long time spans.

Likewise, the difficulty in verifying the accuracy of a system simulation increases rapidly with the system complexity. For instance, all of the input and output variables of the dual-duct system cannot practically be monitored at the same time. Under these circumstances the accuracy of the components of the simulation must be examined.

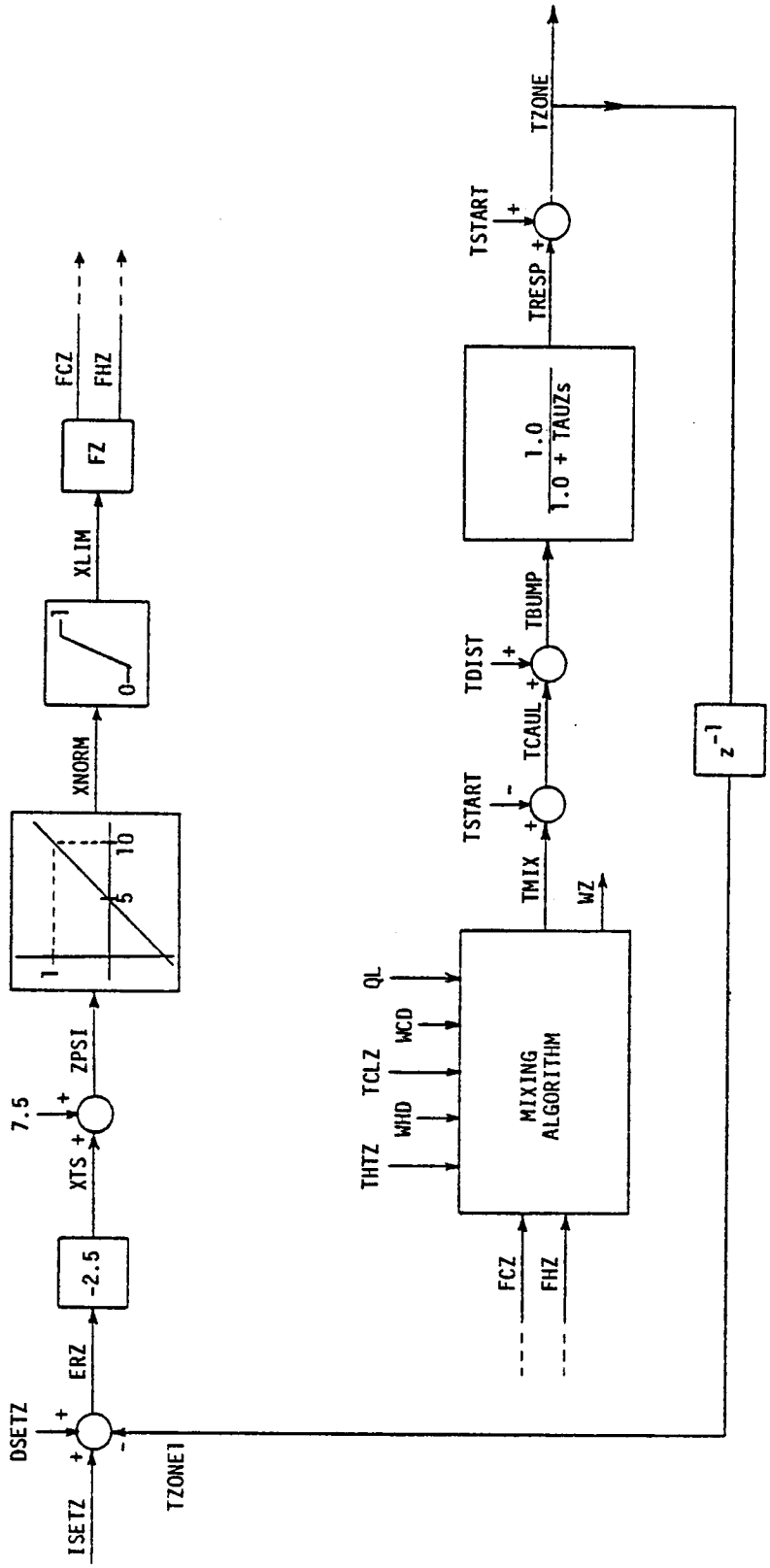


Figure 4.7. Zone temperature control loop.

Simulation segments such as ZFEED, DAMPER, TTRTN, WWRTN, CLIMAT, XLEFT, XRIGHT, COLD, and PSYSUN were written to be accurate within 10% of their design data. That does not imply that they will maintain that measure of accuracy over all operating conditions. Subroutines HOT and ZONE were based largely on intuition and engineering judgement since detailed measurements of variables were not available.

No gross errors have yet been observed in the system simulation. Although not ideal, the dual-duct model was detailed enough to satisfy the requirement of indicating whether:

(a) A new control strategy would disrupt the system stability.

(b) A new control strategy would decrease the total energy use in the system.

The next chapter presents the simulation results of two different operating strategies for the dual-duct system.

CHAPTER 5

SIMULATION RESULTS

In order to compare relative energy usage and system stability, two sets of dual-duct simulations using different operating strategies were conducted. This chapter presents the results of those simulations and discusses their significance.

Operating Strategies

Many of the input variables of the dual-duct system can not be manipulated to decrease the overall energy usage or to affect the system stability. Among those manipulable input variables that can influence total system energy use or stability are the zone temperature setpoints and the minimum outside air damper position. Design information indicated that the zone temperature setpoints were originally 72F. In addition, the minimum outside air damper was initially set manually to admit 9,000 CFM. The first simulation set was thus conducted to indicate the performance of this original dual-duct system.

Practical experience with the existing dual-duct air handling units eventually led to the modified operating system now in effect at the plant. Under this current system, the zone setpoints are 74F and the minimum outside air damper is set to admit 6,000 CFM. The low pressure steam valve for the heating coils is manually closed so that the hot duct is off. As a result, the hot duct temperature is identical to the supply air temperature. To indicate the performance of the modified dual-duct system, zone setpoints, minimum air flow, and hot duct

parameters were changed and a second simulation set was conducted. All remaining input parameters were indentical to the simulation for the original system.

Simulation Results and Discussion

Both figures and tables are used to display pertinent simulation results concerning the dual-duct system stability and energy usage. The system was simulated as being inoperative at time zero, so the greatest transient phenomena was exhibited in the few minutes following system start-up. This transient activity was plotted for the following variables (FORTRAN variable names are included):

(a) The supply air temperature, TSUP.

(b) The cold duct temperature, TCOLD.

(c) The cold duct air flow, FLOWC (or SUMCZ).

(d) The hot duct temperature, THOT.

(e) The temperature of air from the hot duct entering the zones, THTZ.

(f) The temperature of air from the cold duct entering the zones, TCLZ.

(g) The temperature of representative zones four and five, TZONE(4) and TZONE (5).

(h) The return air temperature, TRTN.

(i) The exhaust air flow, EXH.

The energy transferred to the cooling coils, QCOLD, the energy transferred from the heating coils, QHOT, and the total system energy supplied, QTOTAL (or ENERGY) are plotted for the length of the simulation run. QTOTAL is the sum of QHOT, QCOLD, and the maximum power

supplied to the return and supply fans.

Tabular data such as steady state values, the time to steady state, minima, and the time to the minima are listed for all of the variables above. This data is also tabulated for:

(a) The outside air temperature, TOUT.

(b) The outside air humidity ratio, WOD.

(c) The hot duct air flow, FLOWH (or SUMFHZ).

(d) The return air himidity ratio, WRTN.

(e) All zone temperature, TZONE(1) - TZONE(9).

(f) All zone humidity ratios, WZ(1) - WZ(9).

A simulation set consisted of four computer runs, one for each season of the year. The following discussion is consequently divided into four portions. Each portion discusses the simulation results for the original and modified system. The two systems are also compared in terms of relative stability and energy usage.

Simulation of Winter Operation. Figure 5.1 shows the straight line approximations of the temperature, relative humidity, and humidity ratio profiles of a typical day in winter. Figures 5.2 and 5.3 illustrate the transient response of the cold duct, hot duct, and supply air temperature for the original and modified system, respectively. Decreasing the minimum outside air flow in the modified system causes increased oscillations in T_{supply}. These oscillations in T_{supply} consequently cause oscillations in T_{hot} and T_{cold}. Figures 5.4(a) and 5.5(a) show that the exhaust air flow in the modified system exhibit this same oscillatory nature.

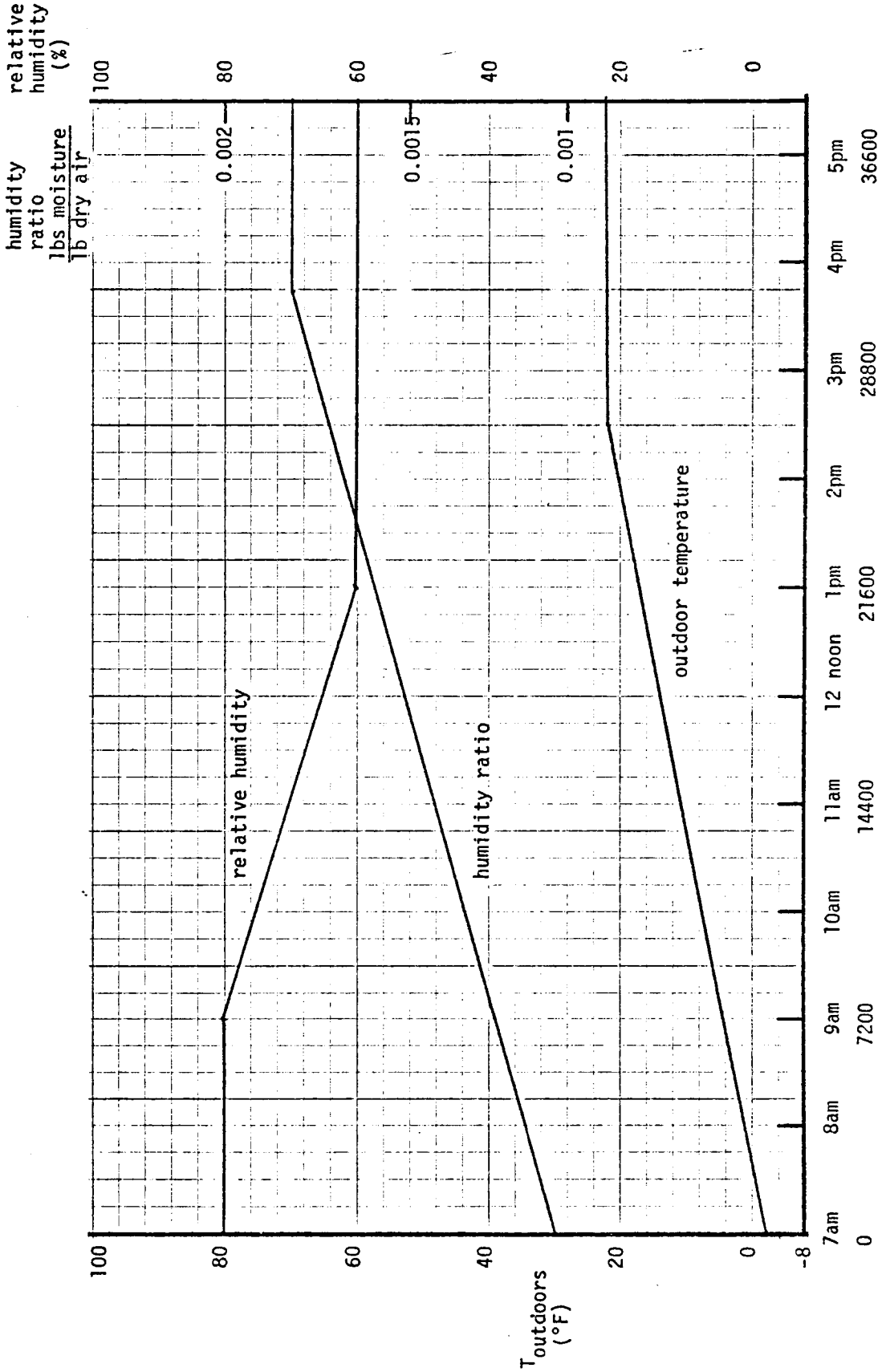


Figure 5.1. Approximate outside air conditions in winter.

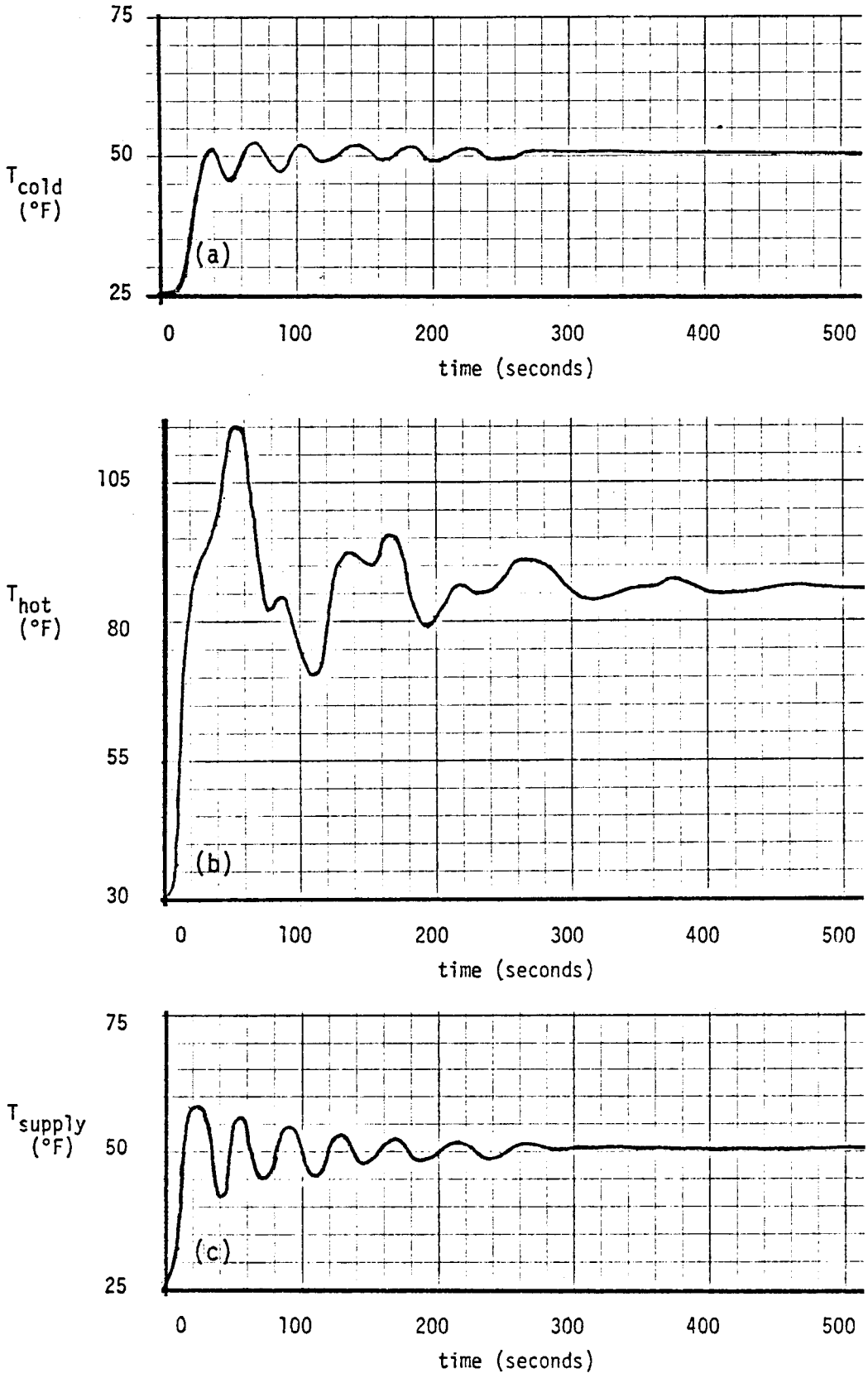


Figure 5.2. Upstream temperatures for the original system in winter.

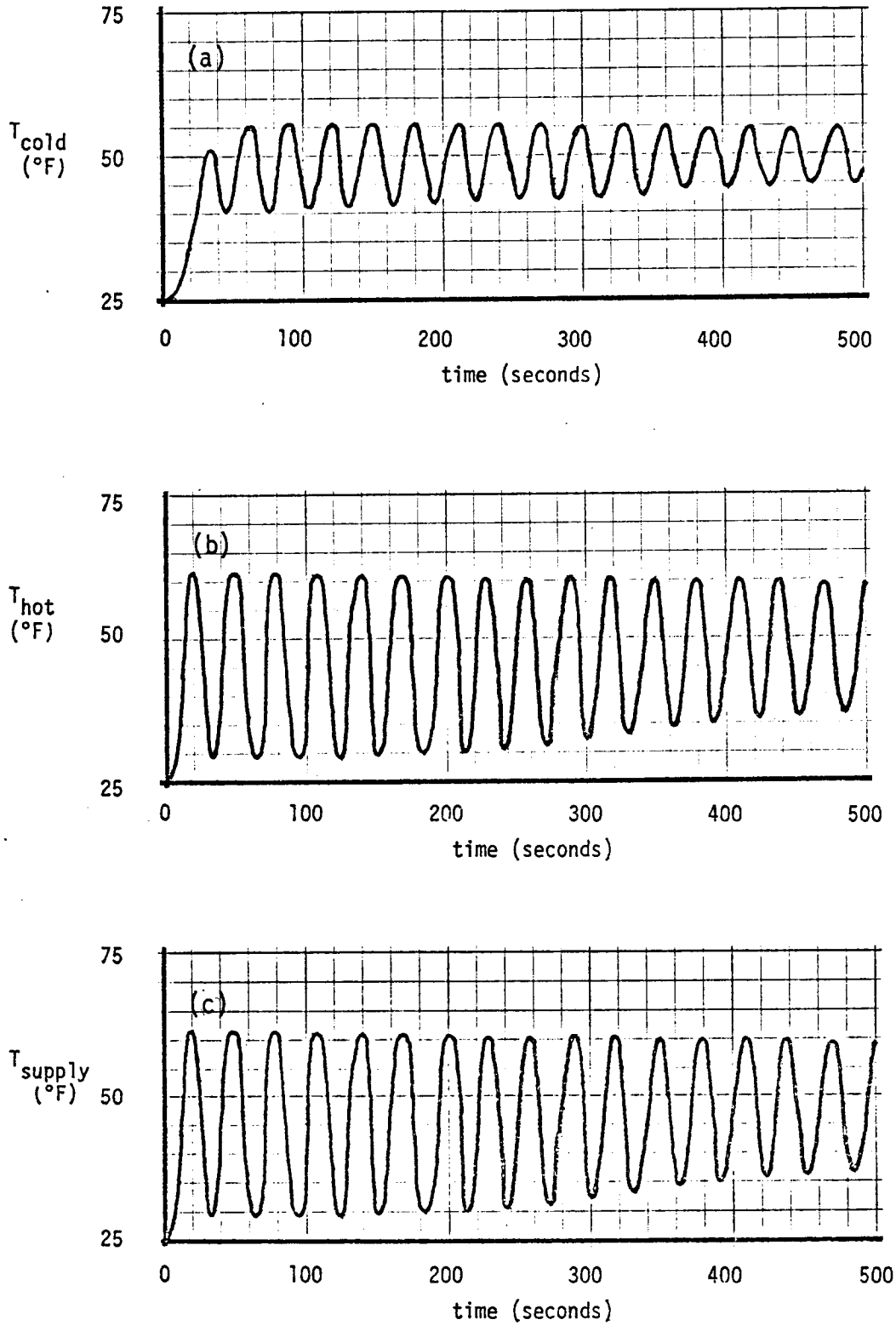


Figure 5.3. Upstream temperatures for the modified system in winter.

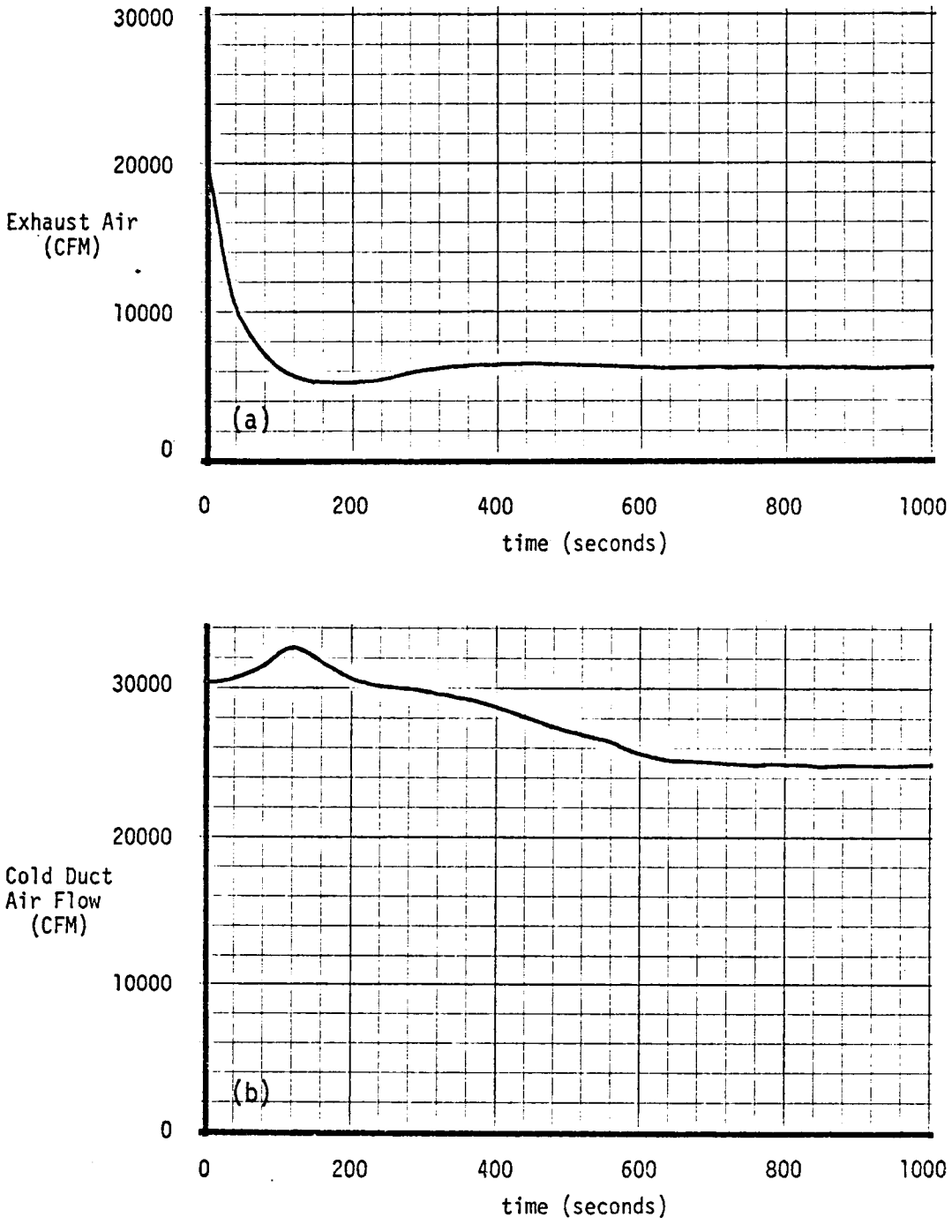


Figure 5.4. Air flows for the original system in winter.

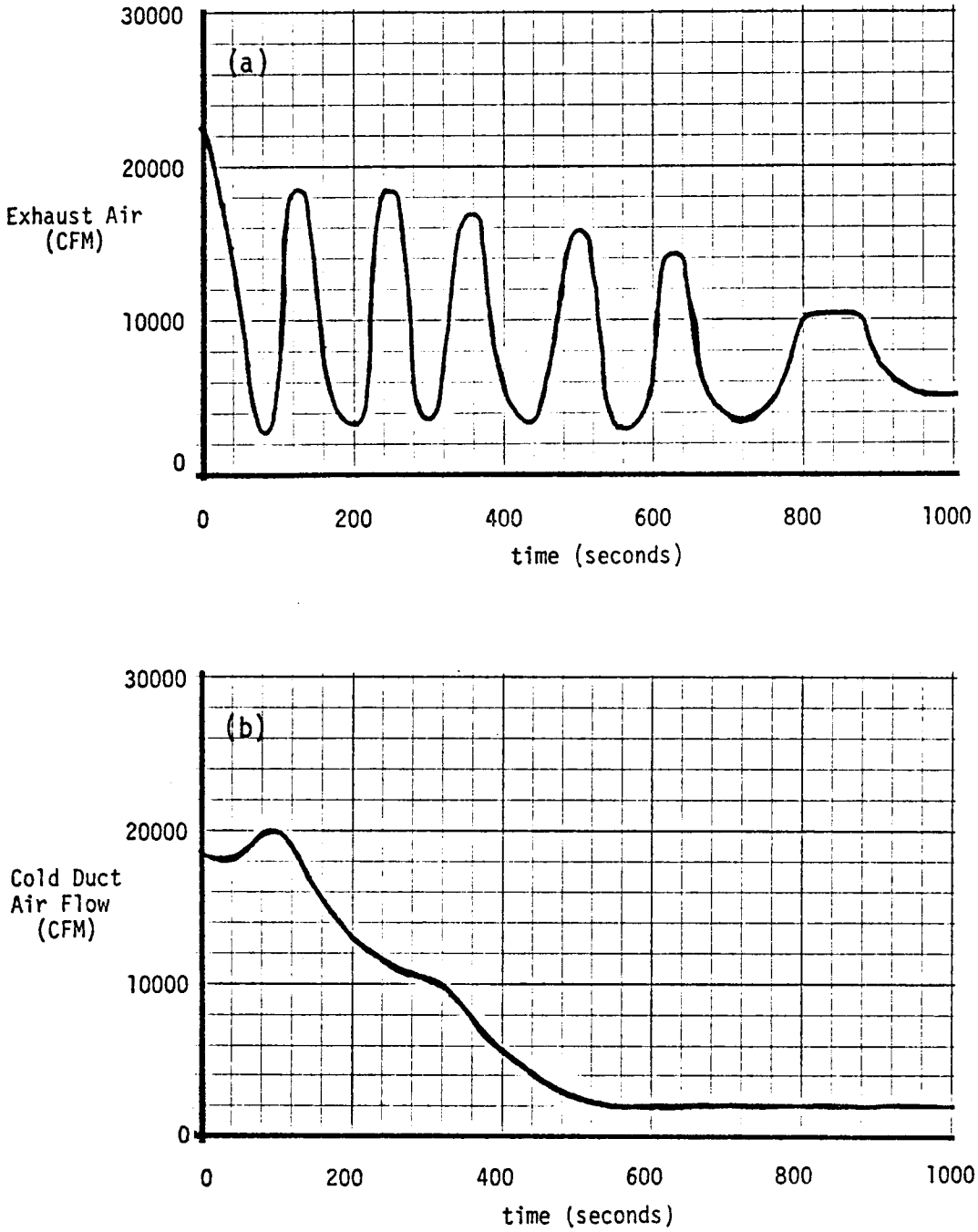


Figure 5.5. Air flows for the modified system in winter.

The cold duct air flows, shown in Figure 5.4(b) and Figure 5.5(b), indicate that less cooling is needed in the modified system because the hot duct is off. Comparison of Figures 5.6(a) and 5.7(a) shows that the transient responses of cold air entering the zones (both the modified and original system) are very similar even though T_{cold} in the modified system is highly oscillatory. Movement of cold air down the duct filters out the high frequency components in the T_{cold} time response.

This same filtering effect is illustrated in Figure 5.6(b). Although the hot duct temperature response is erratic, the time response of the hot air temperature after having moved down the duct is greatly smoothed. Figures 5.8 and 5.9 illustrate that the corresponding transient response of the return air temperature and the temperatures in zones four and five are very similar in both systems.

Figures 5.10 and 5.11 are of primary importance. The modified system is clearly more energy efficient than the original system. Examination of Tables 5.1 and 5.2 shows that the total energy use in the modified system is only 27% of that in the original system. However, Tables 5.3 and 5.4 indicate that the original system maintains the zone temperatures near their setpoint of 72F much more effectively than the modified system can maintain a 74F setpoint. With the hot duct off, the modified system has no adequate source of heated air to raise the zone temperatures. As a result, the simulated zone temperatures in steady state are as much as 7.3 degrees below the established setpoint.

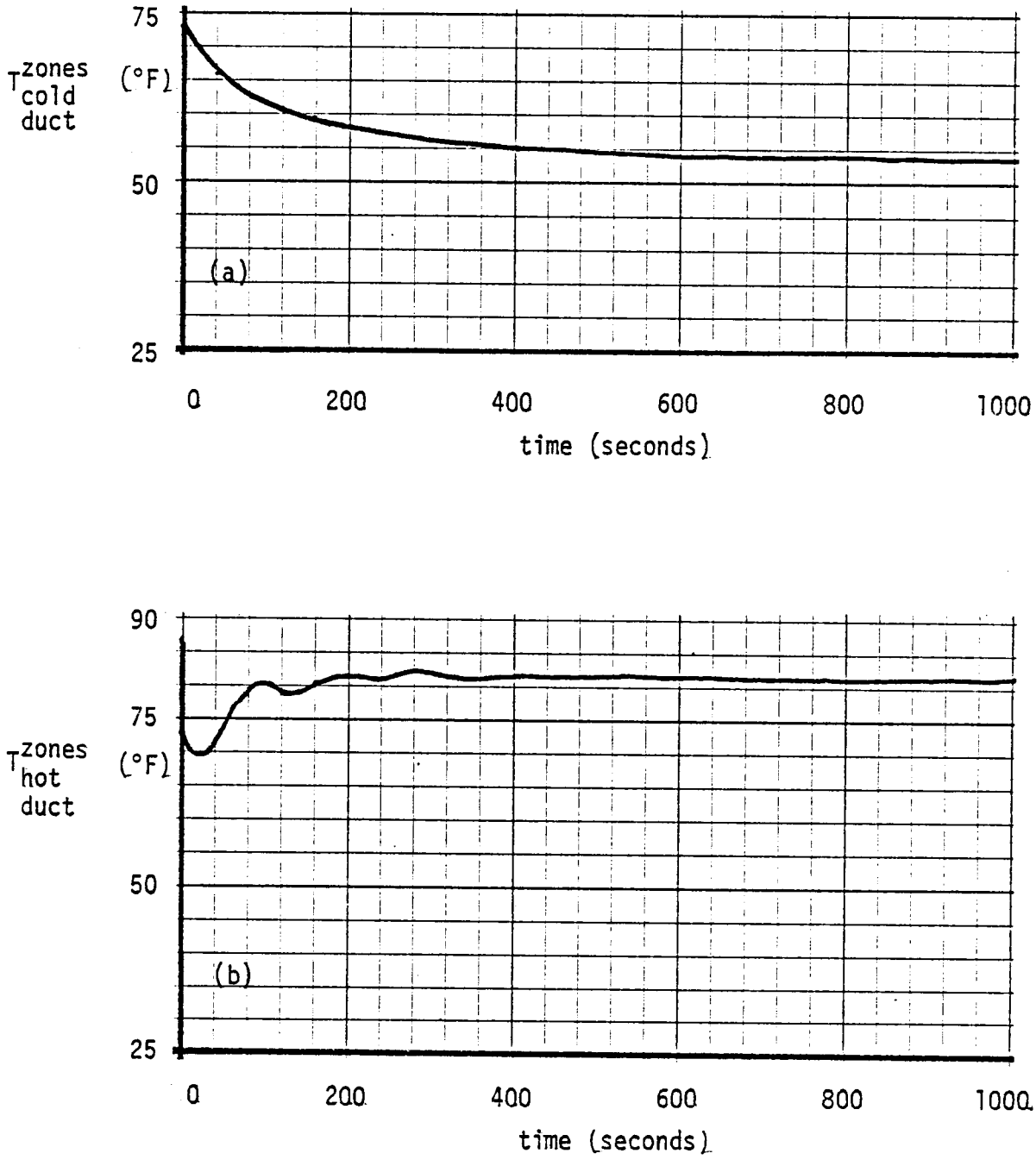
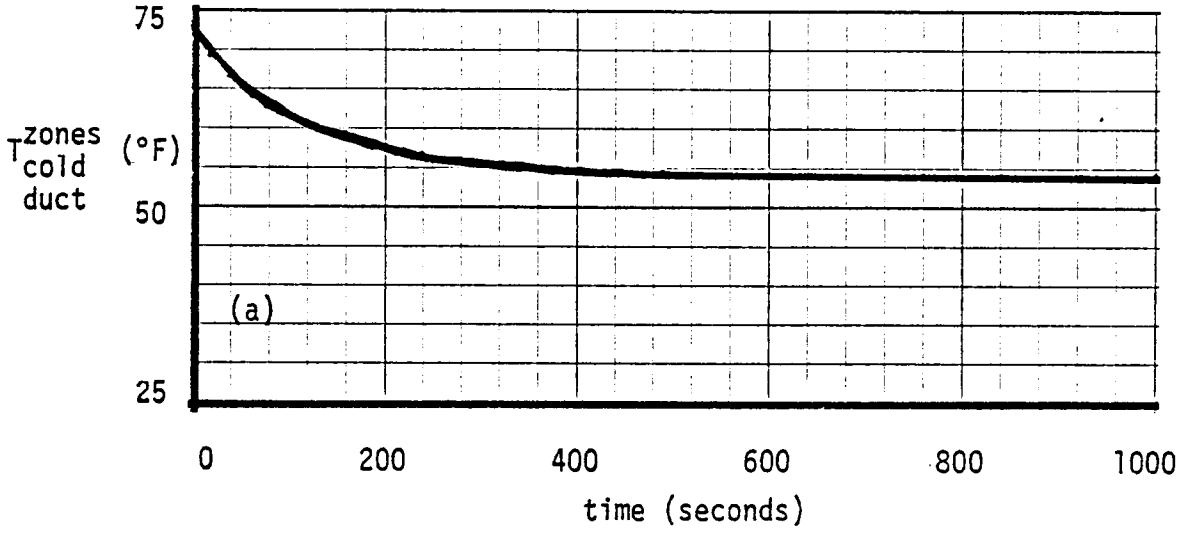


Figure 5.6. Midstream temperatures for the original system in winter.



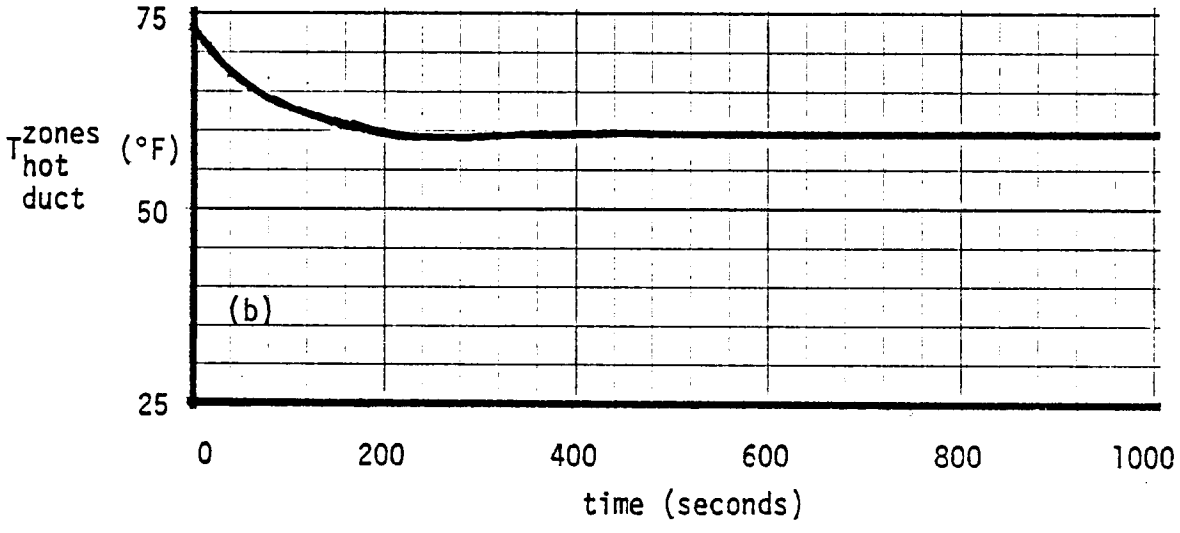


Figure 5.7. Midstream temperatures for the modified system in winter.

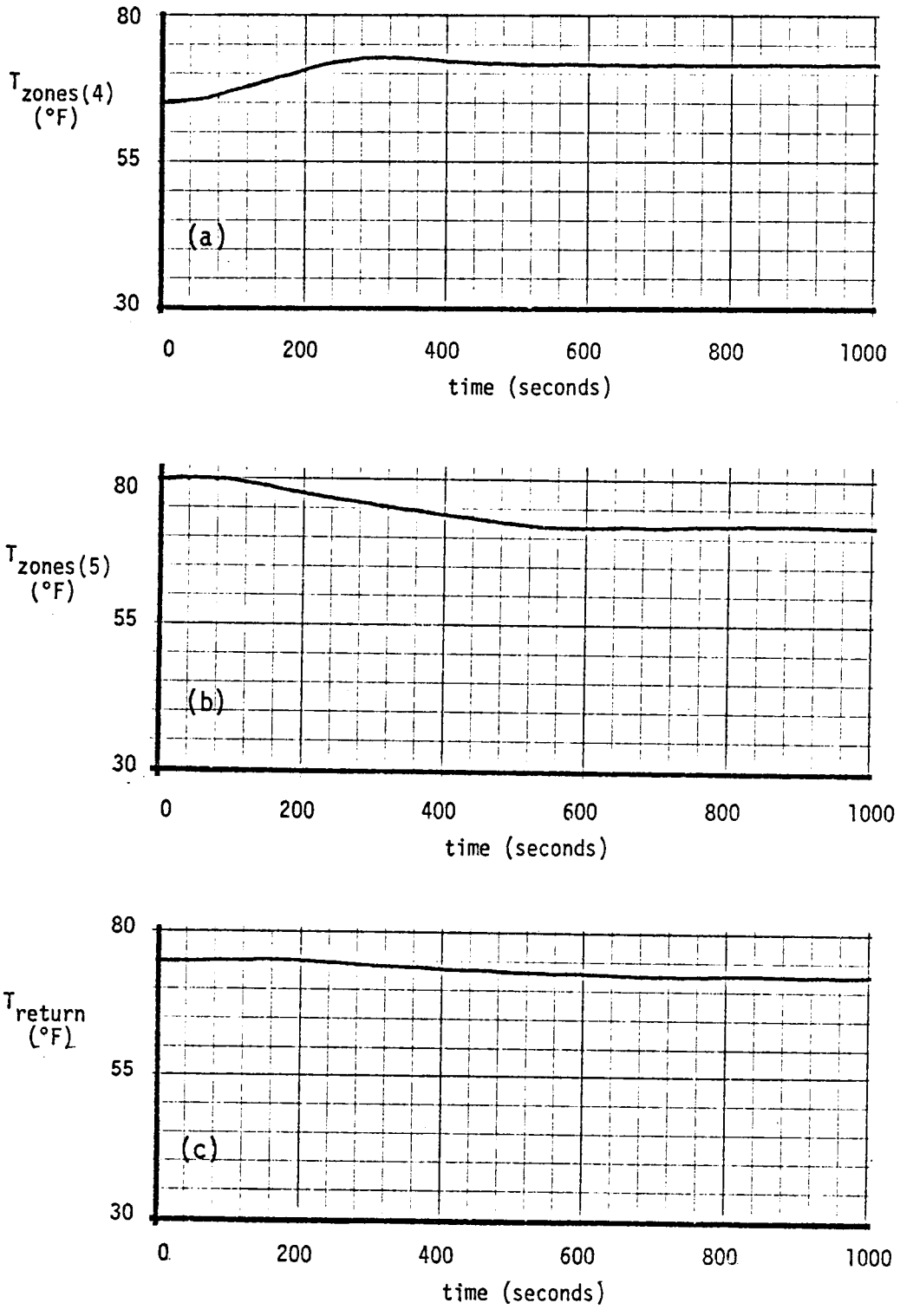


Figure 5.8. Downstream temperatures for the original system in winter.

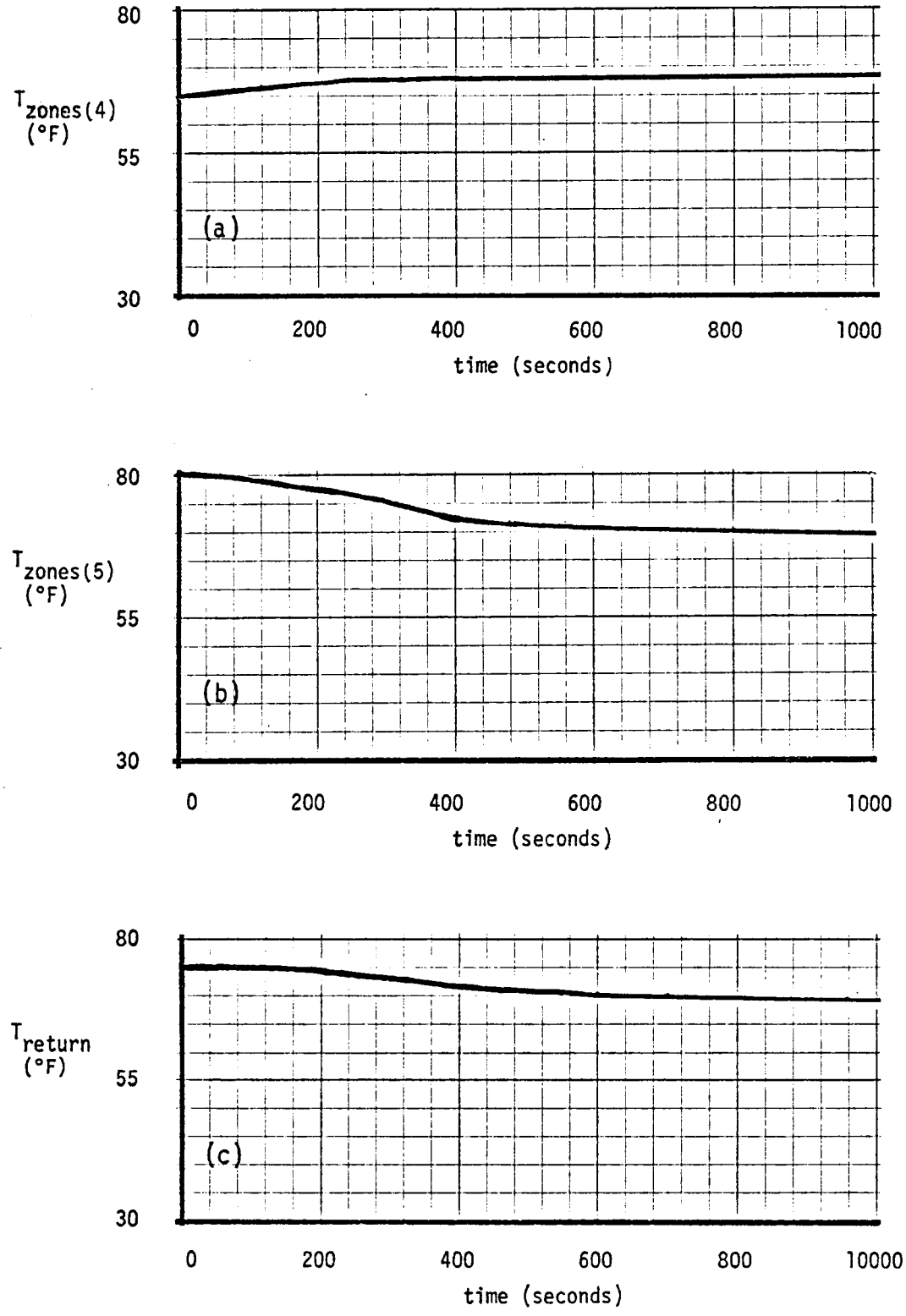


Figure 5.9. Downstream temperatures for the modified system in winter.

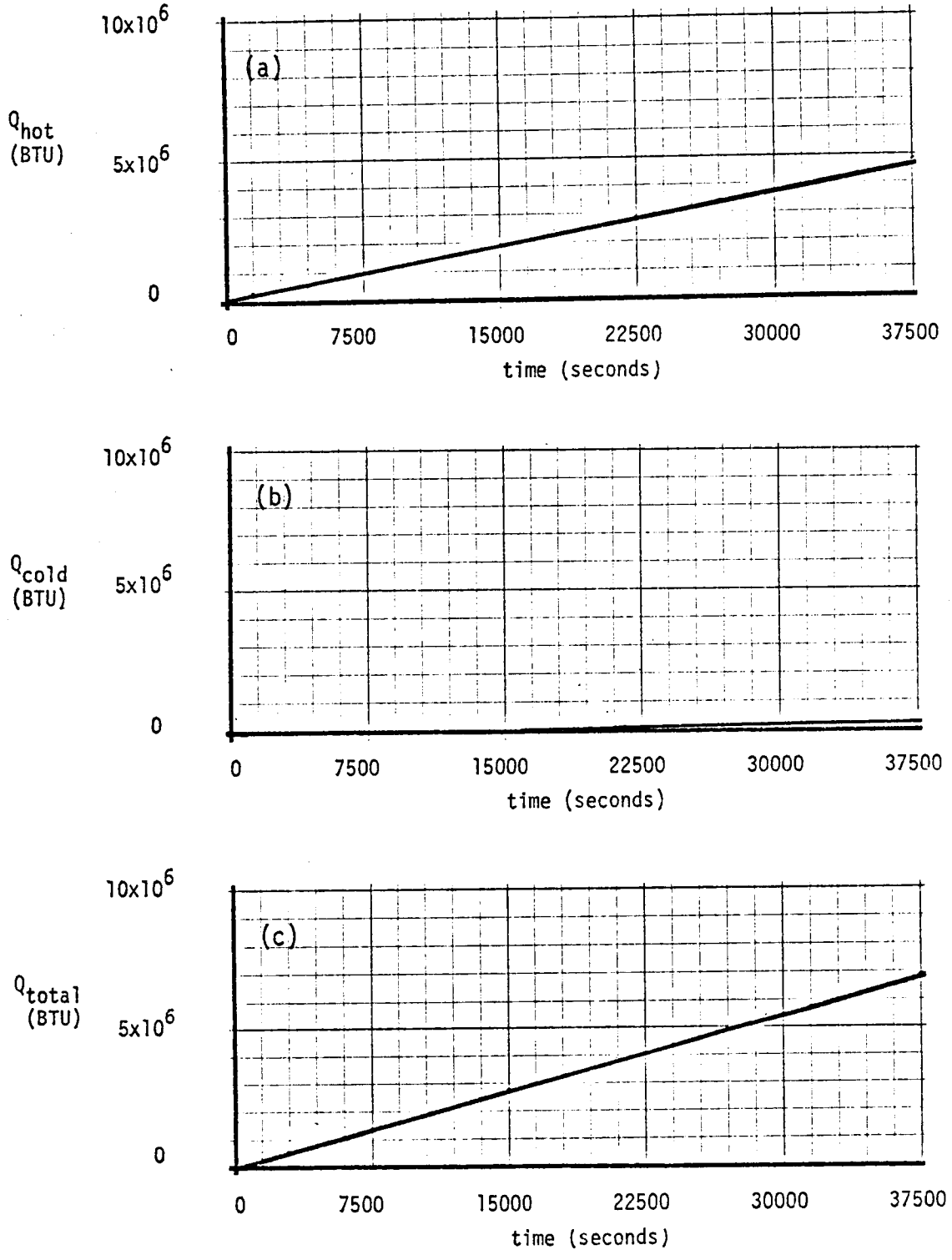


Figure 5.10. Energy use for the original system in winter.

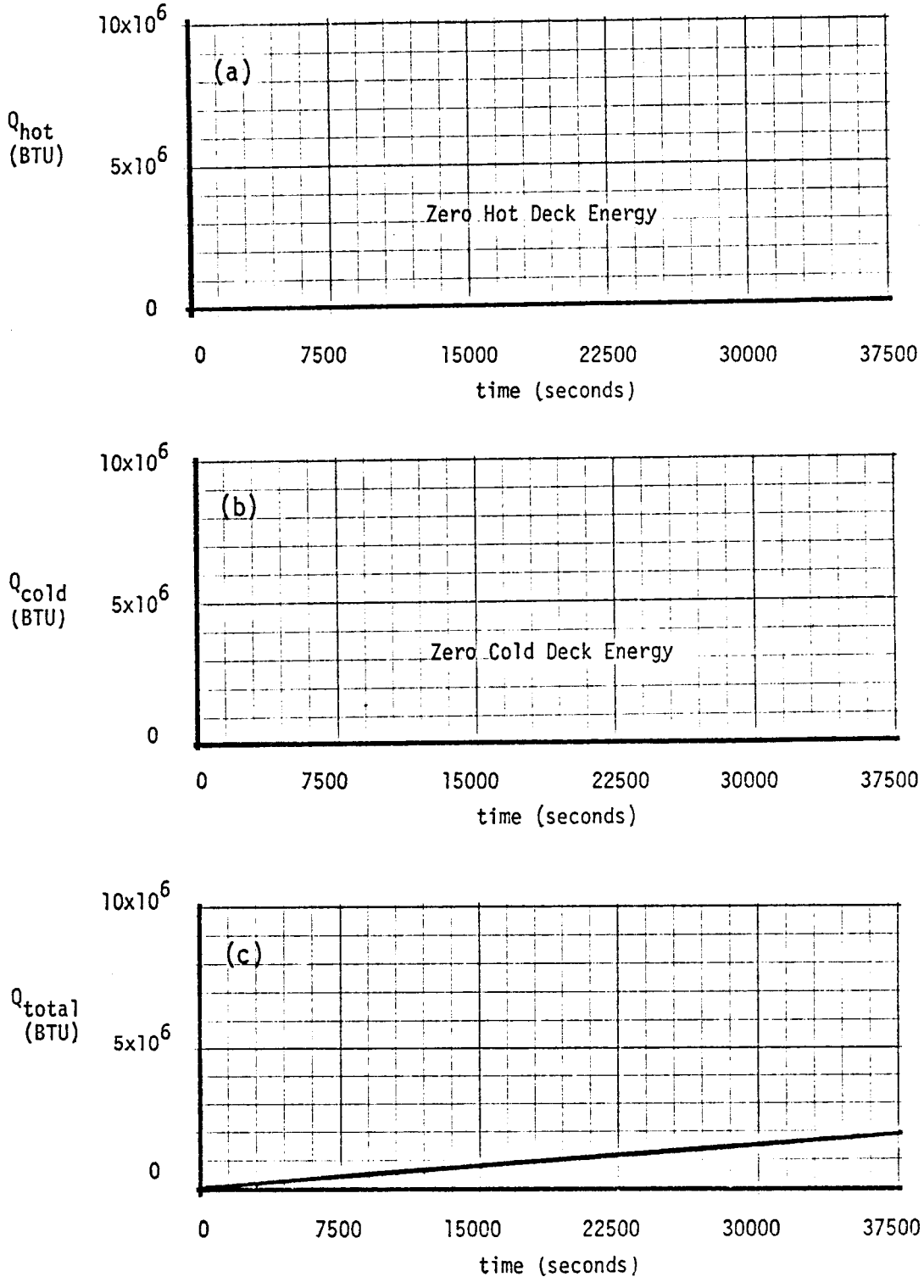


Figure 5.11. Energy use for the modified system in winter.

Table 5.1. Responses for the original system in winter.

	Starting	High Value	Time of High Value (sec)	Low Value	Time of Low Value (sec)	Final Value	Time of Steady State (sec)
TCOLD (°F)	22.2	52.6	105	22.2	0	51.4	375
THOT (°F)	24.5	114.5	54	24.5	0	84.7	678
TSUP (°F)	22.2	57.4	18	22.2	0	52.9	420
EXH (ft^3/min)	20283.	20283.	0	2574.	21	10626	591
FLOWH (ft^3/min)	8368	13753	960	6113	120	12786	840
FLOWC (ft^3/min)	30292	32547	120	24907	960	25874	810
TOUT (°F)	-2	22	27000	-2	0	22	NA
WOD (lbm/lbm)	.0010	.0018	30600	.001	0	.0018	NA
TRTN (°F)	74.8	75	90	73.2	720	73.3	600
WRTN (lbm/lbm)	.0093	.0093	0	.0017	360	.0023	360
QCOLD (BTUs)	0	$.272x10^6$	37800	0	0	$.272x10^6$	NA
QHOT (BTUs)	0	$4.83x10^6$	37800	0	0	$4.83x10^6$	NA
QTOTAL (BTUs)	0	$6.97x10^6$	37800	0	0	$6.97x10^6$	NA
TCLZ (°F)	73.3	73.3	0	54.1	768	55.2	726
THTZ (°F)	72.9	82.4	282	69.6	18	81.2	630

Table 5.2. Responses for the modified system in winter.

	Starting	High Value	Time of High Value (sec)	Low Value	Time of Low Value (sec)	Final Value	Time of Steady State (sec)
TCOLD (°F)	23.6	55.4	93	23.6	0	50.5	1311
THOT (°F)	23.6	62.3	108	23.6	0	52.9	1299
TSUP (°F)	23.6	62.3	180	23.6	0	52.9	1299
EXH (ft^3/min)	22334	22334	0	2905	21	11854	1329
FLOWH (ft^3/min)	20251	36727	510	18424	90	36727	510
FLOWC (ft^3/min)	18409	20236	90	1933	510	1933	510
TOUT (°F)	-2	22.0	27000	-2	0	22.0	NA
WOD (lbm/lbm)	.0010	0.0018	30600	.0010	0	0.0018	NA
TRTN (°F)	74.7	74.9	84	68.8	1350	69.9	1350
WRTN (lbm/lbm)	.0093	.0093	0	.0016	240	.0024	810
QCOLD (BTUs)	0	3.596×10^4	37800	0	0	3.596×10^4	NA
QHOT (BTUs)	0	0	0	0	0	0	NA
QTOTAL (BTUs)	0	1.907×10^6	37800	0	0	1.907×10^6	NA
TCLZ (°F)	73.4	73.4	0	54.1	630	54.4	768
THTZ (°F)	72.9	72.9	0	58.1	372	60.8	1116

Table 5.3. Zone responses for the original system in winter.

	Starting Temperature °F	Lowest Temperature °F	Time of Low Value (seconds)	Steady State Temperature °F	Time of Steady State (seconds)
TZONE(1)	78.0	72.4	630	72.5	630
WZ(1)	0.0093	0.0018	330	0.0024	330
TZONE(2)	74.3	72.4	450	72.5	450
WZ(2)	0.0093	0.0018	330	0.0024	330
TZONE(3)	73.1	72.3	540	72.4	540
WZ(3)	0.0093	0.0017	390	0.0024	390
TZONE(4)	65.0	65.0	0	72.4	510
WZ(4)	0.0093	0.0017	390	0.0024	390
TZONE(5)	80.0	72.2	540	72.4	570
WZ(5)	0.0093	0.0017	450	0.0024	390
TZONE(6)	72.0	72.0	0	72.2	600
WZ(6)	0.0092	0.0016	420	0.0023	420
TZONE(7)	74.8	72.1	270	72.2	540
WZ(7)	0.0092	0.0016	420	0.0023	420
TZONE(8)	74.0	72.1	630	72.2	630
WZ(8)	0.0092	0.0016	420	0.0023	420
TZONE(9)	74.0	72.5	366	72.5	366
WZ(9)	0.0094	0.0018	324	0.0024	324

Table 5.4. Zone responses for the modified system in winter.

	Starting Temperature °F	Lowest Temperature °F	Time of Low Value (seconds)	Steady State Temperature °F	Time of Steady State (seconds)
TZONE(1)	78.0	70.4	1530	71.3	1380
WZ(1)	.0093	.0017	300	.0025	810
TZONE(2)	74.3	70.3	1380	71.3	1380
WZ(2)	.0093	.0016	300	.0025	810
TZONE(3)	73.1	68.3	1440	69.4	1320
WZ(3)	.0093	.0015	270	.0024	930
TZONE(4)	65.0	65.0	0	69.4	600
WZ(4)	.0093	.0015	270	.0024	867
TZONE(5)	80.0	68.5	1500	69.4	1500
WZ(5)	.0093	.0016	360	.0024	930
TZONE(6)	72.0	65.4	1320	66.7	1170
WZ(6)	.0092	.0014	300	.0023	900
TZONE(7)	74.8	65.4	1380	66.7	1260
WZ(7)	.0092	.0014	300	.0023	900
TZONE(8)	74.0	65.4	1350	66.7	1230
WZ(8)	.0092	.0014	300	.0023	900
TZONE(9)	74.0	69.6	456	71.5	948
WZ(9)	.0094	.0016	216	.0025	834

Simulation of Spring Operation. Figure 5.12 reveals the approximations used to represent a typical day in the spring. The corresponding transient responses of the cold duct, hot duct, and supply air temperature in the original and modified system are similar, as shown by Figures 5.13 and 5.14. Figures 5.15 and 5.16 show that while the transient exhaust flows in both systems are similar, the transient cold duct flow in the original system is much greater than in the modified system. The transient temperature responses of cold air entering the zones, shown in Figures 5.17(a) and 5.18(a), are practically identical in both systems.

Since the hot duct remains operative in the original system, the temperature of the hot air entering the zone in Figure 5.17(b) is greater than in Figure 5.18(b). Temperature responses of the return air and zones four and five in both systems (Figures 5.19 and 5.20) are comparable.

Inspection of Figures 5.21 and 5.22 discloses that the modified system also uses less energy than the original system on a typical spring day. Tables 5.5 and 5.6 reveal that only 45% of the original total system energy is required by the modified system. Tables 5.7 and 5.8 show that both systems maintain the steady-state zone temperatures close to their respective setpoints.

Simulation of Summer Operation. Figure 5.23 illustrates the approximate conditions of an average day in summer. Figures 5.24 and 5.25 exhibit that in both systems, the transient responses of the matching cold duct, hot duct, and return air temperatures are nearly alike.

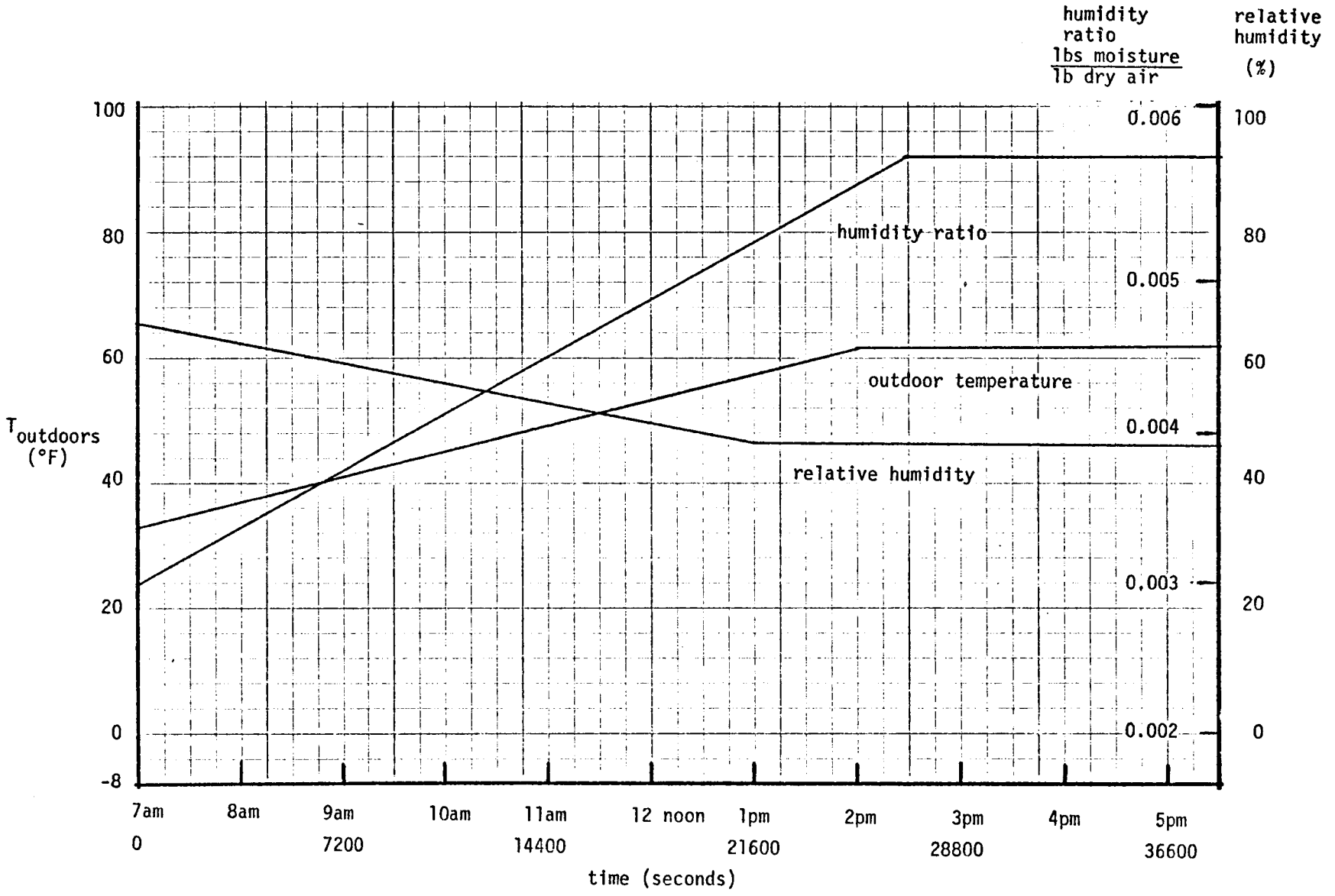


Figure 5.12. Approximate outside air conditions in spring.

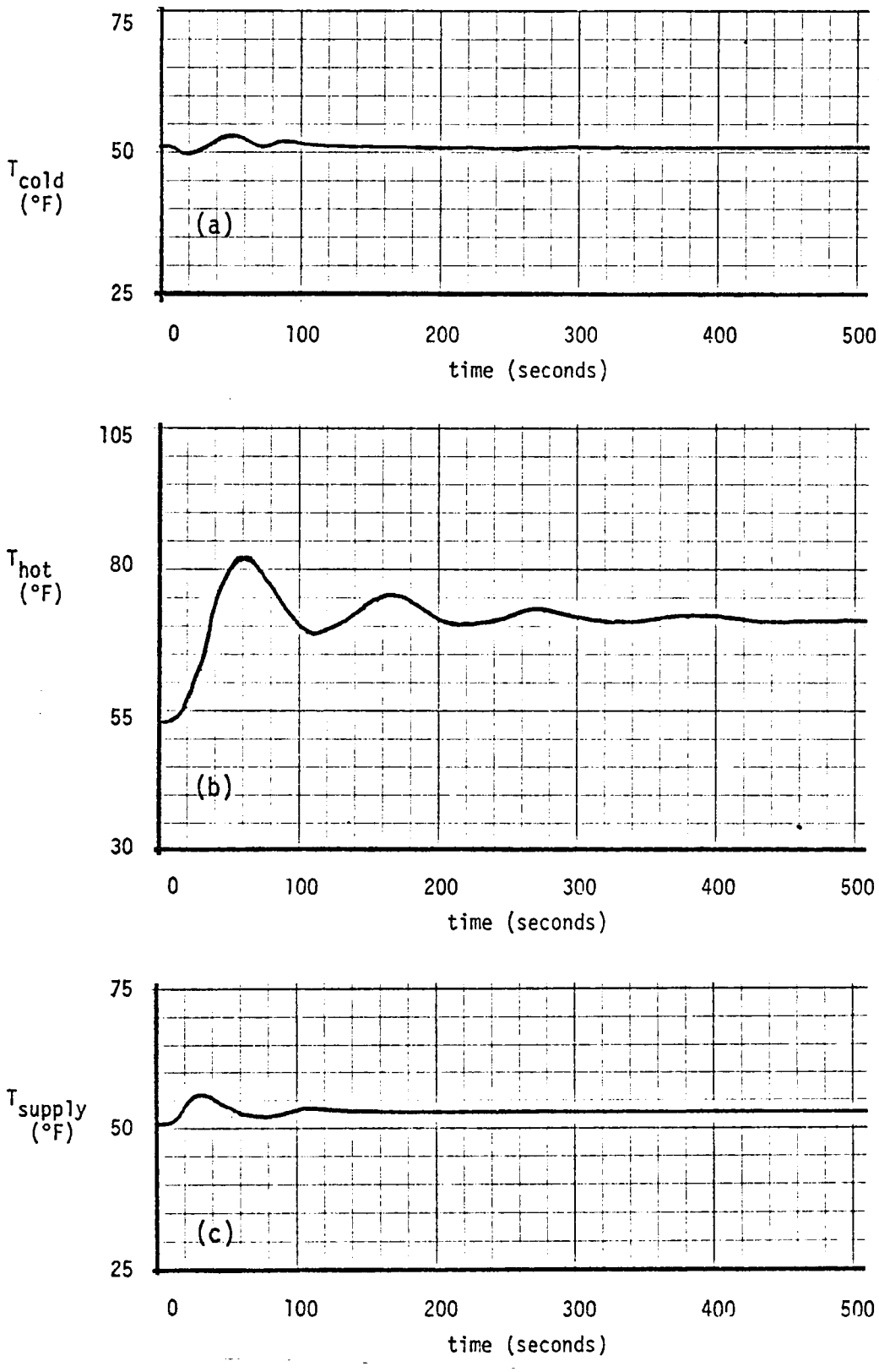


Figure 5.13. Upstream temperatures for the original system in spring.

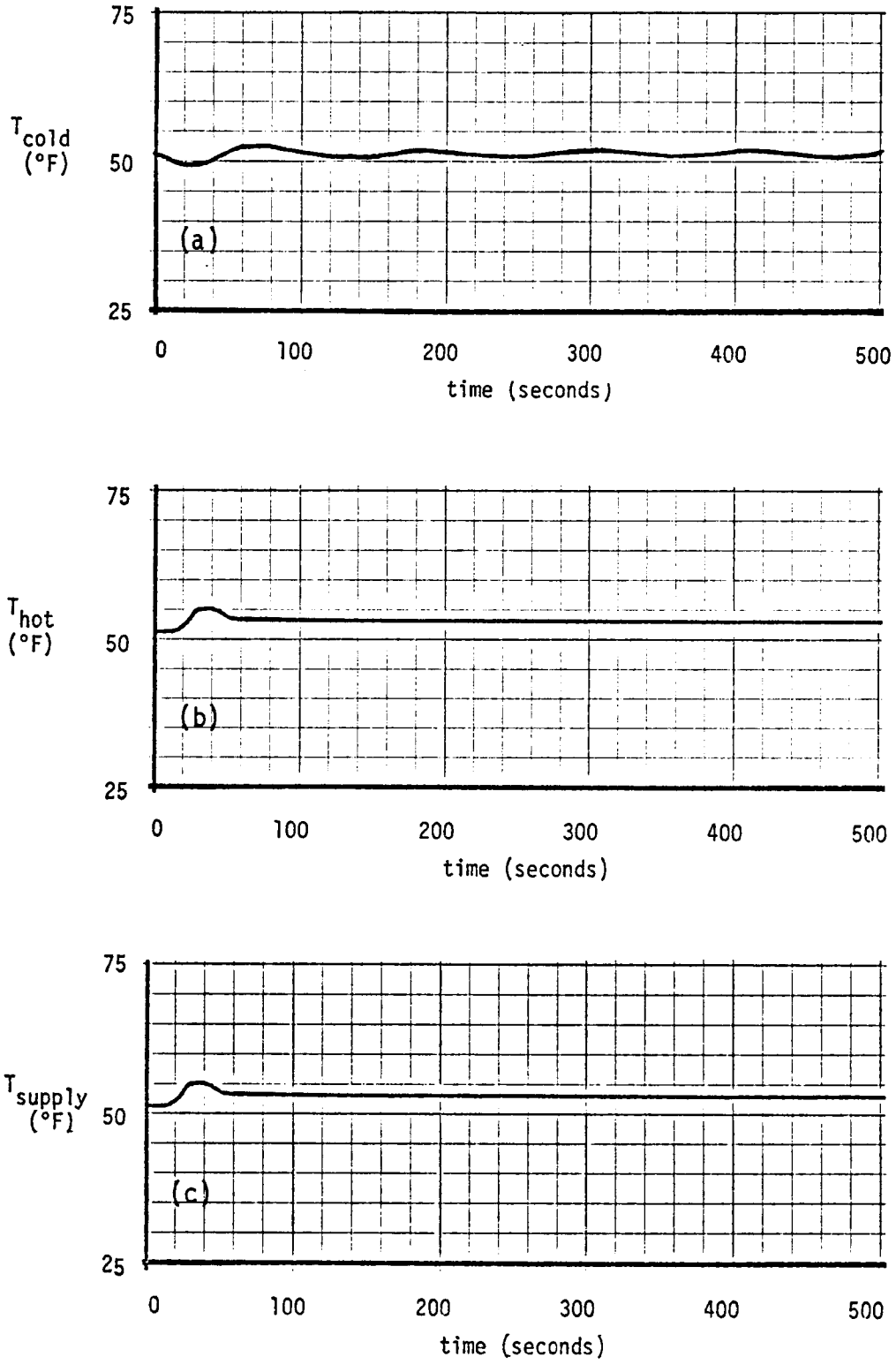


Figure 5.14. Upstream temperatures for the modified system in spring.

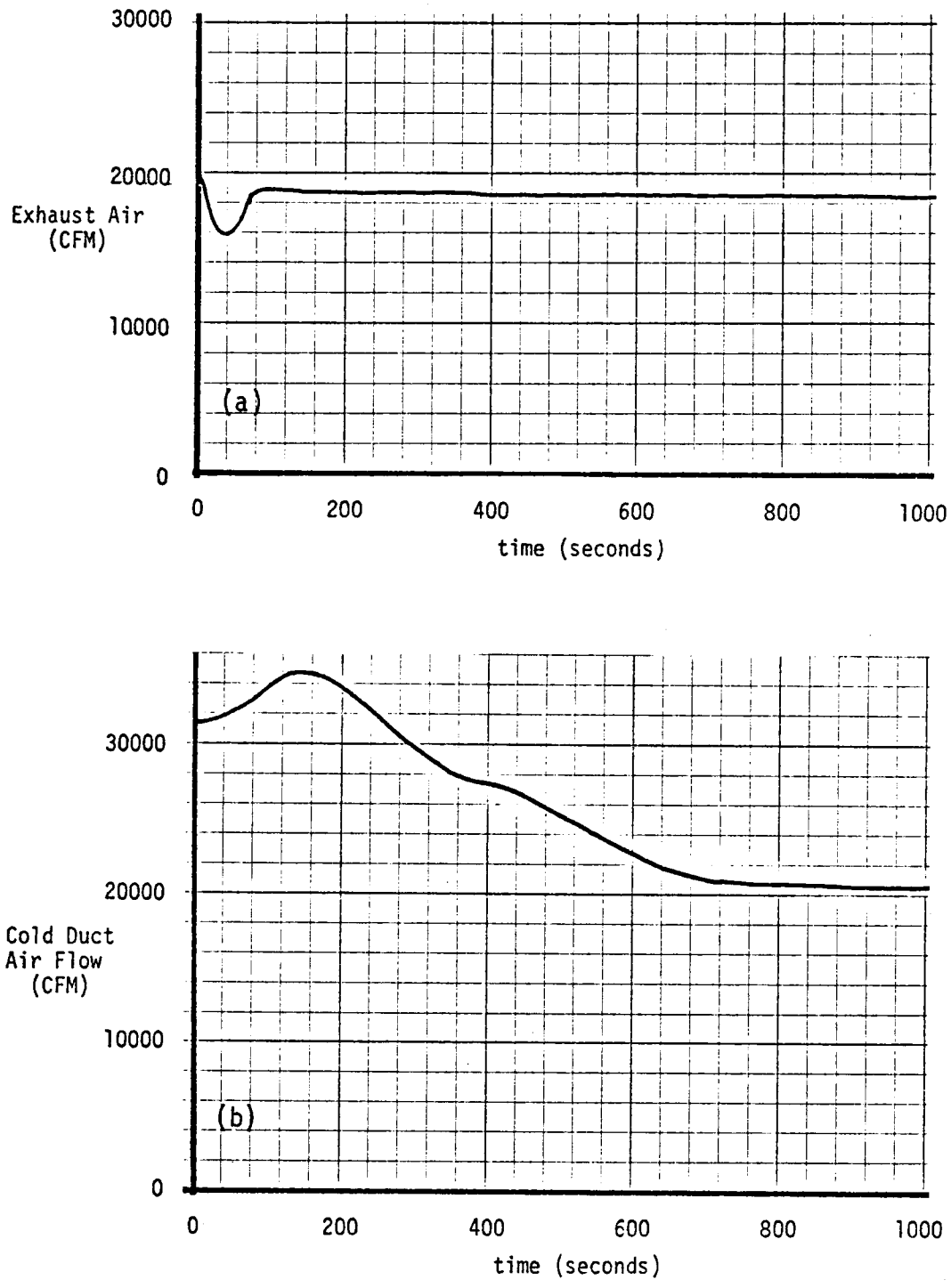


Figure 5.15. Air flows for the original system in spring.

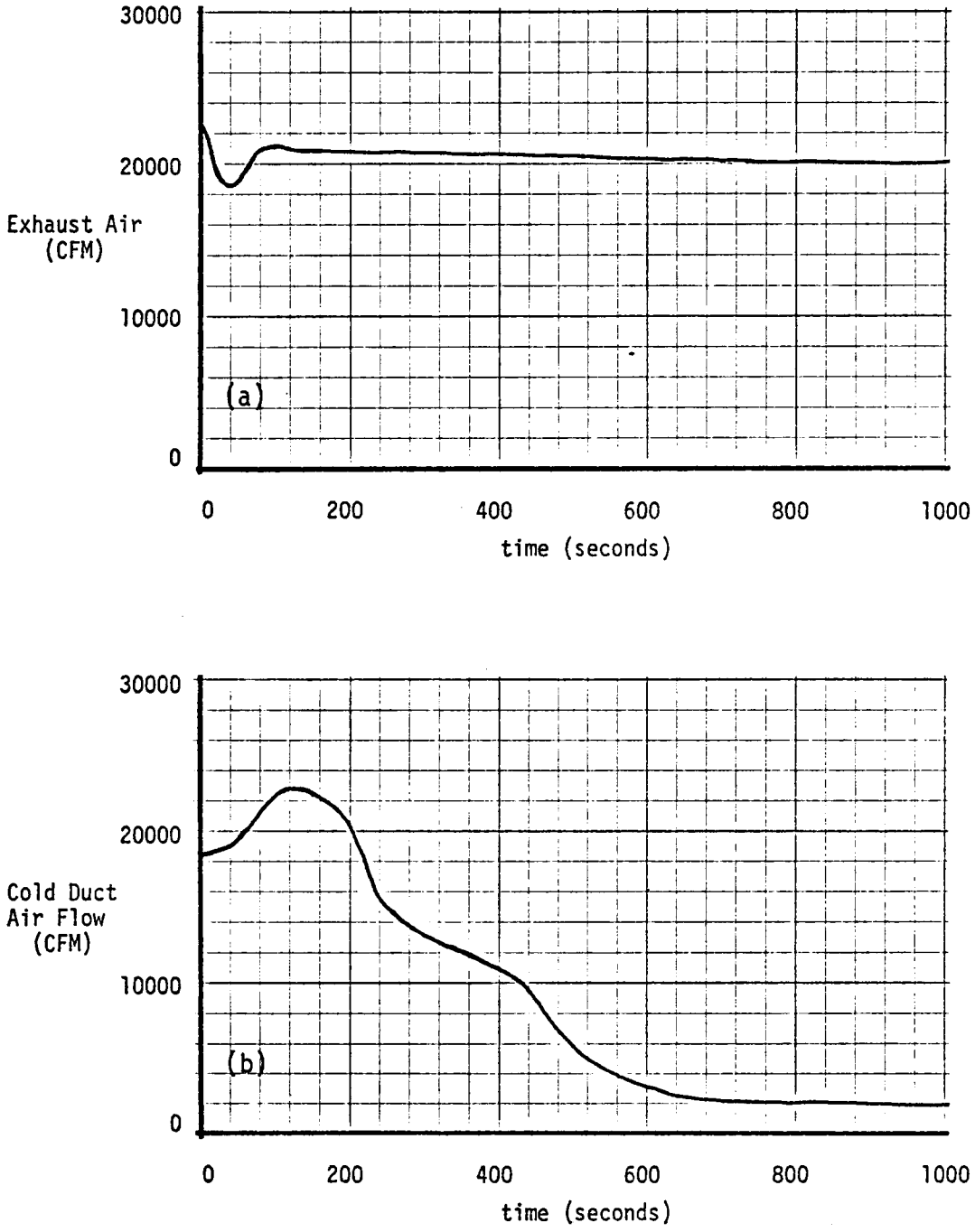


Figure 5.16. Air flows for the modified system in spring.

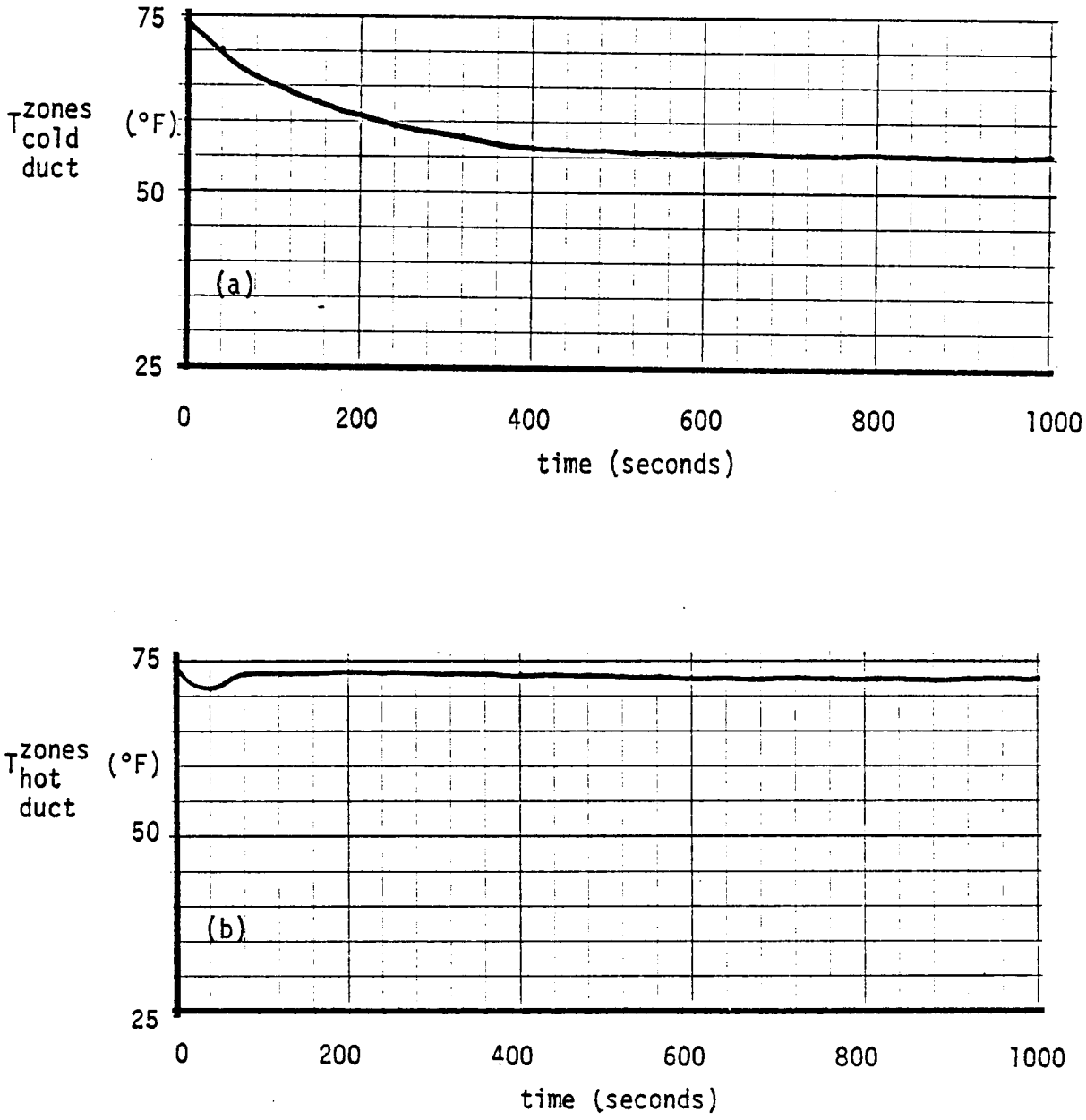


Figure 5.17. Midstream temperatures for the original system in spring.

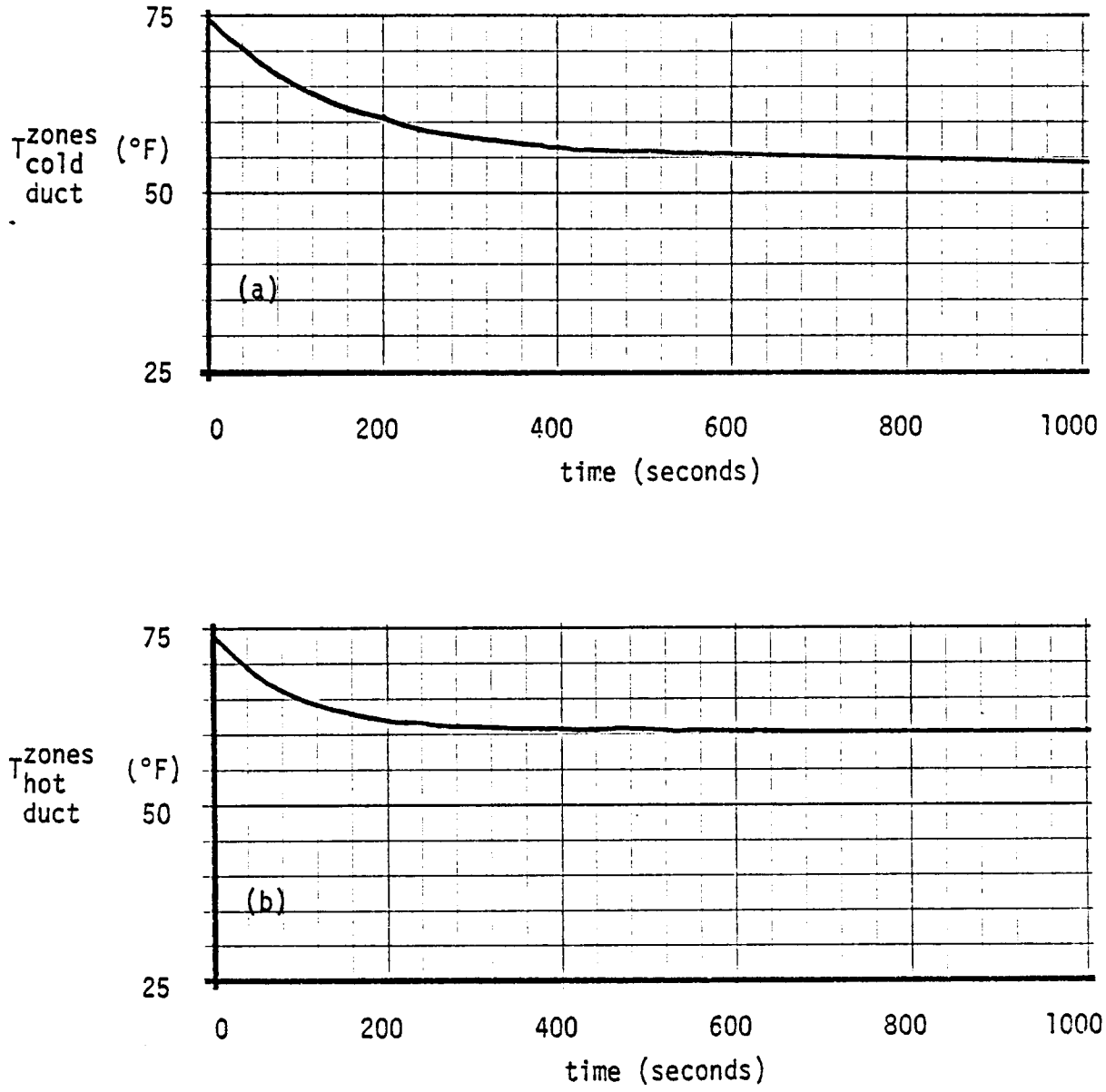
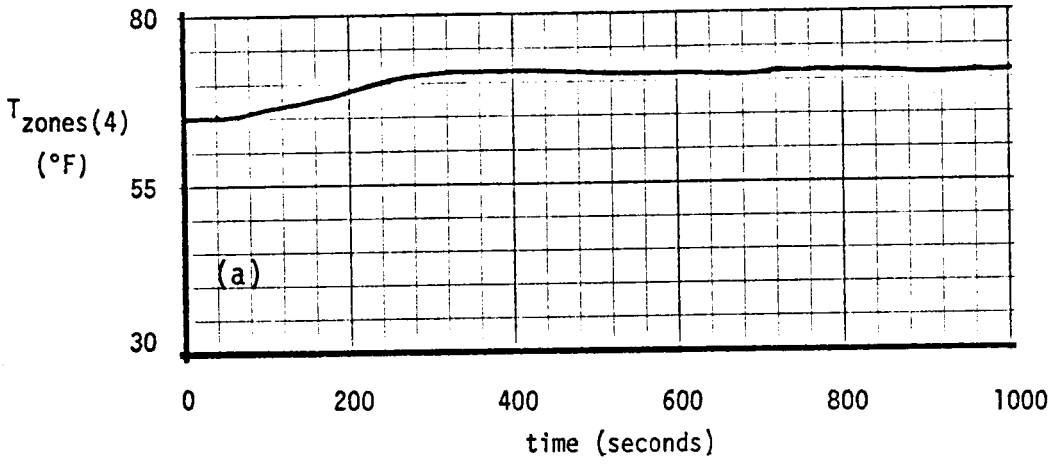
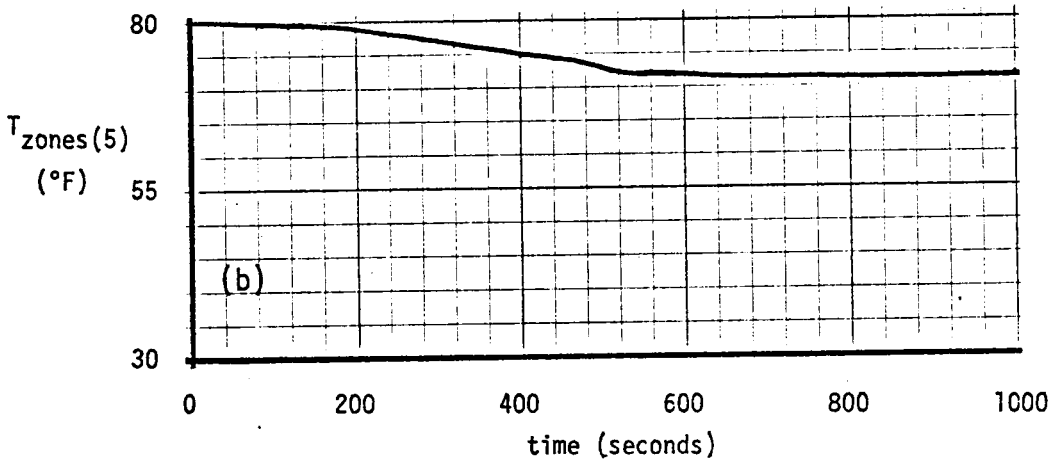


Figure 5.18. Midstream temperatures for the modified system in spring.





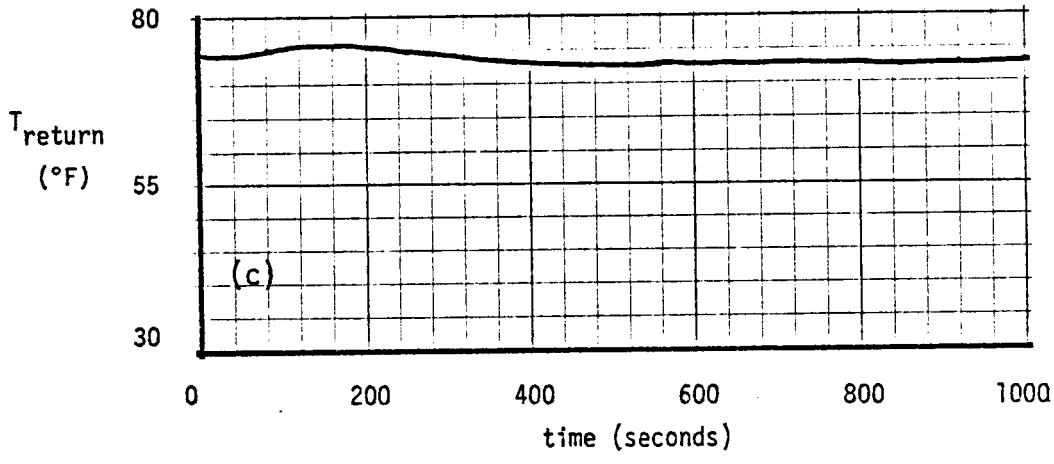


Figure 5.19. Downstream temperatures for the original system in spring.

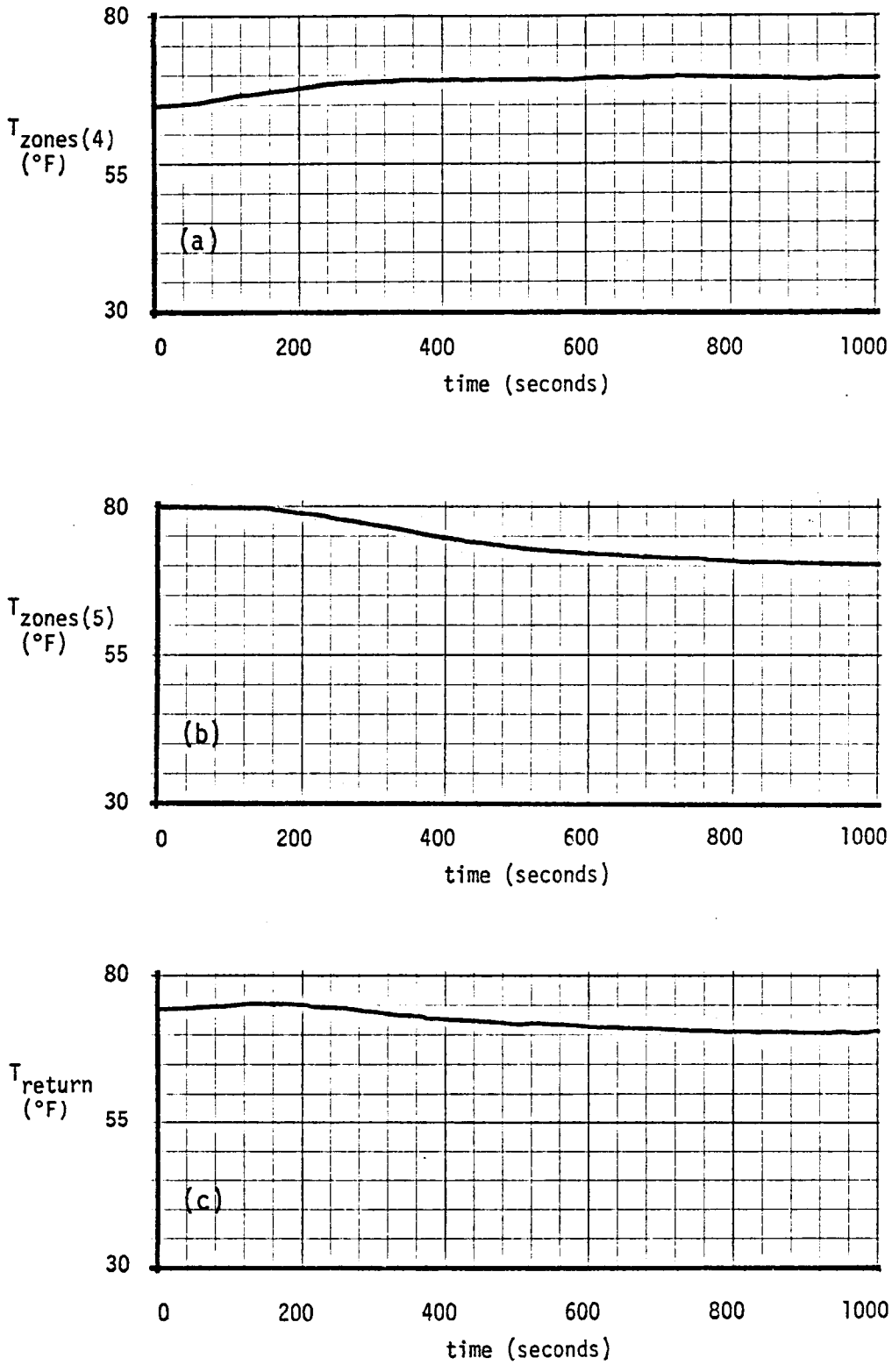


Figure 5.20. Downstream temperatures for the modified system in spring.

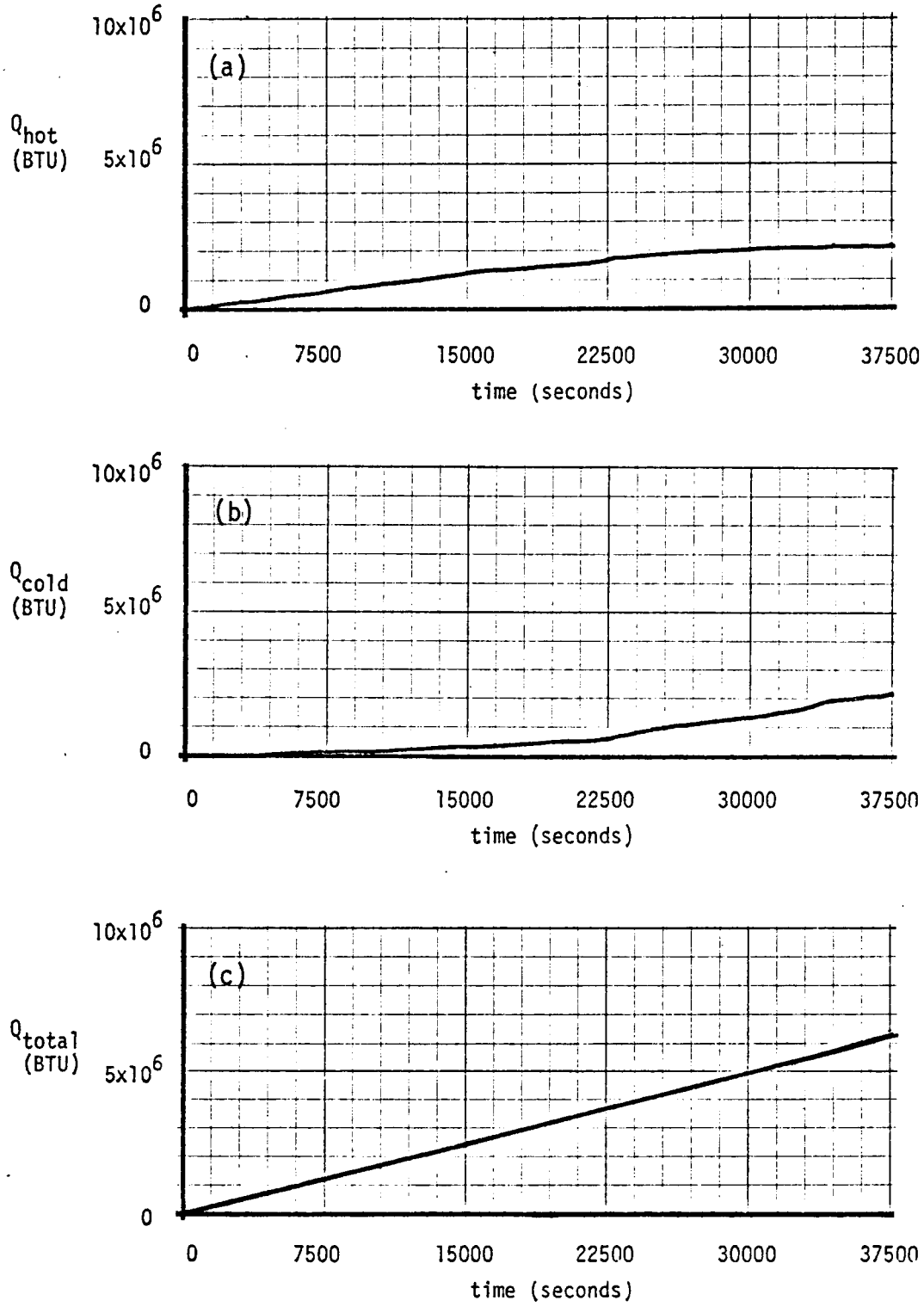


Figure 5.21. Energy use for the original system in spring.

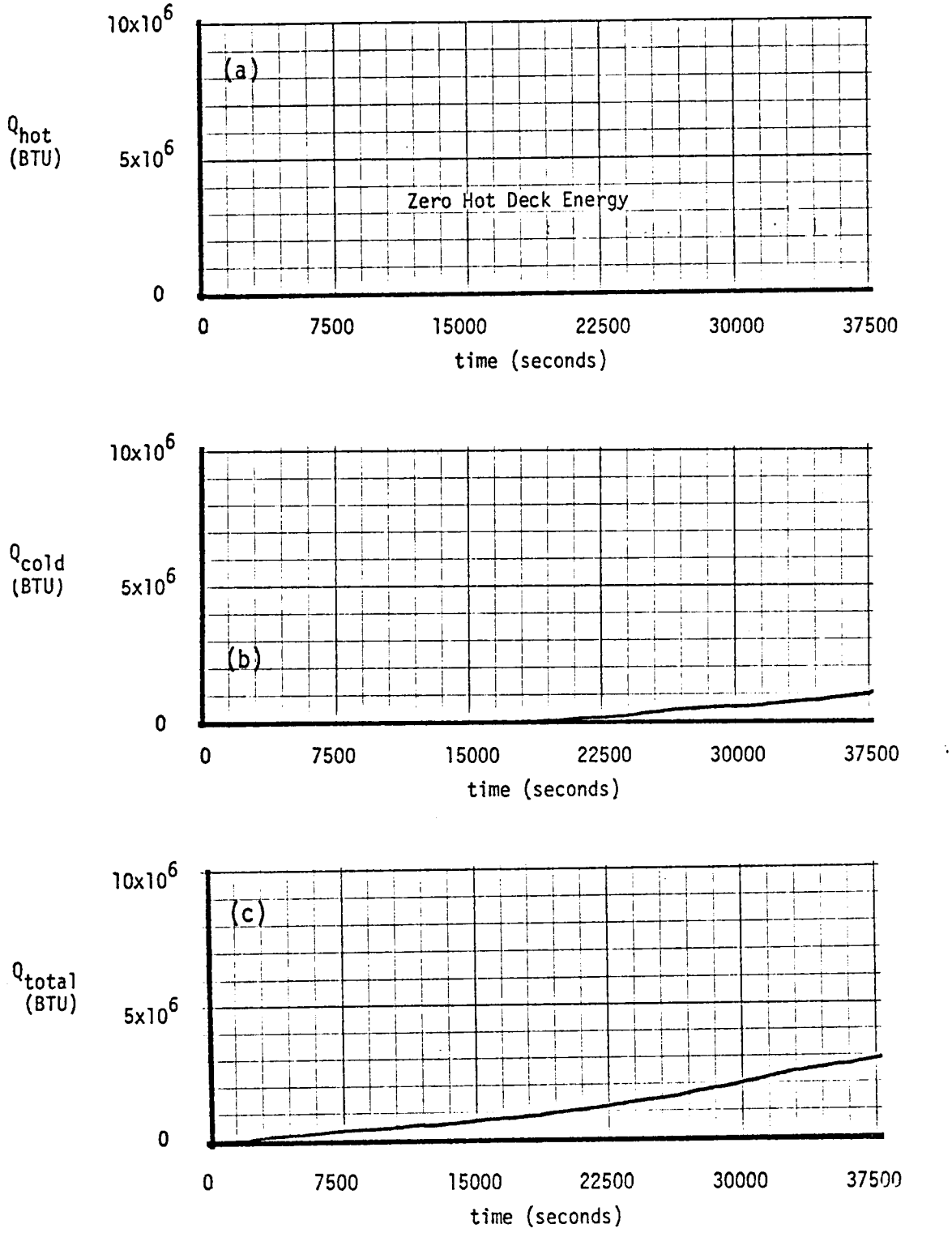


Figure 5.22. Energy use for the modified system in spring.

Table 5.5. Responses for the original system in spring.

	Starting	High Value	Time of High Value (sec)	Low Value	Time of Low Value (sec)	Final Value	Time of Steady State (sec)
TCOLD (°F)	51	51.1	25500	49.6	21	55.1	462
THOT (°F)	53.7	82.4	63	53.7	0	79.1	402
TSUP (°F)	51.0	67.6	28500	51.0	0	67.6	660
EXH (ft^3/min)	20282.	29660.	18300	6104	27	29660.	564
FLOWH (ft^3/min)	7150	18101.	990	3959	120	11196	780
FLOWC (ft^3/min)	31510	34701	120	20559	990	27464	870
TOUT (°F)	36.0	62	25200	36.0	0	62.0	NA
WOD (lbm/lbm)	.0030	.0058	26700	.0030	0	.0058	NA
TRTN (°F)	74.8	75.5	120	73.0	6.60	73.4	660
WRTN (lbm/lbm)	.0093	.0093	0	.0034	150	.0061	630
QCOLD (BTUs)	0	2.27×10^6	37800	0	0	2.27×10^6	NA
QHOT (BTUs)	0	2.316×10^6	37800	0	0	2.316×10^6	NA
QTOTAL (BTUs)	0	6.457×10^6	37800	0	0	6.457×10^6	NA
TCLZ (°F)	74.2	74.2	0	55.3	873	58.3	588
THTZ (°F)	74.1	77.6	37800	70.8	36	77.6	672

Table 5.6. Responses for the modified system in spring.

	Starting	High Value	Time of High Value (sec)	Low Value	Time of Low Value (sec)	Final Value	Time of Steady State (sec)
TCOLD (°F)	51.4	60.2	22200	49.1	24	53.6	687
THOT (°F)	51.4	67.1	25200	51.4	0	67.1	690
TSUP (°F)	51.4	67.1	25500	51.4	0	67.1	660
EXH (ft^3/min)	22334	32660	18600	18751	27	32660	744
FLOWH (ft^3/min)	20251	36727	690	15672	120	24478	690
FLOWC (ft^3/min)	18409	22988	120	1933	690	14182	690
TOUT (°F)	36.0	62.0	25200	36.0	0	62.0	NA
WOD (lbm/lbm)	.0030	.0058	26700	.0030	0	.0058	NA
TRTN (°F)	74.7	75.3	90	70.1	1590	74.6	693
WRTN (lbm/lbm)	.0093	.0093	0	.0034	150	.0061	510
QCOLD (BTUs)	0	$1x10^6$	37800	0	0	$1x10^6$	NA
QHOT (BTUs)	0	0	0	0	0	0	NA
QTOTAL (BTUs)	0	$2.9x10^6$	37800	0	0	$2.9x10^6$	NA
TCLZ (°F)	74.3	74.3	0	54.5	1044	57.0	918
THTZ (°F)	74.0	74.0	0	60.8	672	69.9	672

Table 5.7. Zone responses for the original system in spring.

	Starting Temperature °F	Lowest Temperature °F	Time of Low Value (seconds)	Steady State Temperature °F	Time of Steady State (seconds)
TZONE(1)	78.0	72.3	690	72.6	690
WZ(1)	.0093	.0035	150	.0061	150
TZONE(2)	74.3	72.3	570	72.6	510
WZ(2)	.0093	.0035	150	.0061	150
TZONE(3)	73.1	72.1	570	72.5	570
WZ(3)	.0093	.0034	150	.0061	540
TZONE(4)	65.0	65	0	72.5	570
WZ(4)	.0093	.0034	150	.0061	540
TZONE(5)	80.0	72.1	600	72.5	570
WZ(5)	.0093	.0034	150	.0061	540
TZONE(6)	72.0	71.8	600	72.2	600
WZ(6)	.0092	.0033	180	.0060	420
TZONE(7)	74.8	71.8	600	72.2	600
WZ(7)	.0092	.0033	180	.0060	420
TZONE(8)	74.0	71.8	600	72.2	600
WZ(8)	.0092	.0033	180	.0060	420
TZONE(9)	74.0	72.3	588	72.7	390
WZ(9)	.0094	.0035	132	.0062	132

Table 5.8. Zone responses for the modified system in spring.

	Starting Temperature °F	Lowest Temperature °F	Time of Low Value (seconds)	Steady State Temperature °F	Time of Steady State (seconds)
TZONE(1)	78.0	71.6	1680	74.0	1350
WZ(1)	.0093	.0035	150	.0061	750
TZONE(2)	74.3	71.6	1770	74.0	1230
WZ(2)	.0093	.0035	150	.0061	750
TZONE(3)	73.1	69.7	1530	73.8	1530
WZ(3)	.0093	.0034	180	.0061	420
TZONE(4)	65.0	65.0	0	73.8	690
WZ(4)	.0093	.0034	180	.0061	420
TZONE(5)	80.0	69.7	2100	73.8	1200
WZ(5)	.0093	.0034	180	.0061	420
TZONE(6)	72.0	66.8	1530	73.4	1200
WZ(6)	.0092	.0033	210	.0060	300
TZONE(7)	74.8	70.1	1590	73.4	1260
WZ(7)	.0092	.0033	210	.0060	300
TZONE(8)	74.0	66.8	1560	73.4	1230
WZ(8)	.0092	.0033	210	.0060	300
TZONE(9)	74.0	71.5	930	74.1	930
WZ(9)	.0094	.0035	138	.0062	660

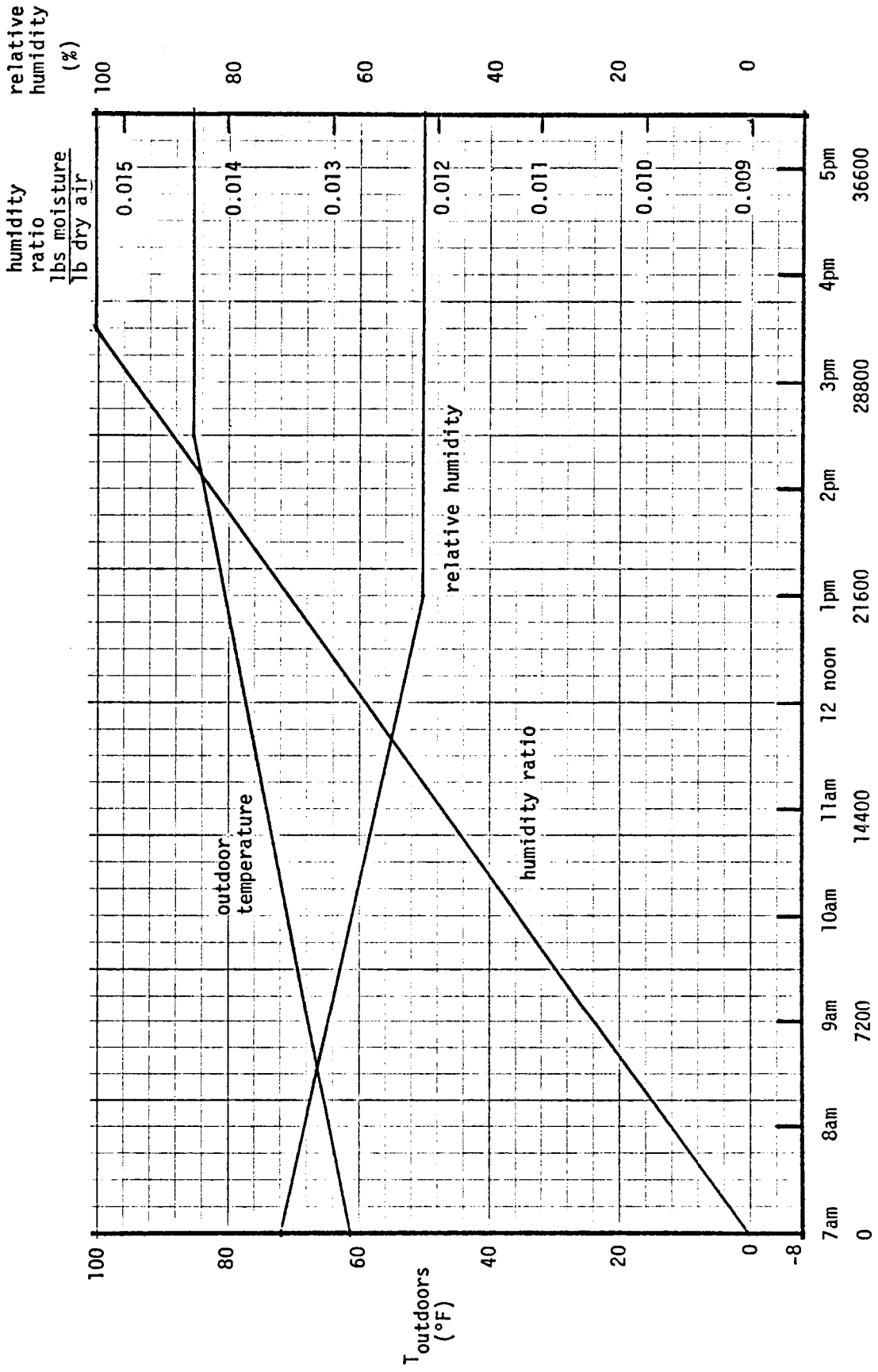


Figure 5.23. Approximate outside air conditions in summer.

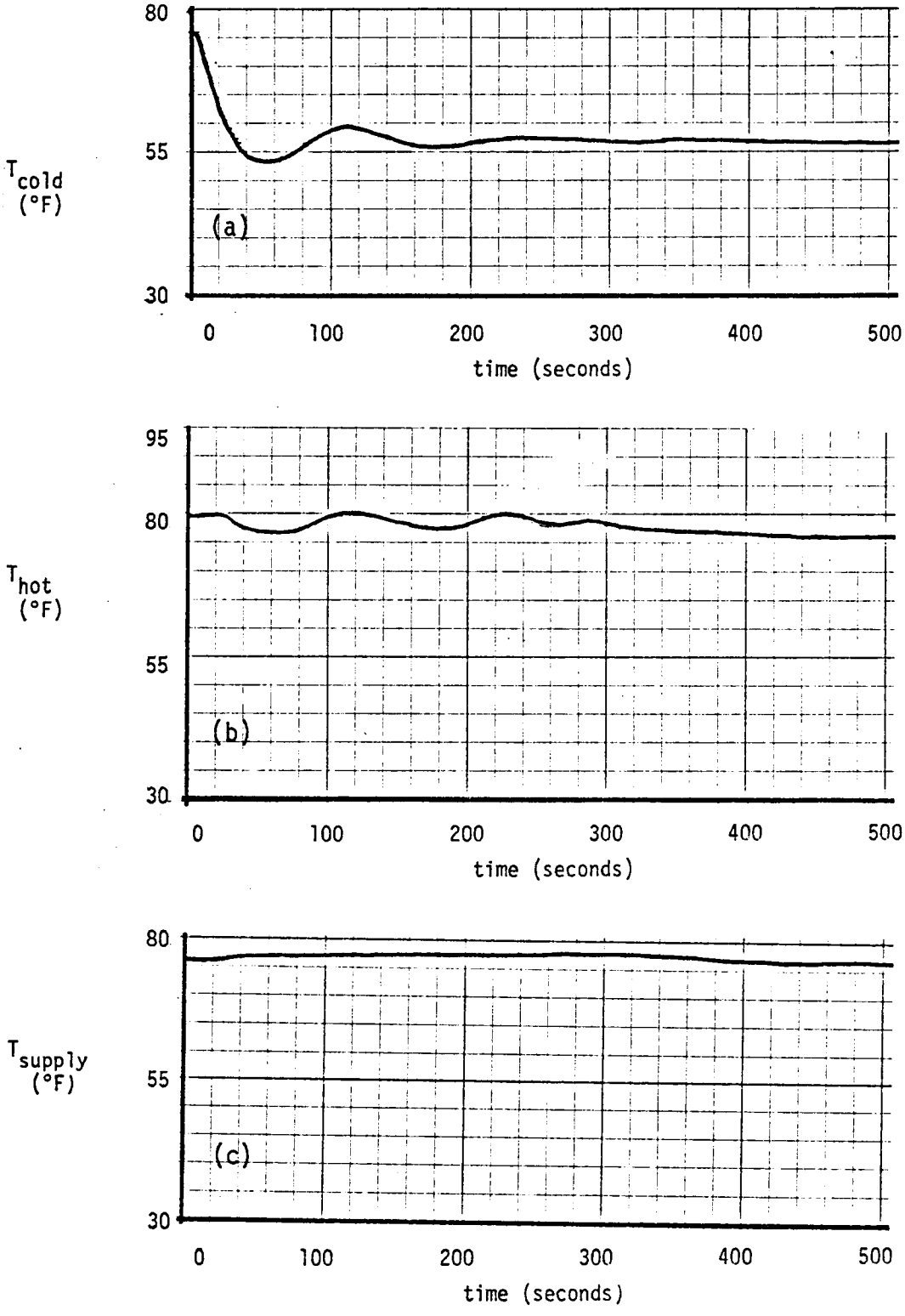


Figure 5.24. Upstream temperatures for the original system.

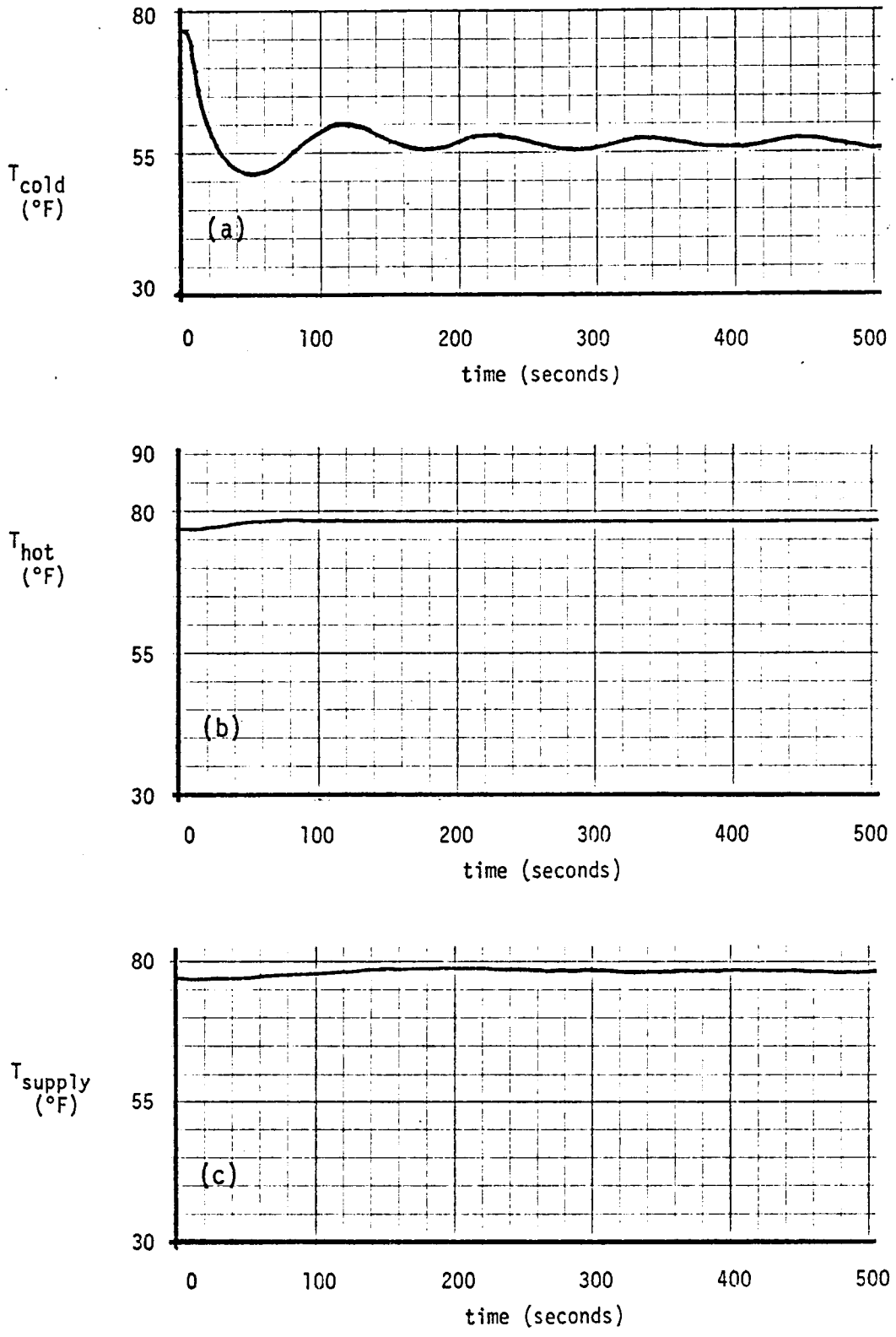


Figure 5.25. Upstream temperatures for the modified system in summer.

Because the outside air temperature is 62F or greater throughout the summer simulation, the supply air temperature control is disconnected. Consequently, Figures 5.26(a) and 5.27(a) show a constant exhaust flow equal to the normal leakage experienced when the maximum air dampers are closed. The cold duct transient air flow (Figure 5.26(b)) for the original system is greater than that in the modified system (Figure 5.27(b)).

Corresponding values for the cold and hot duct air temperatures entering the zones are practically identical in both systems (Figures 5.28 and 5.29). Also, Figures 5.30 and 5.31 show that the temperature response for zone four, zone five, and the return air in each system are closely matched.

Energy savings in the modified system are not as marked in the summer time (Figures 5.32 and 5.33) as are the savings during the winter and spring. Values for Q_{total} from Tables 5.9 and 5.10 indicate that the modified system uses 91% of the total system energy that the original system uses. Tables 5.11 and 5.12 show that the zone temperatures in the modified and original system simulations remain near their respective setpoints.

Simulation of Fall Operation. Figure 5.34 details the approximation of the outside air conditions for an average day in the fall. Figures 5.35 and 5.36 indicate the short-term cold duct, hot duct, and supply air temperature variation for the original and modified system. The hot duct temperature of the original system is slightly oscillatory but quickly settles to a stable value. Figures 5.37(a) and 5.38(a)

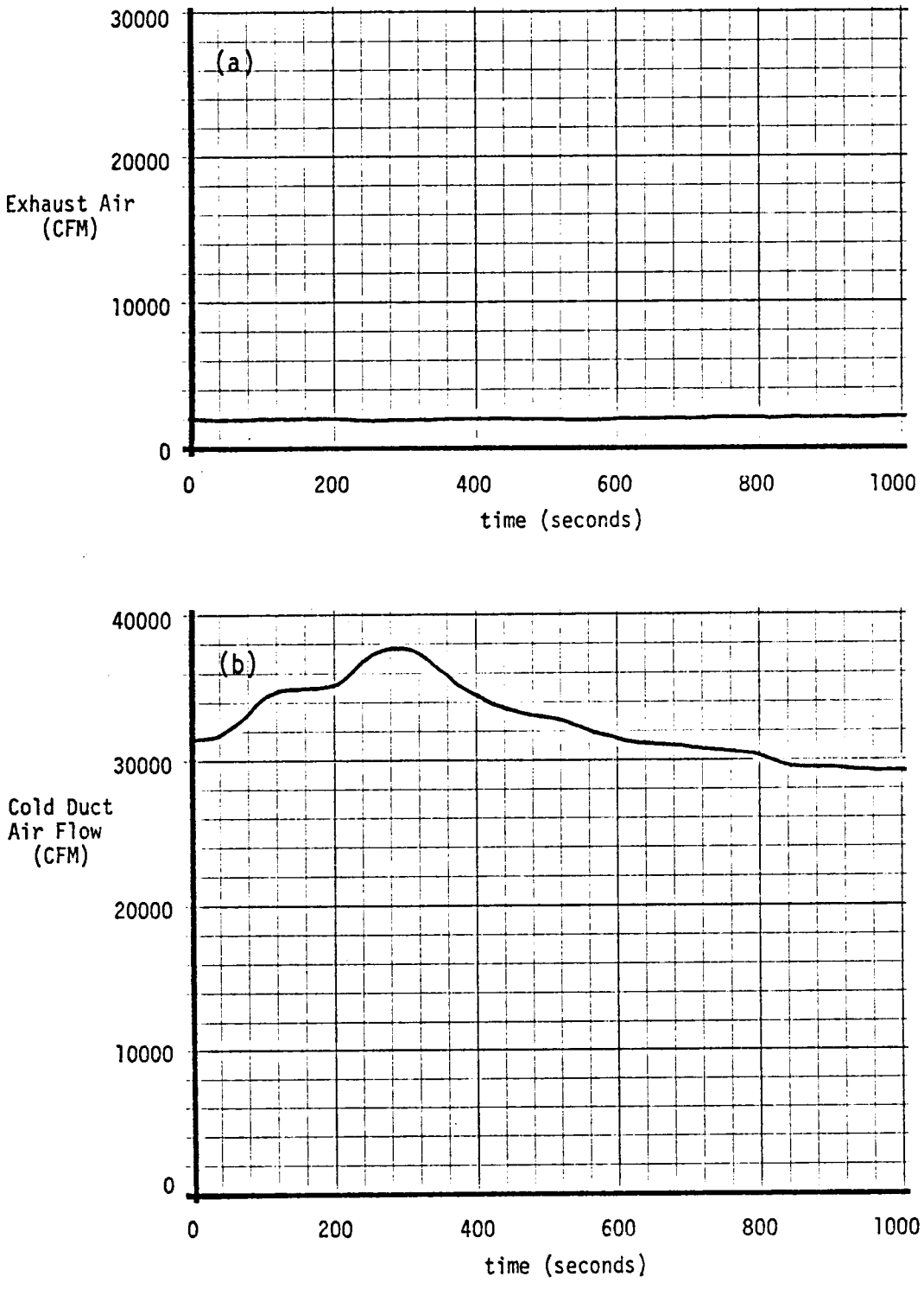


Figure 5.26. Air flows for the original system in summer.

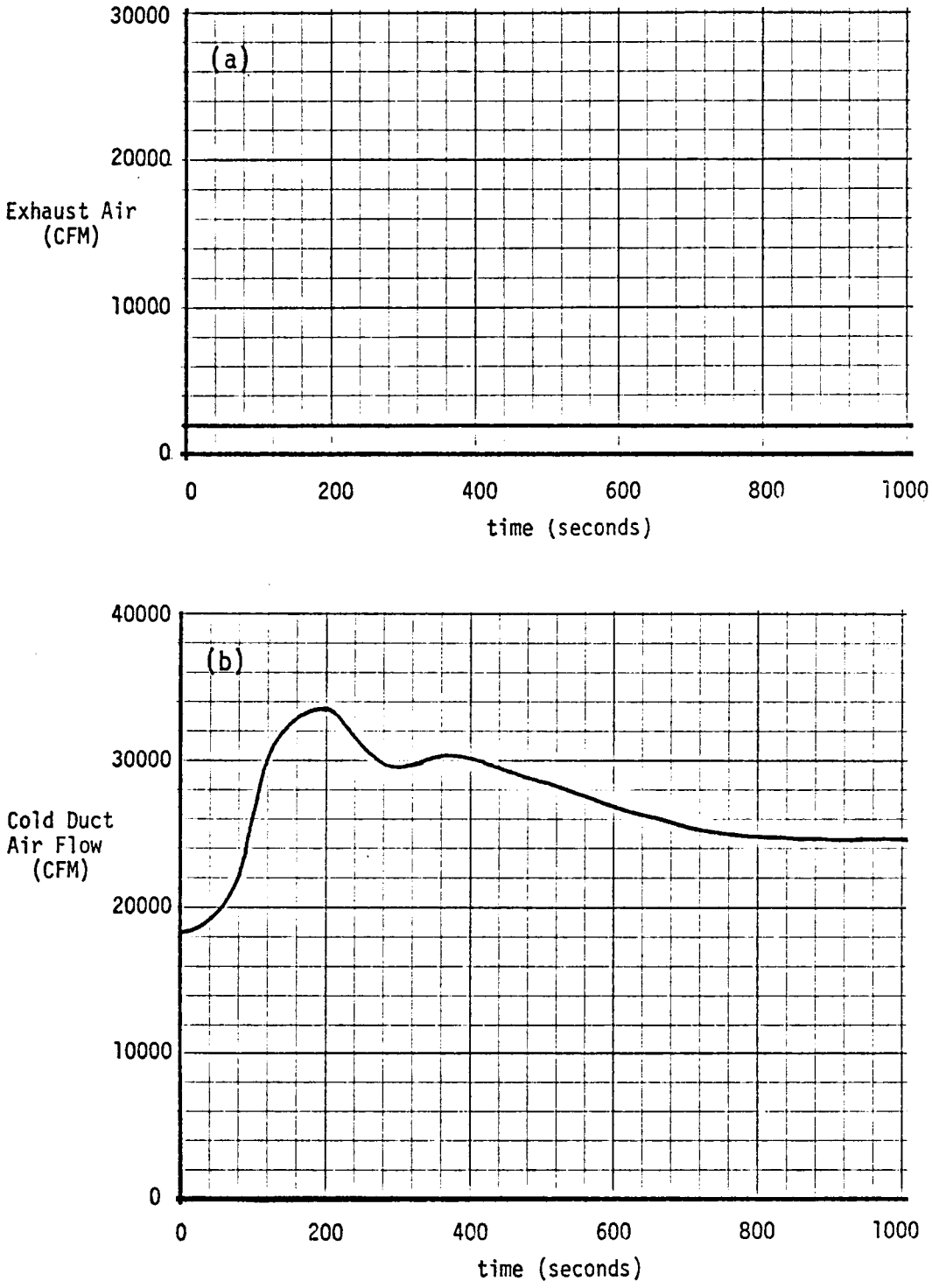
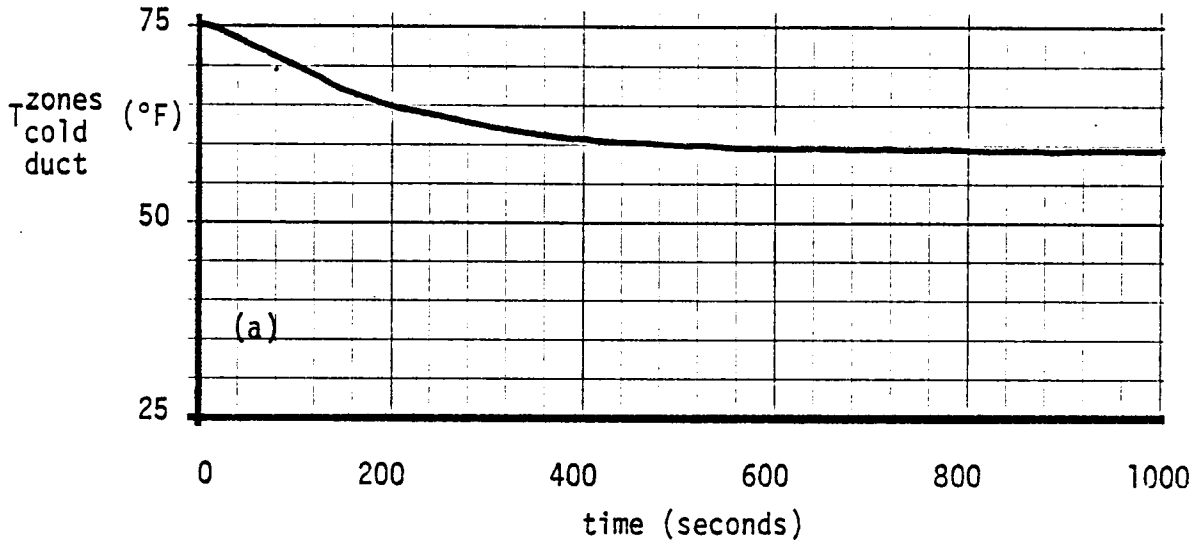


Figure 5.27. Air flows for the modified system in summer.



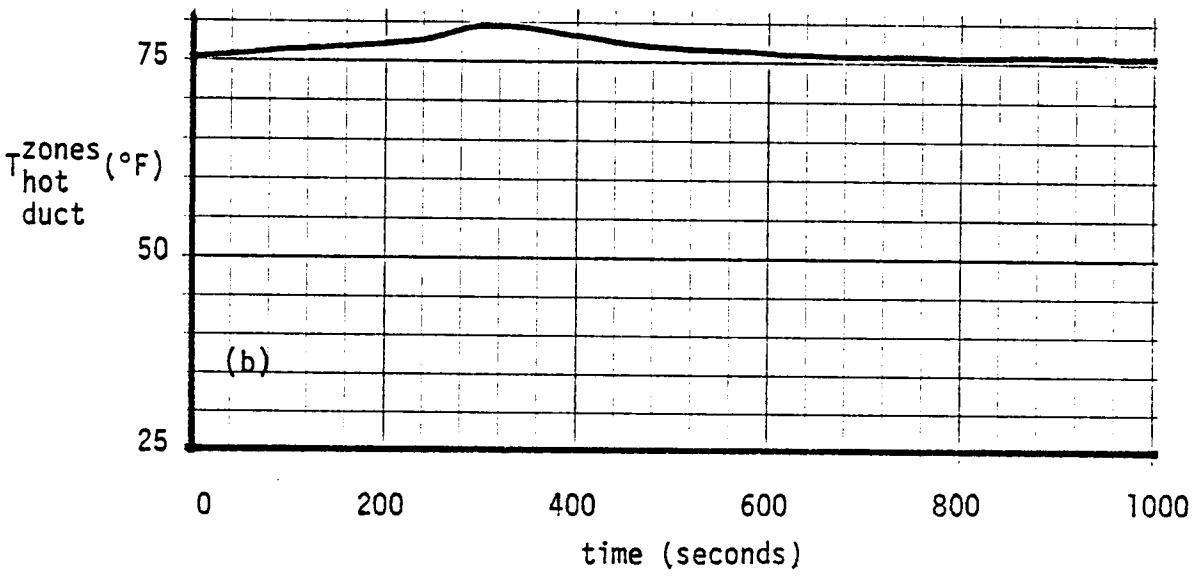
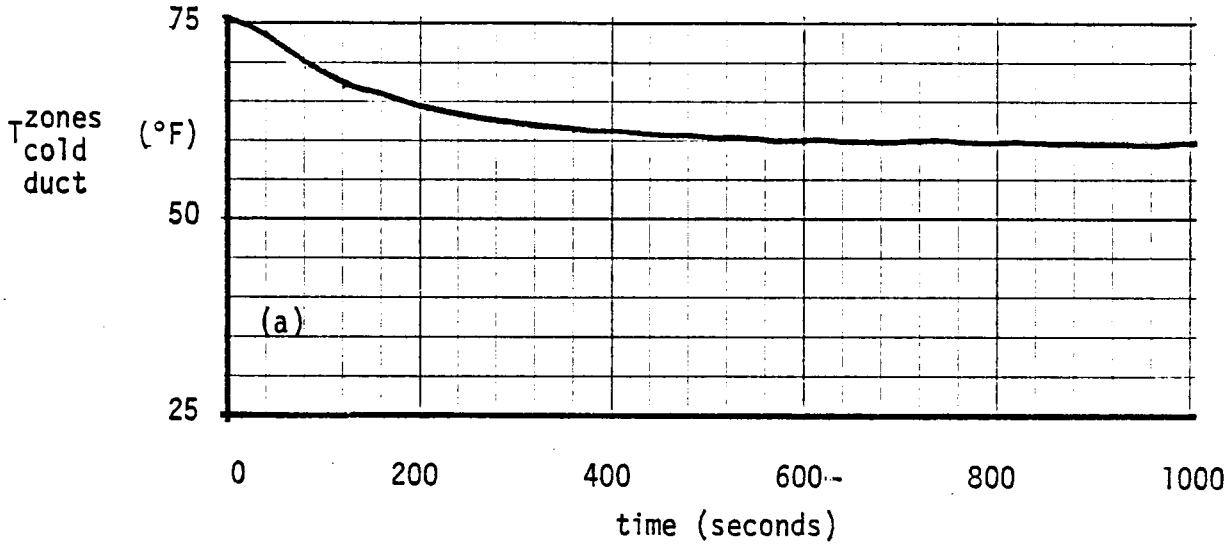


Figure 5.28. Midstream temperatures for the original system in summer.



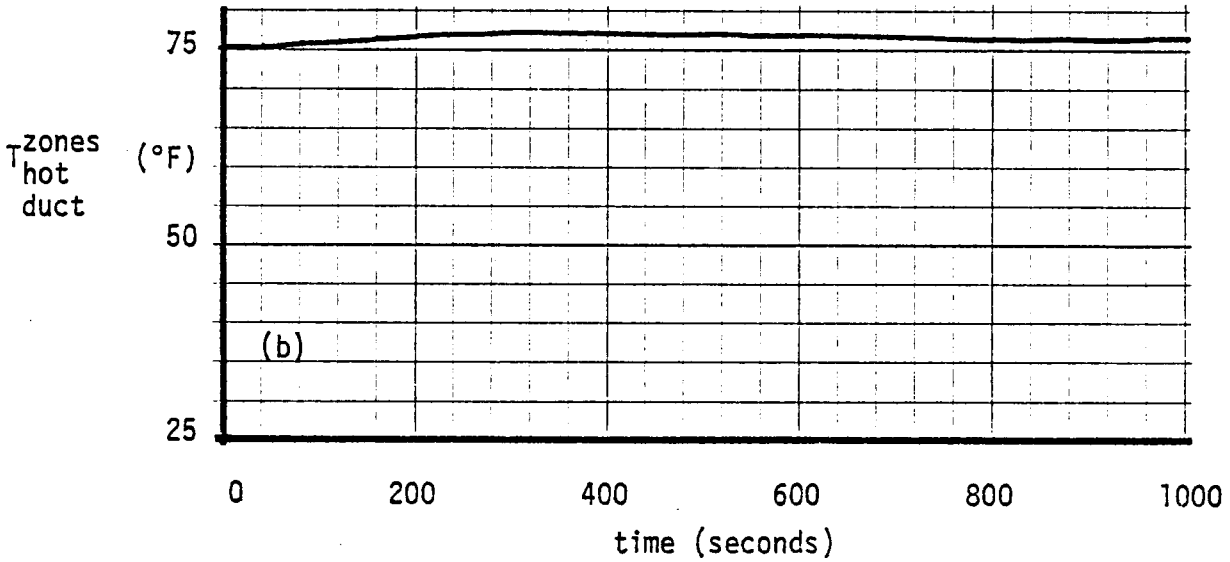


Figure 5.29. Midstream temperatures for the modified system in summer.

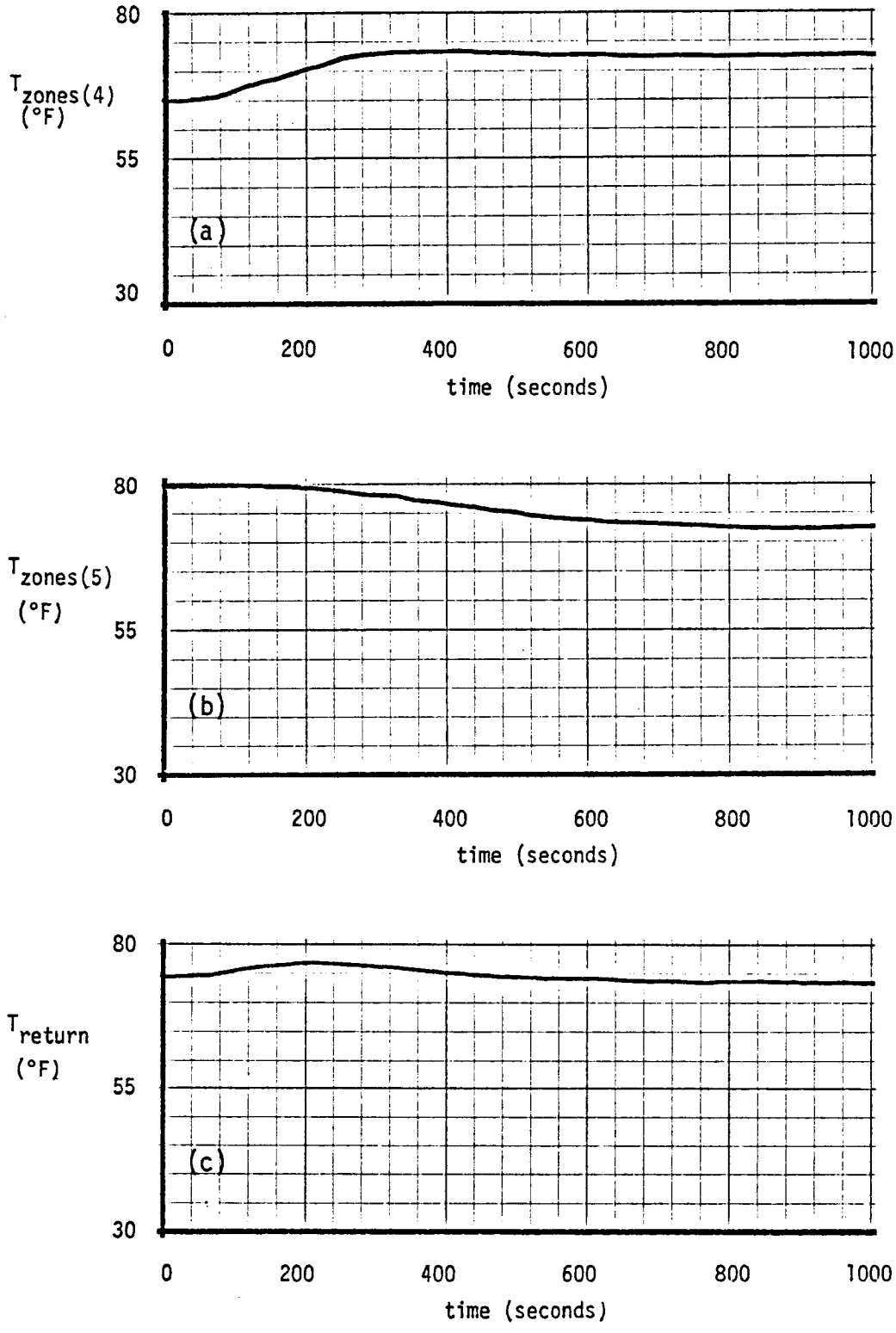


Figure 5.30. Downstream temperatures for the original system in summer.

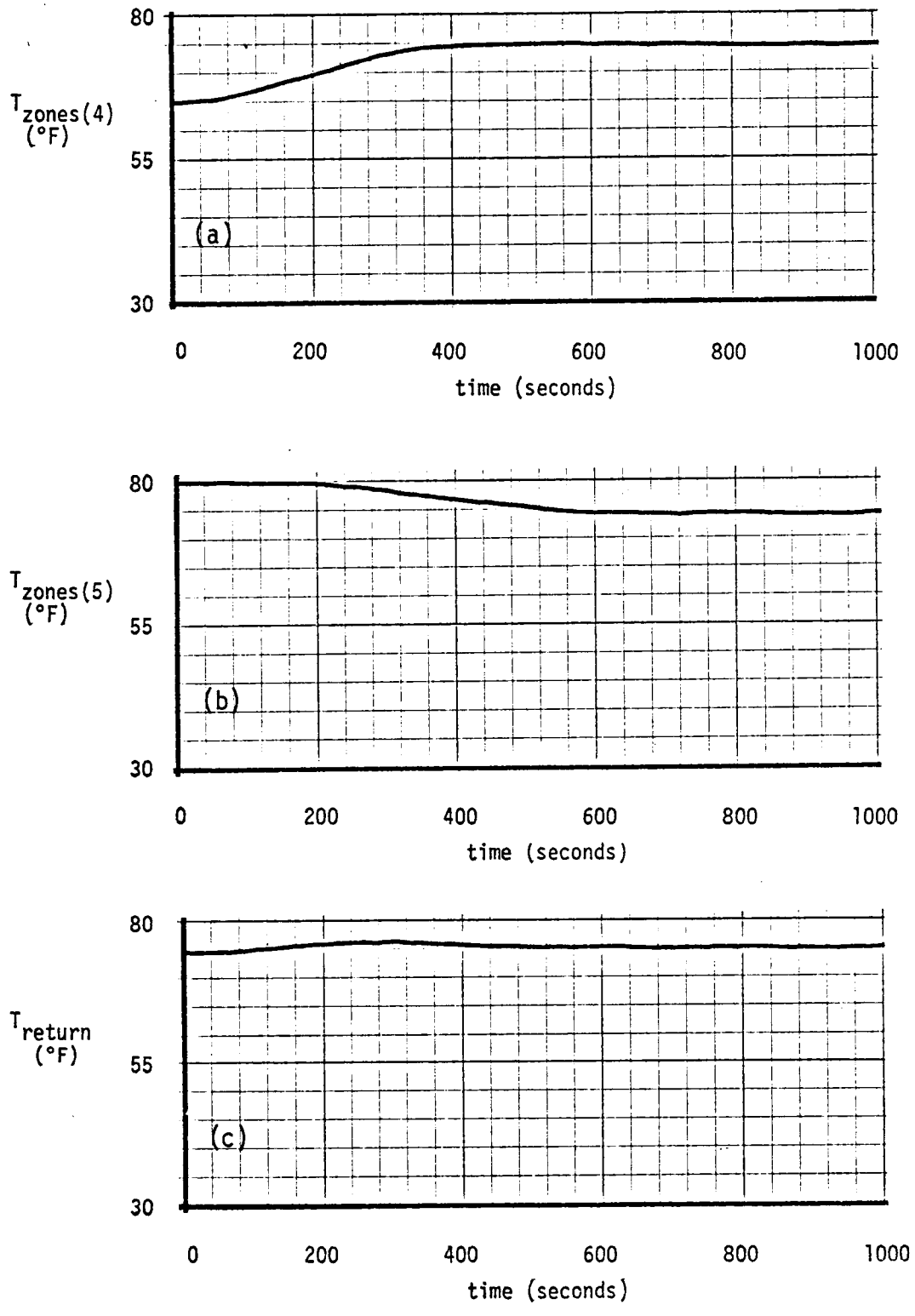


Figure 5.31. Downstream temperatures for the modified system in summer.

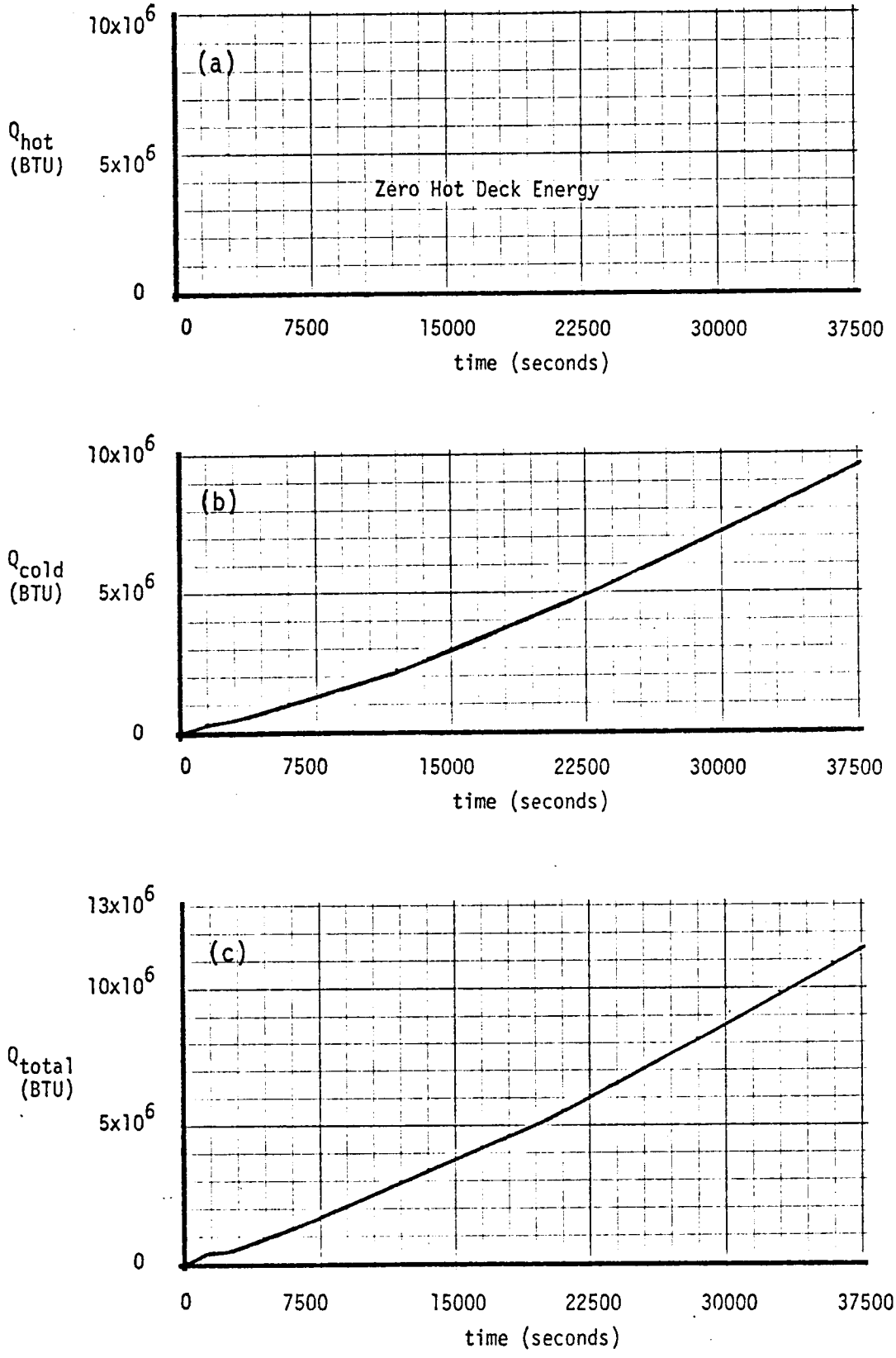


Figure 5.32. Energy use for the original system in summer.

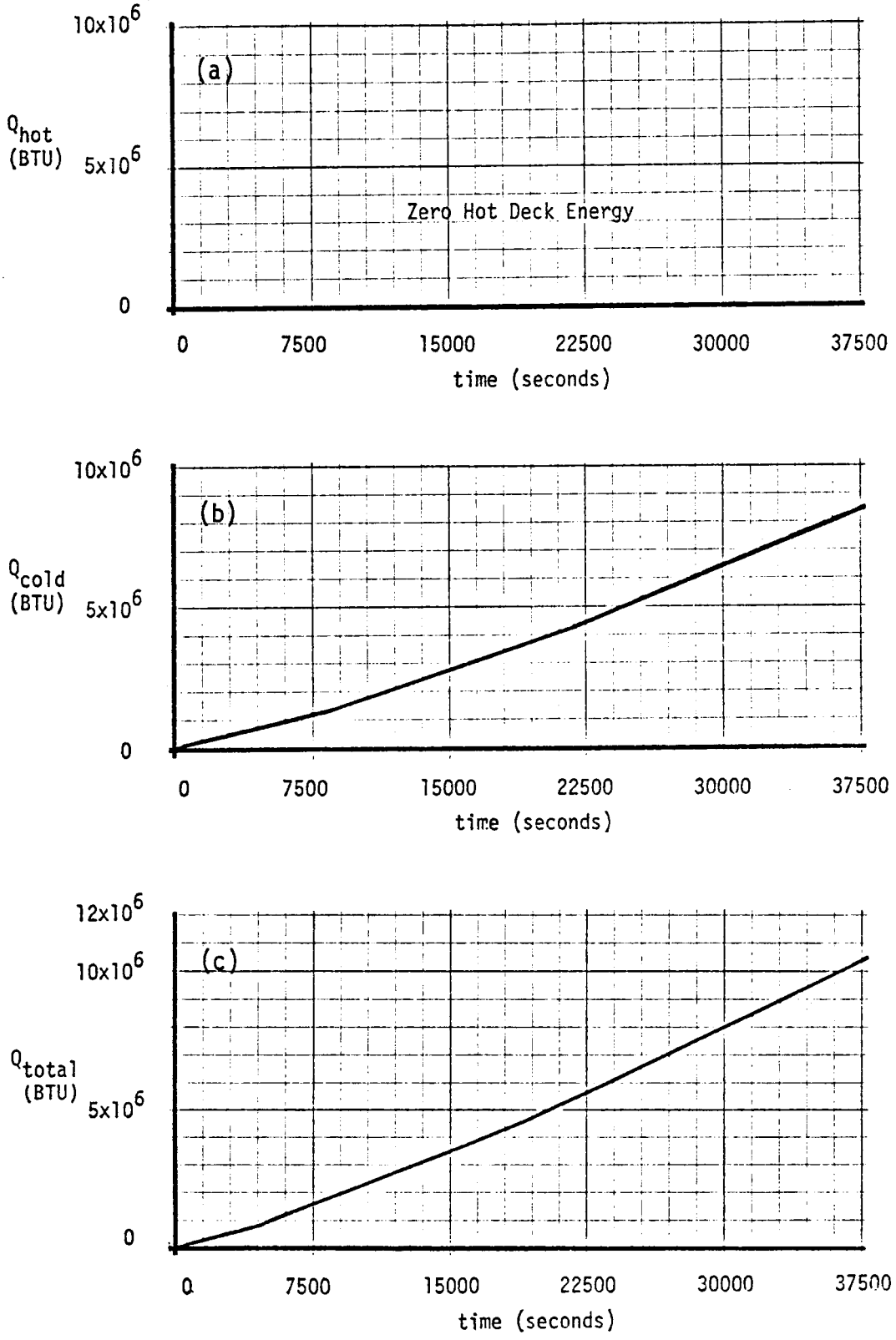


Figure 5.33. Energy use for the modified system in summer.

Table 5.9. Responses for the original system in summer.

	Starting	High Value	Time of High Value (sec)	Low Value	Time of Low Value (sec)	Final Value	Time of Steady State (sec)
TCOLD (°F)	76.7	76.7	0	53.7	54	59.2	1227
THOT (°F)	79.4	83.1	27000	76.0	1020	83.1	810
TSUP (°F)	76.7	83.1	27000	76.0	1020	83.1	810
EXH (ft^3/min)	2000	2000	0	2000	0	2000	0
FLOWH (ft^3/min)	7150	10781	1380	903	270	5135	1650
FLOWC (ft^3/min)	31510	37757	270	27879	1380	33525	870
TOUT (°F)	62.0	87.0	27000	62.0	0	87.0	NA
WOD (lbm/lbm)	.0088	.0152	30300	.0088	0	.0152	NA
TRTN (°F)	74.8	76.3	180	73.4	990	73.7	999
WRTN (lbm/lbm)	.0093	.0113	29700	.0090	60	.0113	540
QCOLD (BTUs)	0	9.65×10^6	37800	0	0	9.65×10^6	NA
QHOT (BTUs)	0	589	37800	0	0	589	NA
QTOTAL (BTUs)	0	1.152×10^6	37800	0	0	1.152×10^6	NA
TCLZ (°F)	75.1	75.1	0	59.3	1182	61.7	852
THTZ (°F)	75.2	80.2	27300	75.2	0	80.2	918

Table 5.10. Responses for the modified system in summer.

	Starting	High Value	Time of High Value (sec)	Low Value	Time of Low Value (sec)	Final Value	Time of Steady State (sec)
TCOLD (°F)	77.1	77.1	0	51.6	51	58.3	750
THOT (°F)	77.1	82.8	26700	77.1	0	82.8	600
TSUP (°F)	77.1	82.8	26700	77.1	0	82.8	600
EXH (ft^3/min)	2000.00	2000	0	2000	0	2000	0
FLOWH (ft^3/min)	20359	20359	0	6122	210	10054	750
FLOWC (ft^3/min)	18301	33595	180	18301	0	28606	750
TOUT (°F)	62.0	87.0	27000	62.1	0	87.0	NA
WOD (lbm/lbm)	.0088	.0152	30300	.0088	0	.0152	NA
TRTN (°F)	74.7	76.4	180	74.7	0	75.3	720
WRTN (lbm/lbm)	.0093	.0111	30000	.0090	30	.0111	690
QCOLD (BTUs)	0	8.57×10^6	37800	0	0	8.576×10^6	NA
QHOT (BTUs)	0	0.000	0	0	0	0.000	NA
QTOTAL (BTUs)	0	1.050×10^7	37800	0	0	1.050×10^7	NA
TCLZ (°F)	75.1	75.1	0	59.3	1080	61.0	600
THTZ (°F)	75.1	80.0	27000	75.1	0	80.0	738

Table 5.11. Zone responses for the original system in summer.

	Starting Temperature °F	Lowest Temperature °F	Time of Low Value (seconds)	Steady State Temperature °F	Time of Steady State (seconds)
TZONE(1)	78.0	72.7	1080	73.0	1020
WZ(1)	.0093	.0092	30	.0112	360
TZONE(2)	74.3	72.7	900	73.0	900
WZ(2)	.0093	.0090	63	.0112	360
TZONE(3)	73.1	72.5	600	72.8	660
WZ(3)	.0093	.0090	60	.0113	510
TZONE(4)	65.0	65.0	0	72.8	660
WZ(4)	.0093	.0092	90	.0113	510
TZONE(5)	80.0	72.5	810	72.8	810
WZ(5)	.0093	.0090	60	.0113	510
TZONE(6)	72.0	72.0	0	72.5	660
WZ(6)	.0092	.0090	60	.0114	480
TZONE(7)	74.8	72.2	660	72.5	660
WZ(7)	.0092	.0089	60	.0114	480
TZONE(8)	74.0	72.2	660	72.5	660
WZ(8)	.0092	.0089	60	.0114	480
TZONE(9)	74.0	72.7	750	73.0	474
WZ(9)	.0094	.0090	42	.0112	342

Table 5.12. Zone responses for the modified system in summer.

	Starting Temperature °F	Lowest Temperature °F	Time of Low Value (seconds)	Steady State Temperature °F	Time of Steady State (seconds)
TZONE(1)	78.0	74.5	720	74.7	720
WZ(1)	.0093	.0084	60	.0110	300
TZONE(2)	74.3	74.3	0	74.7	660
WZ(2)	.0093	.0086	60	.0110	420
TZONE(3)	73.1	73.1	0	74.5	450
WZ(3)	.0093	.0090	60	.0111	570
TZONE(4)	65.0	65.0	0	74.5	480
WZ(4)	.0093	.0080	39	.0111	570
TZONE(5)	80.0	74.3	630	74.5	570
WZ(5)	.0093	.0084	87	.0111	570
TZONE(6)	72.0	72.0	0	74.3	690
WZ(6)	.0092	.0089	90	.0112	720
TZONE(7)	74.8	74.0	690	74.3	690
WZ(7)	.0092	.0083	60	.0112	720
TZONE(8)	74.0	74.0	0	74.3	690
WZ(8)	.0092	.0086	60	.0112	420
TZONE(9)	74.0	74.0	0	74.7	660
WZ(9)	.0094	.0083	43	.0110	327

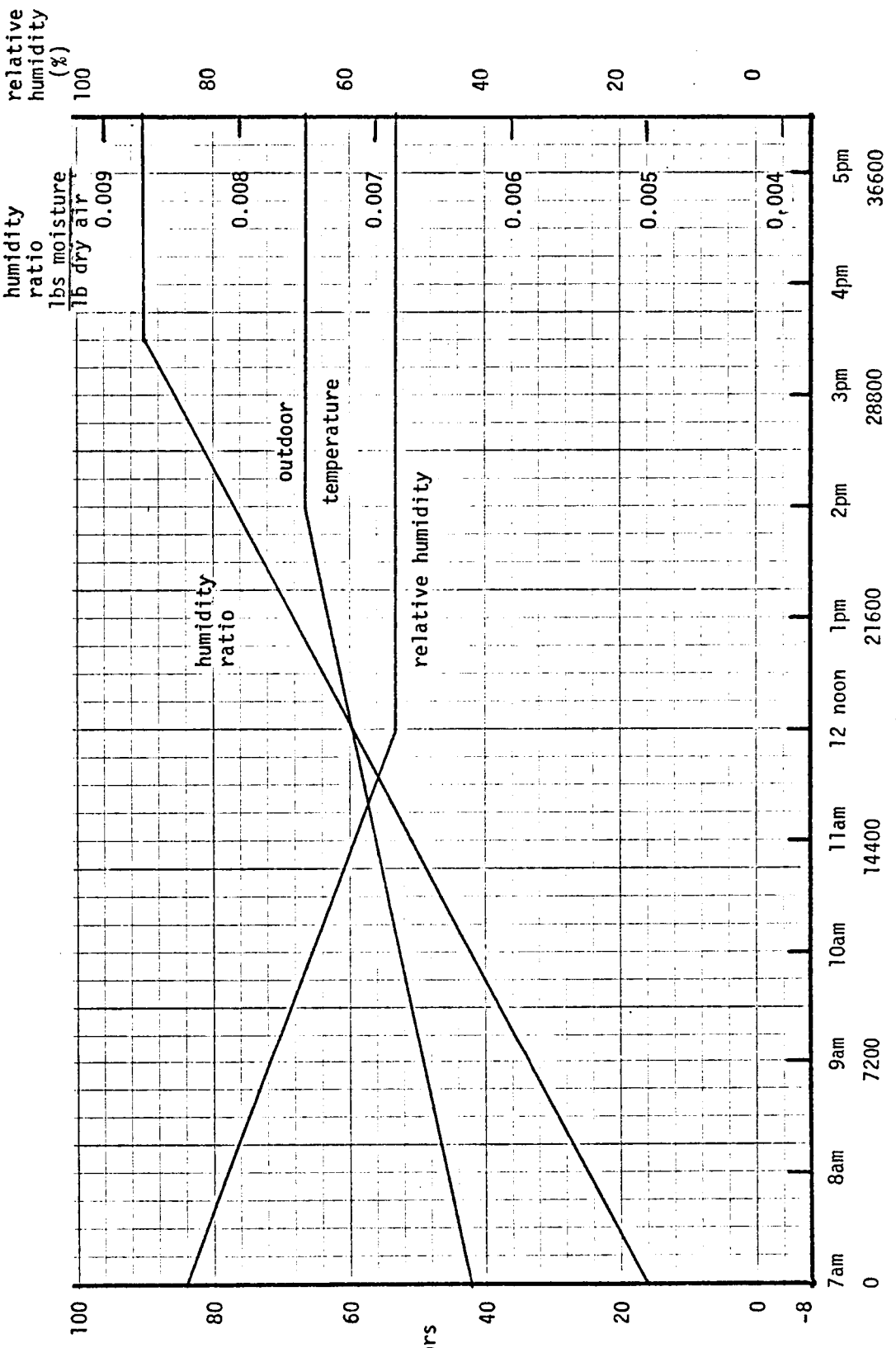


Figure 5.34. Approximate outside air conditions in fall.

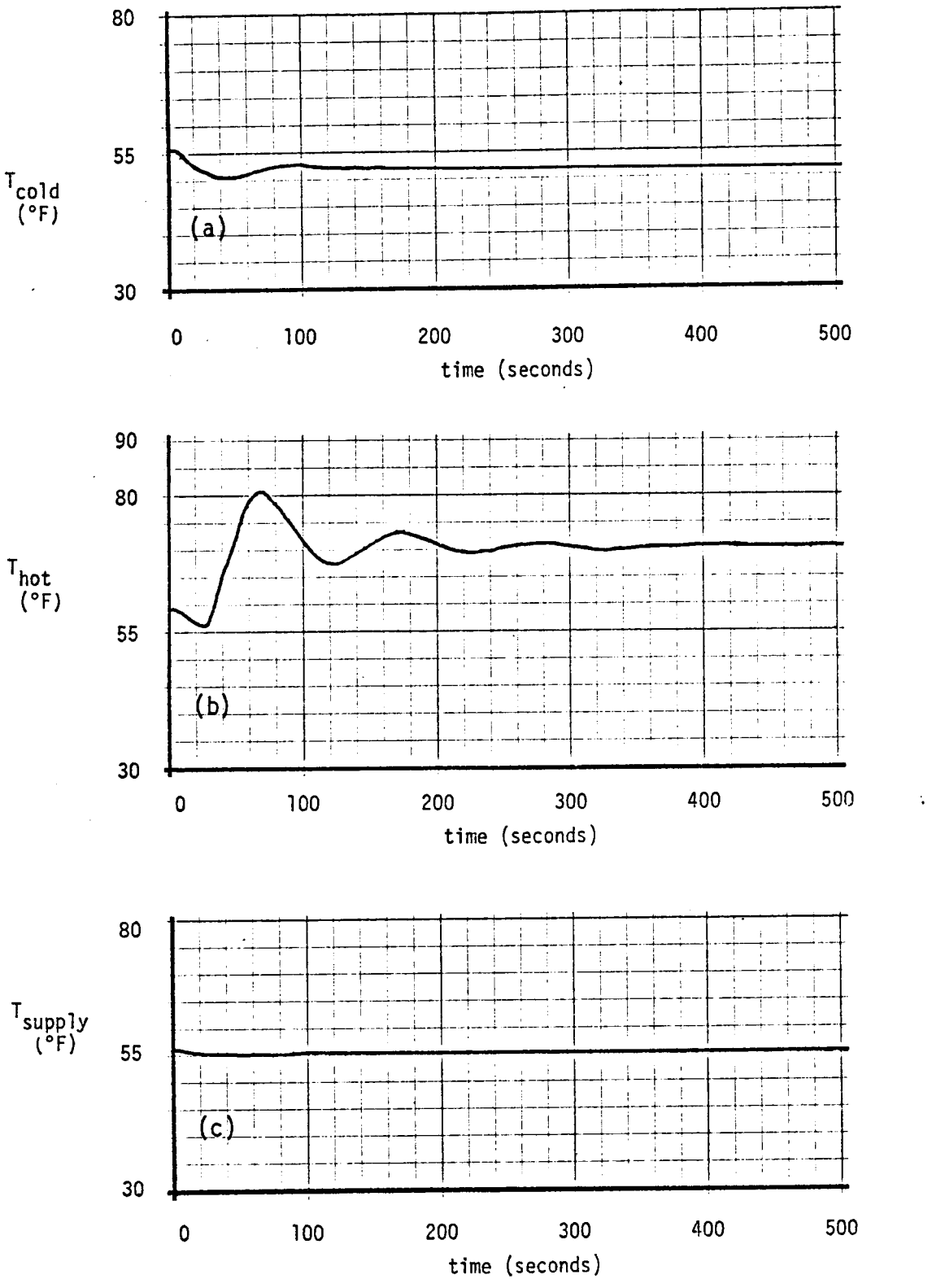


Figure 5.35. Upstream temperatures for the original system in fall.

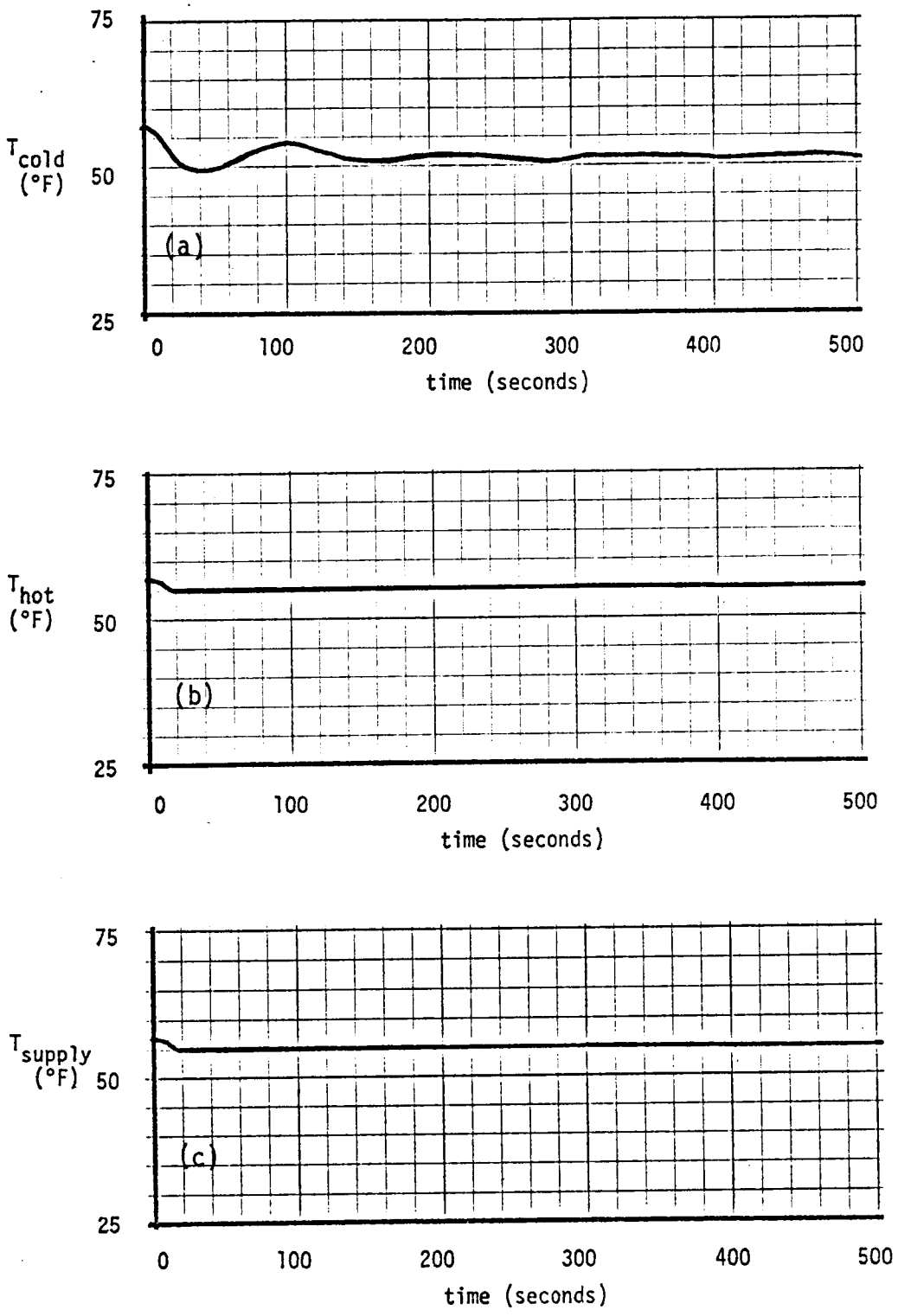


Figure 5.36. Upstream temperatures for the modified system in fall.

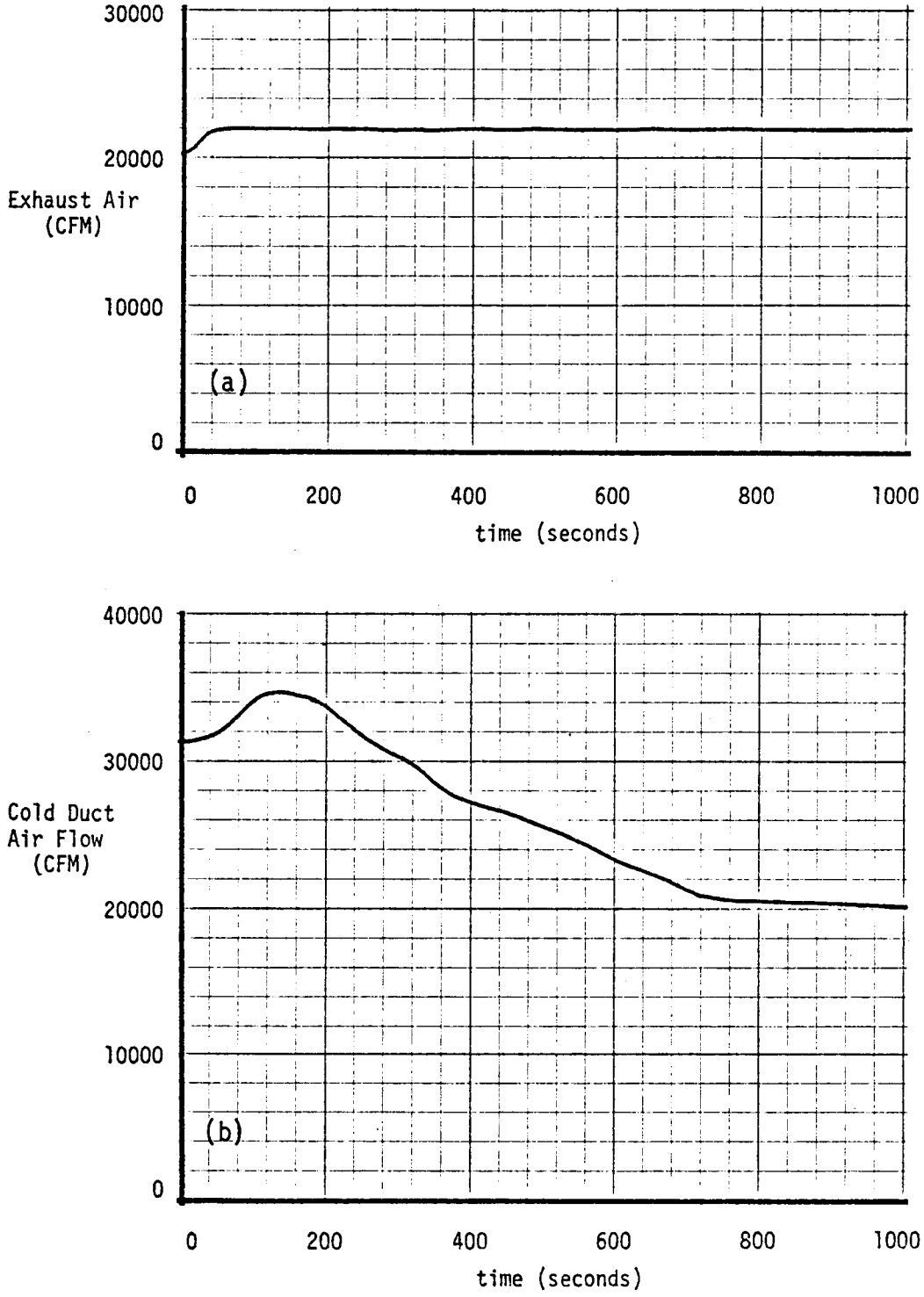


Figure 5.37. Air flows for the original system in fall.

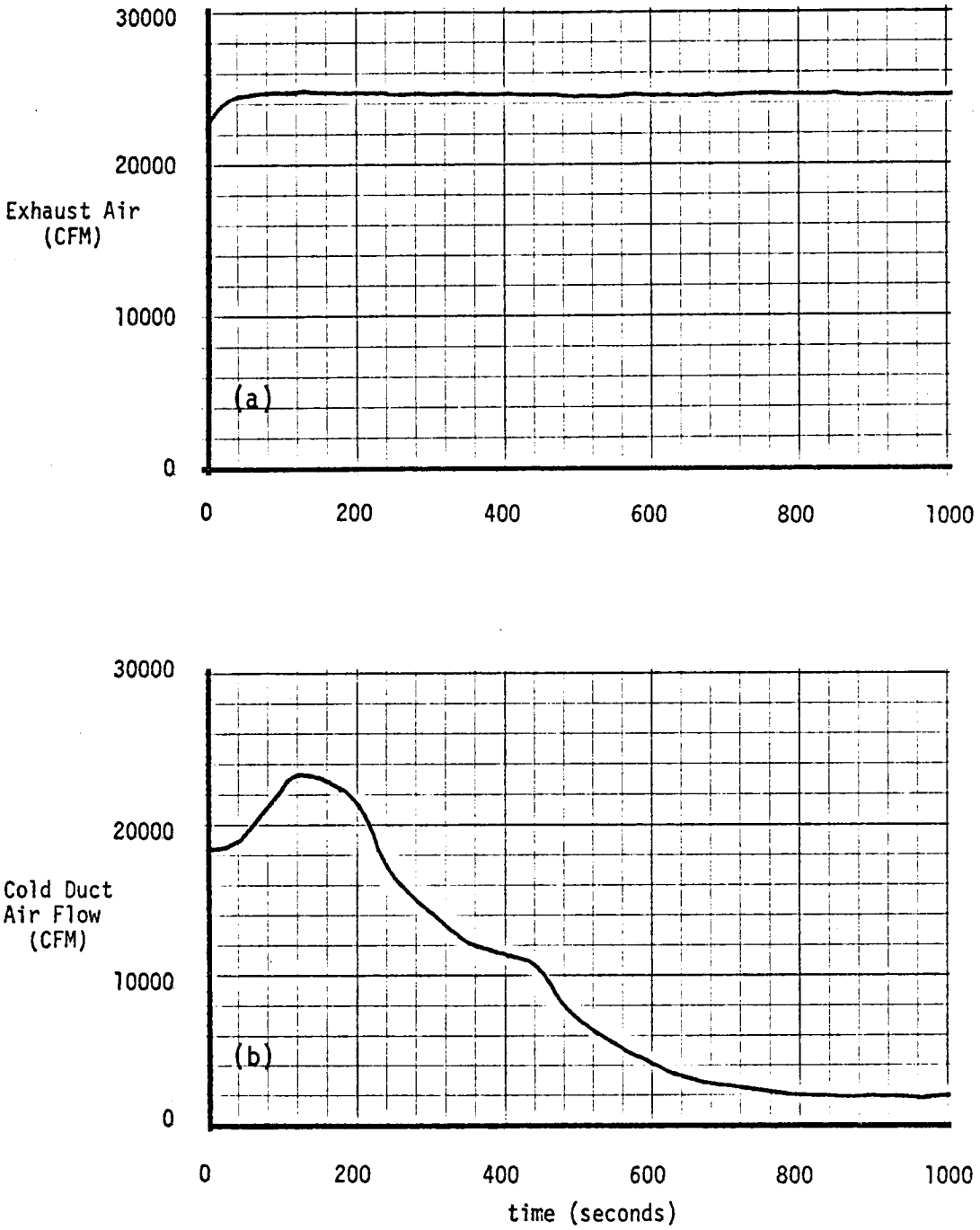


Figure 5.38. Air flows for the modified system in fall.

disclose that the exhaust flow in both systems rapidly reaches a stable value.

The cold duct air flow in the original system remains considerably larger than that in the modified system (Figures 5.37(b) and 5.38(b)). Only slight differences exist between the transient response of cold air entering the zones in the original and the modified system (Figures 5.39(a) and 5.40(b)).

The hot duct flows shown in Figures 5.39(b) and 5.40(b) reflect that the hot duct is shut off in the modified system. As previously shown in simulations for other seasons, the temperature responses of zones four and five and of the return air are practically identical in both systems (Figures 5.41 and 5.42).

Figures 5.43 and 5.44 show significant differences between the energy used in the two systems. Tables 5.13 and 5.14 disclose that the modified system uses 58% of the energy that is used in the original system. Tables 5.15 and 5.16 indicate that both systems are capable of maintaining steady-state zone temperatures with little error.

Summary

Obviously, different operating strategies can drastically affect the amount of energy used by a dual-duct system. Differing strategies can also affect system stability. Several important conclusions can be drawn from the results presented above.

Specifically, the simulations indicate that the current dual-duct operating system is much more effective in conserving energy than the original operating system. Energy savings occur in all four seasons,

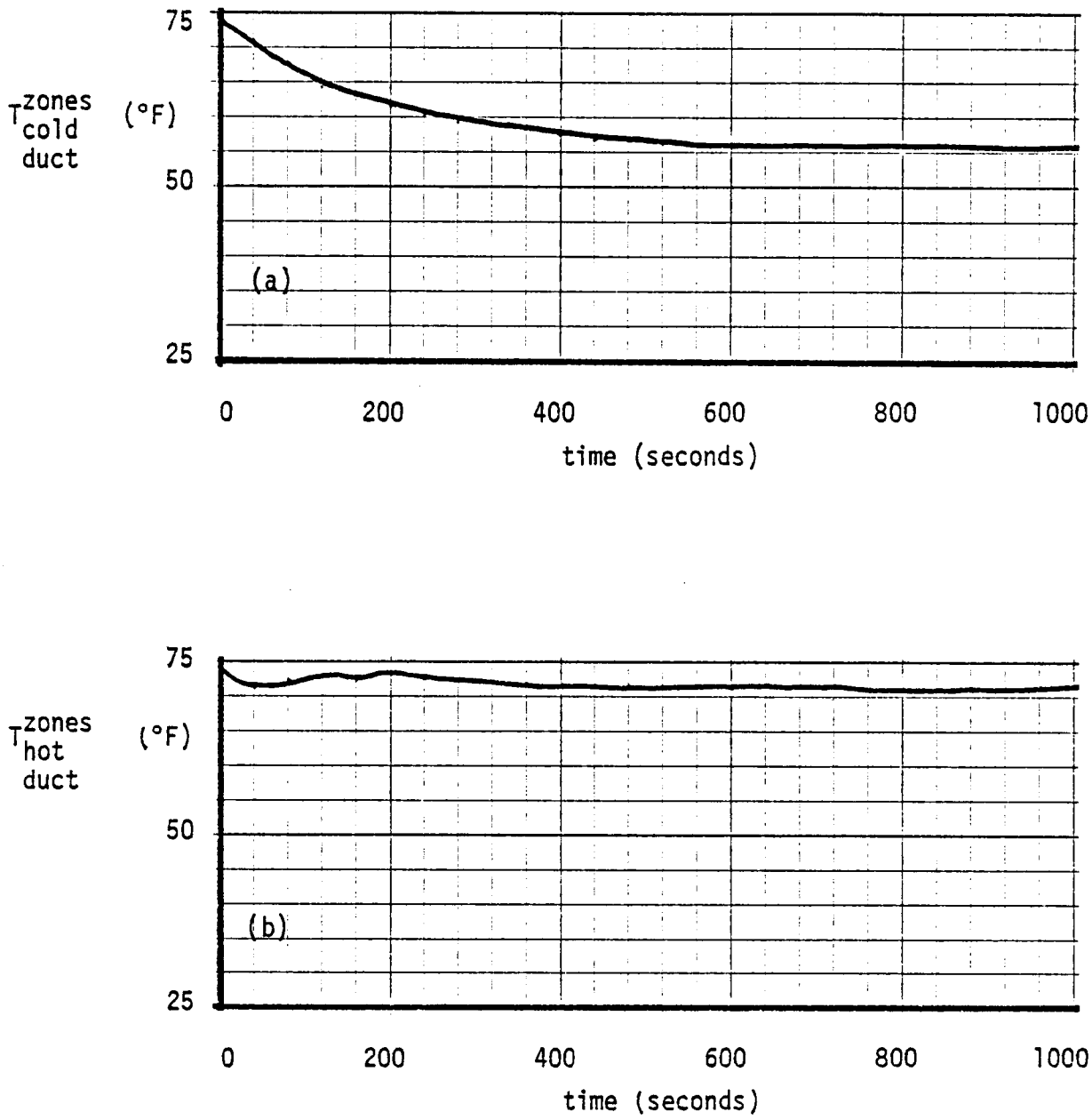


Figure 5.39. Midstream temperatures for the original system in fall.

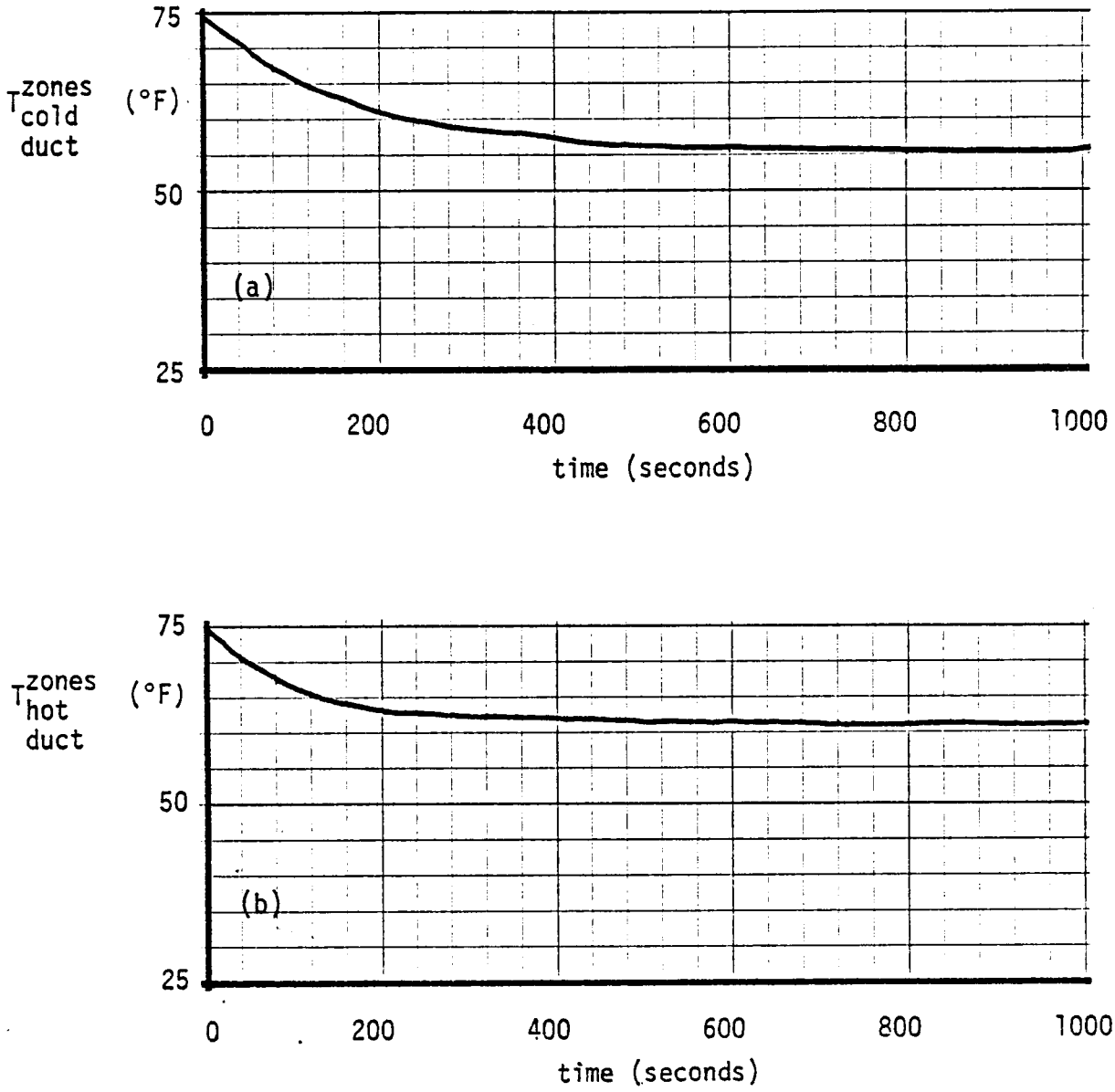


Figure 5.40. Midstream temperatures for the modified system in fall.

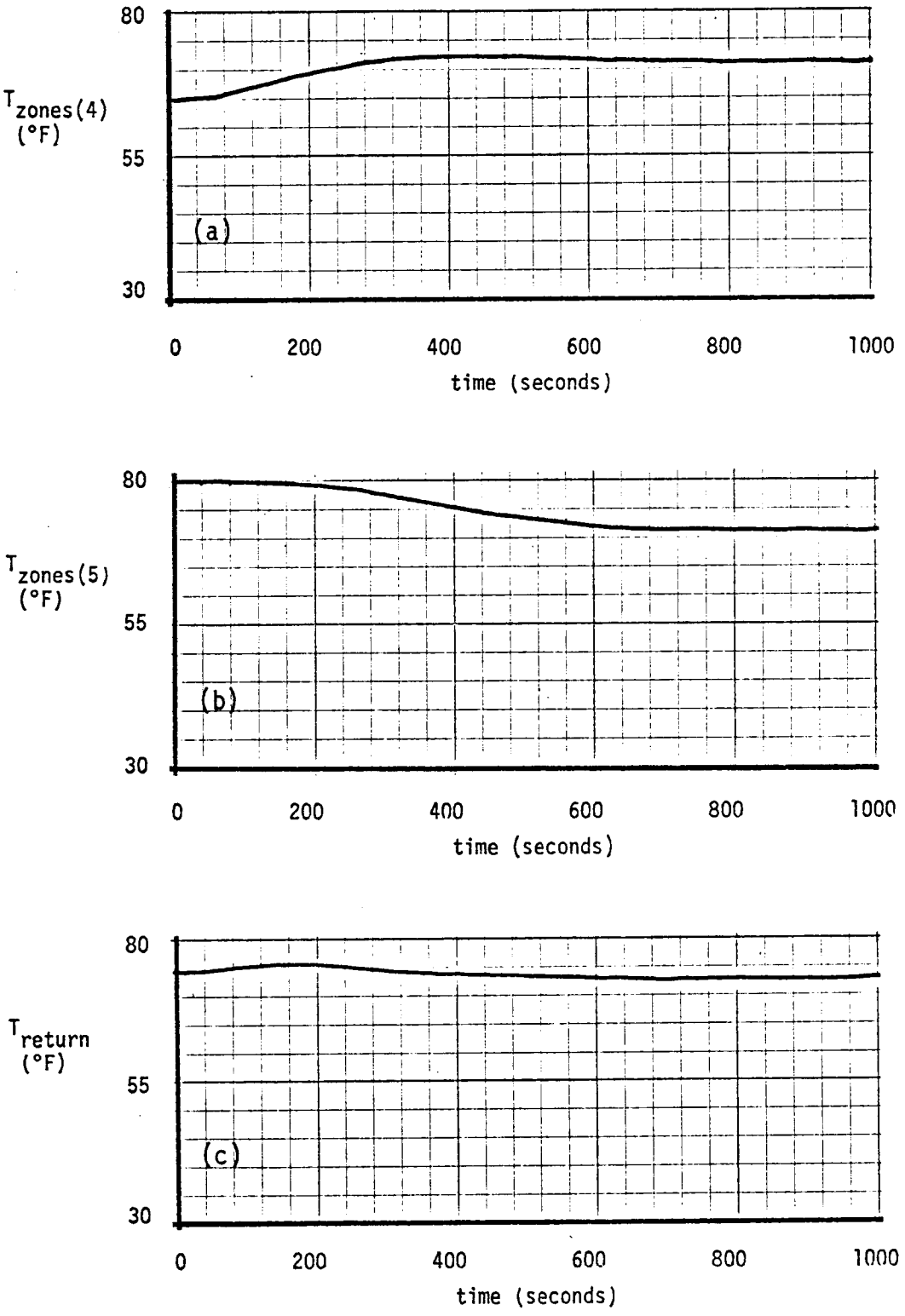


Figure 5.41. Downstream temperatures for the original system in fall.

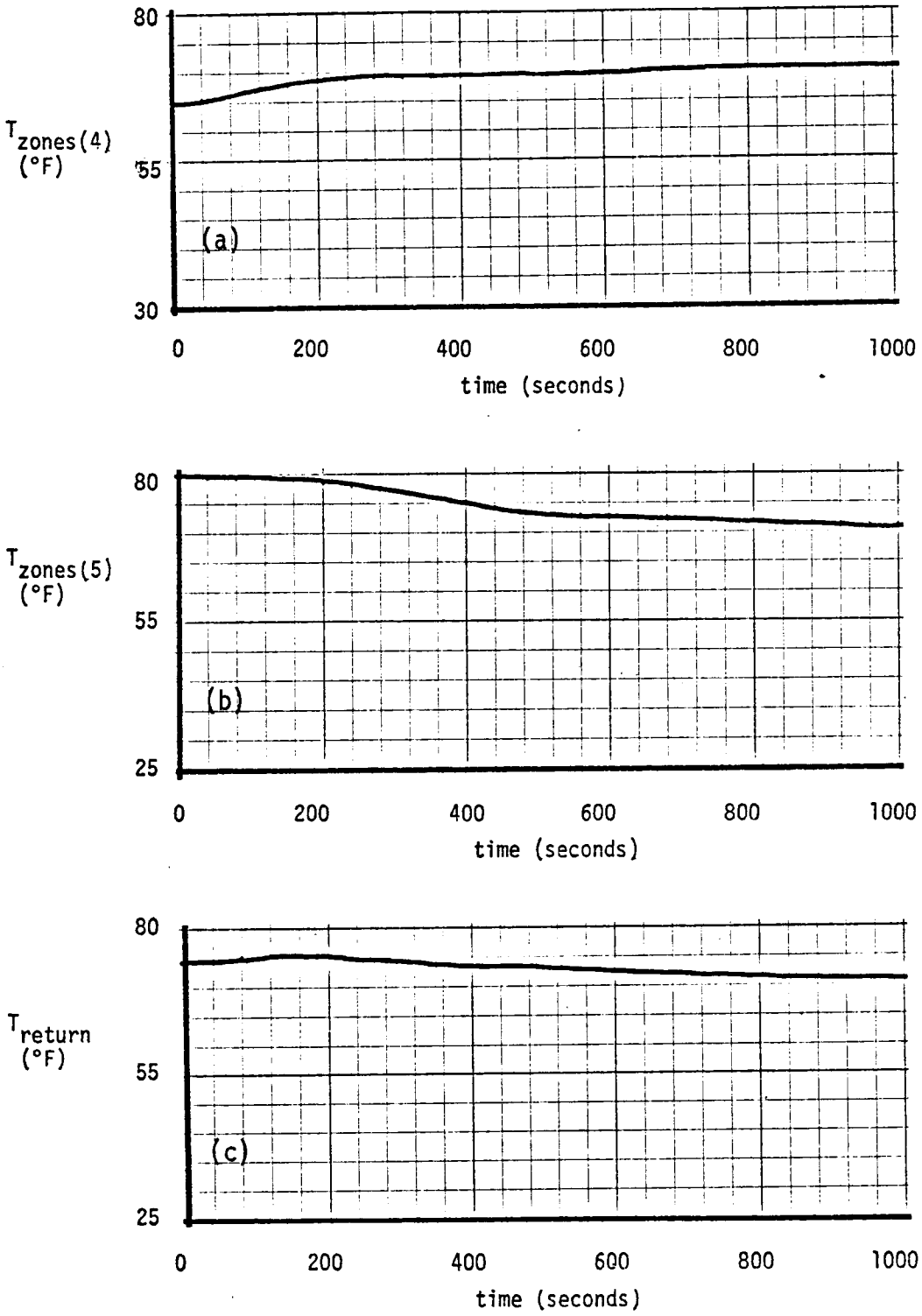


Figure 5.42. Downstream temperatures for the modified system in fall.

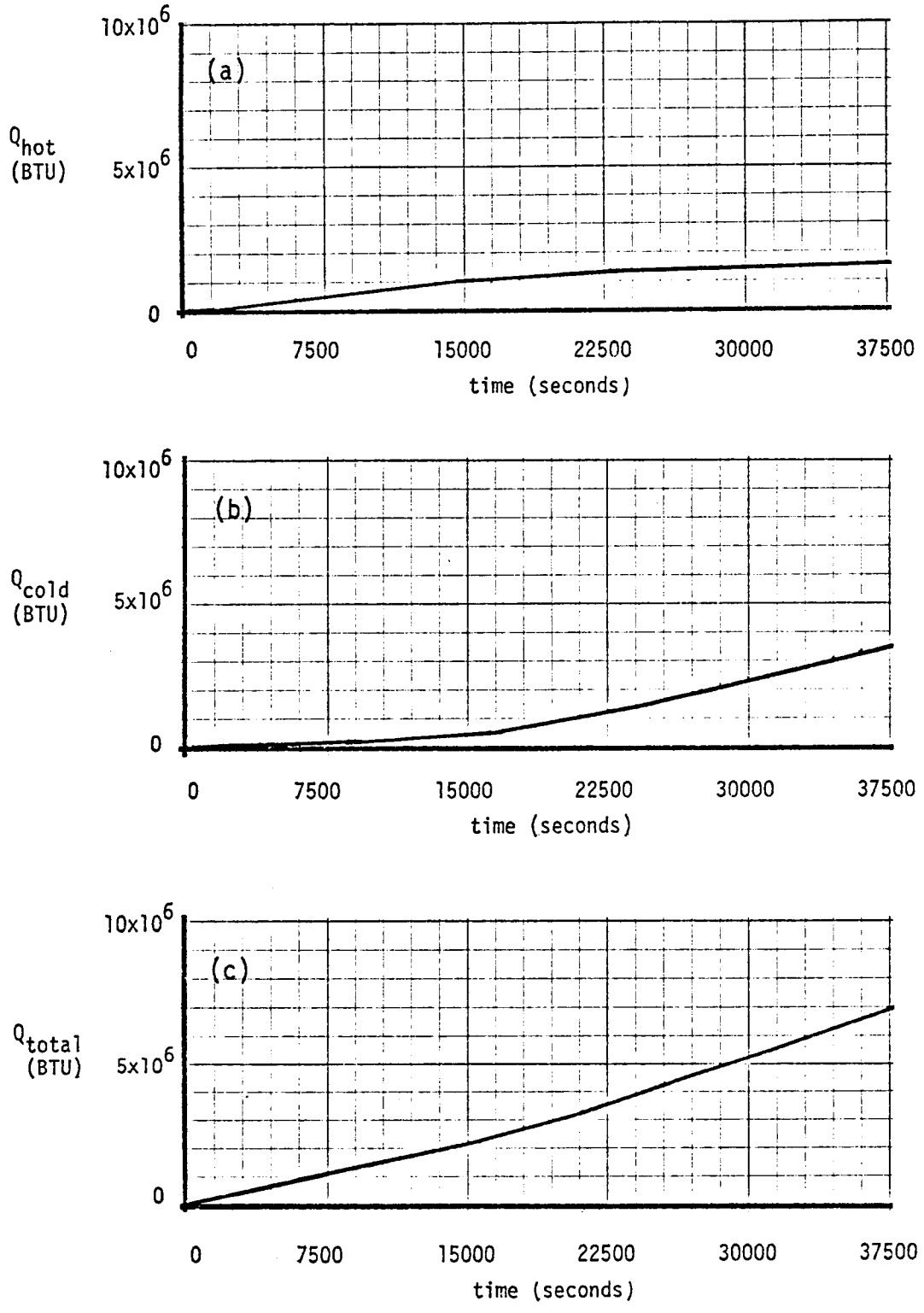


Figure 5.43. Energy use for the original system in fall.

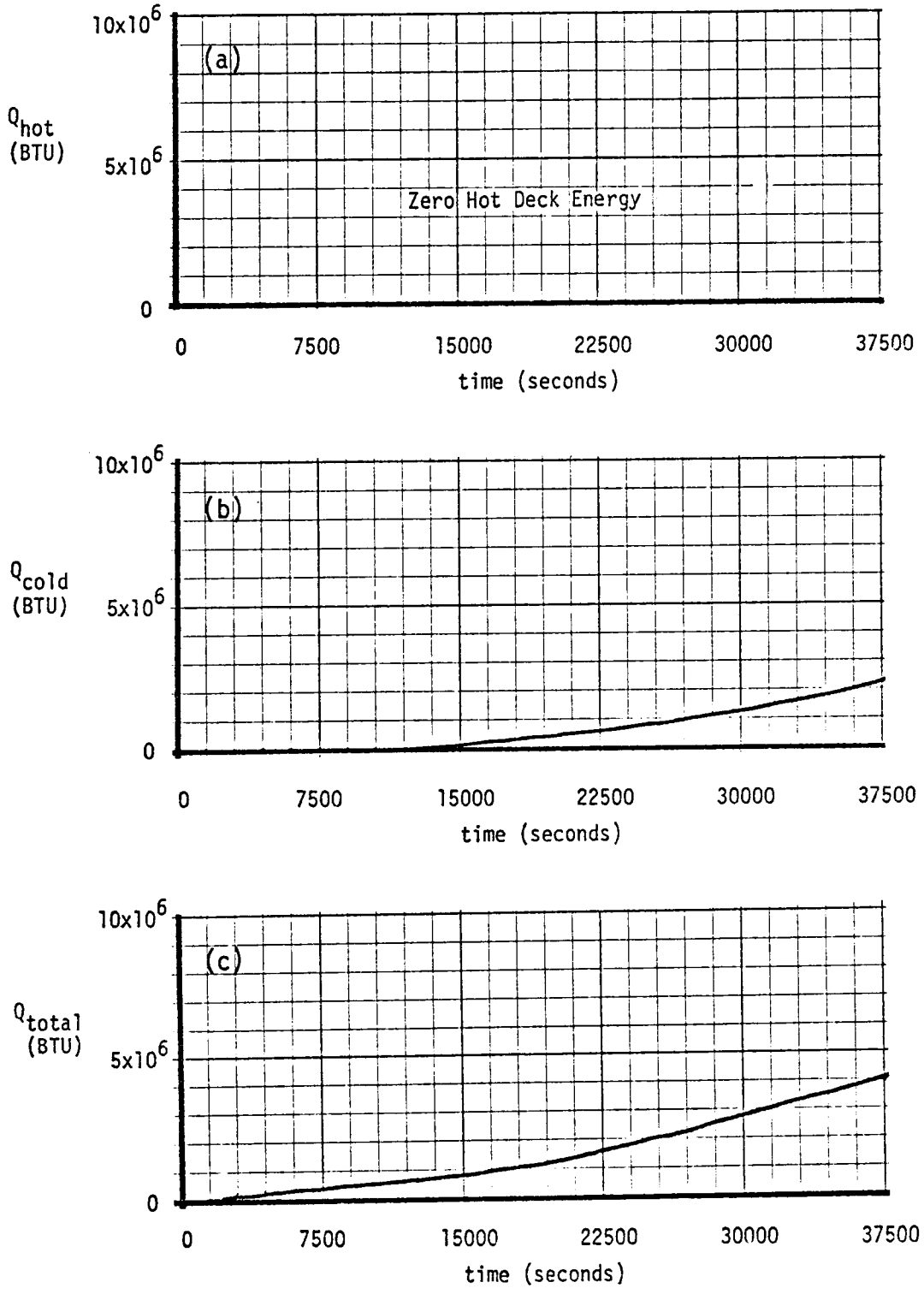


Figure 5.44. Energy use for the modified system in fall.

Table 5.13. Responses for the original system in fall.

	Starting	High Value	Time of High Value (sec)	Low Value	Time of Low Value (sec)	Final Value	Time of Steady State (sec)
TCOLD (°F)	56.3	56.3	0	51.3	39	56.2	582
THOT (°F)	59.0	81.7	25200	56.6	24	81.7	552
TSUP (°F)	56.3	73.6	25200	55.1	300	73.6	300
EXH (ft^3/min)	20282	29660	11700	20282	0	29660	21
FLOWH (ft^3/min)	7150	18319	1080	3755	120	9203	810
FLOWC (ft^3/min)	31510	29457	26100	20341	1080	29457	900
TOUT (°F)	43.0	68.0	25200	43.0	0	68.0	NA
WOD (lbm/lbm)	.0050	.0084	31300	.0050	0	.0084	NA
TRTN (°F)	74.8	75.6	120	73.0	690	73.5	690
WRTN (lbm/lbm)	.0093	.0093	0	.0054	90	.0087	90
QCOLD (BTUs)	0	3.591×10^6	37800	0	0	3.59×10^6	NA
QHOT (BTUs)	0	1.606×10^6	37800	0	0	1.606×10^6	NA
QTOTAL (BTUs)	0	7.07×10^6	37800	0	0	7.068×10^6	NA
TCLZ (°F)	74.4	74.4	0	55.9	870	59.2	870
THTZ (°F)	74.3	79.3	25500	71.9	654	79.3	654

Table 5.14. Responses for the modified system in fall.

	Starting	High Value	Time of High Value (sec)	Low Value	Time of Low Value (sec)	Final Value	Time of Steady State (sec)
TCOLD (°F)	56.6	56.6	0	52.1	837	54.4	837
THOT (°F)	56.6	56.6	0	47.3	678	73.1	837
TSUP (°F)	56.6	56.6	0	54.8	18	73.1	480
EXH (ft^3/min)	22334	32660	12300	22334	0	32660	18
FLOWH (ft^3/min)	20251	36727	780	15170	120	18425	780
FLOWC (ft^3/min)	18409	23490	120	1933	780	20235	780
TOUT (°F)	43.0	68.0	25200	43.0	0	68.0	660
WOD (lbm/lbm)	.0050	0.0084	.30300	.0050	0	.0084	480
TRTN (°F)	74.7	75.4	120	71.4	1260	74.9	960
WRTN (lbm/lbm)	.0093	.0093	0	.0054	90	.0087	930
QCOLD (BTUs)	0	2.21×10^6	37800	0	0	2.21×10^6	NA
QHOT (BTUs)	0	0	C	0	0	0	NA
QTOTAL (BTUs)	0	4.08×10^6	37800	0	0	4.08×10^6	NA
TCLZ (°F)	74.4	74.4	0	55.0	780	73.8	1050
THTZ (°F)	74.2	74.2	0	62.1	546	58.0	546

Table 5.15. Zone responses for the original system in fall.

	Starting Temperature °F	Lowest Temperature °F	Time of Low Value (seconds)	Steady State Temperature °F	Time of Steady State (seconds)
TZONE(1)	78.0	72.3	750	72.7	750
WZ(1)	.0093	.0054	120	.0087	330
TZONE(2)	74.3	72.3	630	72.7	630
WZ(2)	.0093	.0054	120	.0087	330
TZONE(3)	73.1	72.1	570	72.6	570
WZ(3)	.0093	.0054	90	.0087	90
TZONE(4)	65.0	65.0	0	72.6	570
WZ(4)	.0093	.0054	90	.0087	90
TZONE(5)	80.0	72.1	630	72.6	630
WZ(5)	.0093	.0054	90	.0087	90
TZONE(6)	72.0	71.8	510	72.3	510
WZ(6)	.0092	.0053	90	.0086	90
TZONE(7)	74.8	71.8	510	72.3	510
WZ(7)	.0092	.0053	90	.0086	90
TZONE(8)	74.0	71.8	510	72.3	510
WZ(8)	.0092	.0053	90	.0086	90
TZONE(9)	74.0	72.3	672	72.7	672
WZ(9)	.0094	.0054	132	.0088	258

Table 5.16. Zone responses for the modified system in fall.

	Starting Temperature °F	Lowest Temperature °F	Time of Low Value (seconds)	Steady State Temperature °F	Time of Steady State (seconds)
TZONE(1)	78.0	72.8	1170	74.3	840
WZ(1)	.0093	.0054	150	.0087	300
TZONE(2)	74.3	72.7	1350	74.3	990
WZ(2)	.0093	.0054	150	.0087	300
TZONE(3)	73.1	74.1	24600	74.1	1200
WZ(3)	.0093	.0054	90	.0087	90
TZONE(4)	65.0	65.0	0	74.1	1320
WZ(4)	.0093	.0054	90	.0087	90
TZONE(5)	80.0	71.0	1710	74.1	1410
WZ(5)	.0093	.0054	90	.0087	90
TZONE(6)	72.0	68.2	1230	73.8	1230
WZ(6)	.0092	.0053	90	.0086	720
TZONE(7)	74.8	68.2	1320	73.8	1320
WZ(7)	.0092	.0053	120	.0086	720
TZONE(8)	74.0	68.2	1290	73.8	1290
WZ(8)	.0092	.0053	120	.0086	720
TZONE(9)	74.0	72.8	666	74.3	666
WZ(9)	.0094	.0055	84	.0088	84

though they are most significant in winter, spring, and fall. On the average, energy costs are probably more than halved during these three seasons. Most of the energy savings occur because the hot duct is made inoperative. In the past, the hot duct actually overheated the incoming air because the temperature setpoint was dependent on external and not internal conditions. As a result, the cold duct experienced an additional cooling load. Total energy usage thus increased rapidly.

The simulations also indicate that the modified system does not perform ideally under all conditions. Temperatures near or below zero degrees Farenheit cause the supply air temperature to undergo a large damped oscillatory response. Such great temperature extremes are never experienced by the zone temperatures themselves because the interaction with the ambient temperature along the length of the ducts smooths the temperature response. However, mechanical components in the system may experience undue wear if the oscillatory response persists. Zone temperatures may also fall below setpoint values when low external air temperatures exist. Since no steam is supplied to the heating coils, the warmest temperature in the hot duct is that of the supply air. This air flow is controlled to a temperature near 55F, so the hot duct can not supply the heated air necessary to raise the zone temperatures. Under these low temperature conditions. the steam valve could be opened manually to maintain the desired zone temperatures. Of course, the subsequent system energy use would increase.

CHAPTER 6

CONCLUSIONS

A method for developing a dynamic digital simulation of a dual-duct air handling system has been presented. A typical dual-duct system has been described, and the individual system components and control loops of the specific dual-duct system which was studied have been explained in detail. A justification has been given for changing the existing dual-duct pneumatic analog controls to direct digital controls.

The design and operation of a module for applying pneumatic test signals to system components was discussed. A description of the digital and analog data recording devices utilized was also presented. Specific test methods for developing the system transfer functions were also outlined.

An appropriate model for the resulting system transfer functions has been described. Also, an effective computer-aided method for fitting the digital test data to the desired model was discussed.

A detailed development of the simulation program has been included. The Tustin method was extensively used to simulate in sampled-data form the first-order differential equation characteristic of the general transfer function model. An analytical description was given for the development of this sampled-data form. Analytical presentations were also made for the equations describing the resultant temperature and humidity ratio of a mixed airstream. In addition, the theoretical development of an adequate model for a cooling coil has been set forth.

A practical means for estimating the change in temperature of air moving down a duct has been presented. The estimation of sensible and latent heat loads and zone time constants has also been related.

Several subprograms that were written can easily be adapted to a variety of engineering applications. All subroutines involving piecewise linear approximations are in this category as well as the hysteresis simulation segment.

Additionally, two simulation examples using different control strategies were conducted. These simulations illustrated that important differences in total system energy use and system stability existed between the two control strategies. Significant energy savings were found to occur when the low pressure steam flow to the heating coils was blocked, the minimum air damper was closed to admit only 6,000 CFM, and the zone setpoints were raised. This control strategy did not maintain the zone temperatures close enough to their setpoints in winter. Also, some system responses became more oscillatory. However, the simulation results from this strategy indicated that there was no need to supply any heating to the air handling system in spring, summer or fall. Although not ideal, the overall results from the simulation program indicated that effective estimates of the relative worth of a given control strategy could be made.

Further efforts should be directed toward improving the accuracy of the simulation program. Time constants and time delays were generally regarded as invariant. However, these quantities are to a certain degree influenced by the same variables that affect the system gain constants. The overall heat transfer coefficient for the cooling coil

should be measured for a wider range of operating conditions. In addition, a more detailed analysis of the heating coil should be performed. Just as importantly, additional dual-duct system readings should be collected throughout the year to establish a more detailed set of benchmarks.

Improved error reduction techniques should be implemented in subroutine COLD. With this change, a significant decrease in the CPU time necessary to run the simulation program would occur.

Finally, a wide range of control strategies should be tested by the simulation program to determine the most effective means of optimizing the dual-duct system energy usage while still maintaining system stability. With the advent of low-cost, versatile digital controllers, the implementation of detailed control strategies is no longer a limiting factor.

LIST OF REFERENCES

LIST OF REFERENCES

1. C. L. Smith, Digital Computer Process Control, Scranton, Pa: International Textbook, 1972.

2. R. W. Haines, Control Systems for Heating, Ventilating and Air Conditioning, New York, N.Y.: Van Nostrand Reinhold, 1971.

3. C. F. Moore, C. L. Smith, and P. W. Murrill, "Multidimensional Optimization Using PATERN Search," IBM Share Library Program LSU PATE SDA 3552, 1969.

4. F. H. Speckhart and W. L. Green, A Guide to Using CSMP-the Continuous System Modeling Program, Englewood Cliffs, N.J.: Prentice-Hall, 1976.

5. J. A. Cadzow, Discrete-Time Systems, Englewood Cliffs, N.J.: Prentice-Hall, 1973.

6. T. Y. Sun, "Psychrometric Subroutine Uses ASHRAE Algorithms," unidentified publication.

7. C. T. Gosling, Applied Air Conditioning and Refrigeration, London: Applied Science Publishers, 1974.

8. T. G. Hicks, ed., Standard Handbook of Engineering Calculations, New York, N.Y.: McGraw-Hill, 1972.

9. Aerofin Water Coils, Type "C", Aerofin Corporation Bulletin C-58, Lynchburg, Va.: Aerofin Corporation, 1961.

10. Trane Air Conditioning Manual, LaCrosse, Wis.: The Trane Company, 1973.

11. W. F. Stoecker, Procedures for Simulating The Performance of Components and Systems for Energy Calculations, New York, N.Y.: American Society of Heating, Refrigerating, and Air-Conditioning Engineers, 1975.

12. Local Climatological Data, Albany, New York, Dept. of Commerce, National Oceanic and Atmospheric Administration Environmental Data Service, Washington, D.C.: Government Printing Office, 1970.

13. J. W. Jones, et al.,"Simulation of a Dual Duct, Reheat Air-Handling System," American Society of Heating, Refrigerating, and Air-Conditioning Engineers Research Report No. 2358. RP-66-OS, New York, N.Y.: 1968.

14. H. L. Harrison, W. S. Hansen, and R. E. Zelenski, "Development of a Room Transfer Function Model for Use in the Study of Short-Term Transient Response," American Society of Heating, Refrigerating, and Air Conditioning Engineers Research Report No. 2088 RP-52, New York, N.Y.: 1968.

APPENDIX

```
      DIMENSION  DSETZ(10), ISETZ(10), QFIX(10), TSTART(10),
     >FZ(10)
      DIMENSION QL(10),TMIX(10)
      DIMENSION  TAUZ(10)
      DIMENSION TZONEP(10),WZ(10)
      DIMENSION FCZ(10),FHZ(10)
      COMMON DSETZ,ISETZ,QFIX,TSTART,FZ,QL,TAUZ,TAMB,TMIX
      COMMON/A/ FRTN,RFANHP,TRFAN,TSFAN,FMIN
      COMMON/B/ TIME,DELT
      COMMON/C/ QHOT,QCOLD
      COMMON/E/TW2,TDB2,KCOR,GPM,QWATER,K,DPVLV
      REAL ISETZ,KCOR
      INTEGER DAMPRT,COLPRT,HOTPRT
      OPEN(UNIT=1,DEVICE='DSK',ACCESS='SEQIN',
     >FILE='FOR01.DAT',DIALOG)
      READ(1,32)  DELT, FINTIM
      WRITE(3,33) DELT,FINTIM
      READ(1,30)(DSETZ(I), I=1,9)
      WRITE(3,31)(DSETZ(I), I=1,9)
      READ(1,30)(ISETZ(I), I=1,9)
      WRITE(3,31)(ISETZ(I), I=1,9)
      READ(1,30)(QFIX(I), I=1,9)
      WRITE(3,31)(QFIX(I), I=1,9)
      READ(1,30)(TSTART(I), I=1,9)
      WRITE(3,31)(TSTART(I), I=1,9)
      READ(1,30)(FZ(I), I=1,9)
      WRITE(3,31)(FZ(I), I=1,9)
      READ(1,30)(QL(I), I=1,9)
      WRITE(3,31)(QL(I), I=1,9)
      READ(1,30)(TAUZ(I), I=1,9)
      WRITE(3,31)(TAUZ(I), I=1,9)
      READ(1,44) FSUP,RFANHP,SFANHP,FMIN
      WRITE(3,46) FSUP,RFANHP,SFANHP,FMIN
      READ(1,45)  IYEAR
      WRITE(3,47) IYEAR
   30 FORMAT(9F8.0)
   31 FORMAT(1H ,9F8.1)
   32 FORMAT(2F10.0)
   33 FORMAT(1H ,2F10.0)
   44 FORMAT(4F15.0)
   46 FORMAT(1H ,4F15.0)
   45 FORMAT(I10)
   47 FORMAT(1H ,I10)
      FRTN=FSUP-FMIN
      TAMB=75.0
C        2545 BTU/HR = 1 HORSEPOWER
C        2772.3 = 2545.0/(0.85*1.08)
      TRFAN = (2772.3*RFANHP)/FRTN
      TSFAN = (2772.3*SFANHP)/FRTN
      TIME = 0.0
      TIMER = 3.0
```

Figure A.1. Main program.

```
C.....................................................................
C THESE PRINT FLAGS DETERMINE WHETHER OR NOT THE WRITE
C STATEMENTS IN THEIR RESPECTIVE SUBROUTINES ARE ACTIVE,
C I.E.,                 DAMPRT=0
C DEACTIVATES THE WRITE STATEMENTS IN SUBROUTINE DAMPER
      DAMPRT=0
      COLPRT=0
      HOTPRT=0
C.....................................................................
      IFLAG1=0
      WHD=0.009
      WCD=0.009
  100 CONTINUE
      CALL CLIMAT(TOUT,WOD,IYEAR)
      CALL ZONE(WHD,WCD,THTZ,TCLZ,FCZ,FHZ,WZ,TZONEP,SUMFHZ,
     >SUMFCZ,1,9)
      CALL WWRTN(FZ,WZ,WRTN)
      CALL   TTRTN(FZ, TZONEP, TRTN)
      IFLAG2 = 0
  101 CONTINUE
      CALL DAMPER(DAMPRT,TRTN,WRTN,WOD,TOUT,EXH,
     >TSUP,WSUP,PDAMP)
      CALL HOT(HOTPRT,SUMFHZ,TOUT,TSFAN,TSUP,WSUP,THOT,WHD)
      CALL COLD(PRDEL,COLPRT,DTSETC,TSUP,WSUP,SUMFCZ,TCOLD,
     >WCD,PERRCR)
C***********SYSTEM ENERGY SUMMATION*****************
C QCOLD = COOLING COIL ENERGY(FROM SUBROUTINE COLD)
C QHOT = HEATING COIL ENERGY(FROM SUBROUTINE HOT)
C QSFAN = SUPPLY FAN ENERGY
C QRFAN = RETURN FAN ENERGY
      QSFAN=((SFANHP*2545.0)/3600.0)*TIME
      QRFAN=((RFANHP*2545.0)/3600.0)*TIME
      ENERGY=QCOLD+QHOT+QSFAN+QRFAN
      COST=(K1*QCOLD)+(K2*QHOT)+(K3*QSFAN)+(K4*QRFAN)
C***************************************************
      IF(TIME.EQ.0.0) GO TO 103
      IF(IFLAG1.EQ.5) GO TO 103
      GO TO 104
  103 CONTINUE
      CALL ZFEED(TAMB,THOT,TCOLD,THTZ,TCLZ)
  104 CONTINUE
      IF(TIME.EQ.0.0) GO TO 107
      IF(TIME.GT.FINTIM) GO TO 106
      IFLAG3=IFLAG3+1
C     **** IFLAG3 CONTROLS THE PRINTOUT FREQUENCY.
C     **** FOR IFLAG3=18, PRINTING OCCURS EVERY 18 SECONDS.
      IF(TIME.GT.1800.0) TIMER=300.0
      IF(IFLAG3.EQ.TIMER) GO TO 110
      GO TO 108
  107 CONTINUE
      WRITE(3,80)
```

Figure A.1. (Continued)

```
D       WRITE(5,80)
        WRITE(3,81)
D       WRITE(5,81)
        WRITE(3,82)
D       WRITE(5,82)
80      FORMAT(1H ,T2,'TIME',T9,'TOUT',T16,'WOD',T23,'TSUP',
       >T30,'WSUP',T35,'TCOLD',T43,'WCD',T47,'SUMFCZ',T56,
       >'THOT',T63,'WHD',T67,'SUMFHZ',T76,'TRTN',T83,'WRTN',
       >T89,'TW2',T94,'TDB2',T103,'GPM',T107,'QWATER',T116,
       >'KCOR',T125,'PERROR')
81      FORMAT(1H ,T5,'ZONE#1',T17,'ZONE#2',T29,'ZONE#3',T41,
       >'ZONE#4',T53,'ZONE#5',T65,'ZONE#6',T77,'ZONE#7',T89,
       >'ZONE#8',T101,'ZONE#9',T117,'K',T125,'DPVLV')
82      FORMAT(1H ,T3,'THTZ',T10,'TCLZ',T19,'EXH',T28,'QHOT',
       >T39,'QCOLD',T49,'ENERGY')
  110 CONTINUE
        WRITE(3,50) TIME,TOUT,WOD,TSUP,WSUP,TCOLD,WCD,SUMFCZ,
       >THOT,WHD,SUMFHZ,TRTN,WRTN,TW2,TDB2,GPM,QWATER,KCOR,
       >PERROR
D       WRITE(5,50) TIME,TOUT,WOD,TSUP,WSUP,TCOLD,WCD,SUMFCZ,
D      >THOT,WHD,SUMFHZ,TRTN,WRTN,TW2,TDB2,GPM,QWATER,KCOR,
D      >PERROR
   50 FORMAT(1H ,F6.0,1X,3(F5.1,1X,F6.4,1X),F6.0,1X,F5.1,1X,
       >F6.4,1X,F6.0,1X,F5.1,1X,F6.4,1X,2(F5.1,1X),F5.1,1X,
       >F8.0,1X,1PE8.1,1X,0PF5.1)
        WRITE(3,60) (TZONEP(I),WZ(I), I=1,9),K,DPVLV
D       WRITE(5,60) (TZONEP(I),WZ(I), I=1,9),K,DPVLV
   60 FORMAT(1H ,9(F5.1,1X,F6.4),5X,F5.1,5X,F4.1)
        WRITE(3,70) THTZ,TCLZ,EXH,QHOT,QCOLD,ENERGY
D       WRITE(5,70) THTZ,TCLZ,EXH,QHOT,QCOLD,ENERGY
   70 FORMAT(1H ,2(F5.1,2X),F8.2,2X,3(1PE9.3,2X)/)
        IFLAG3=0
  108 CONTINUE
        TIME=TIME+DELT
        IFLAG2=IFLAG2+1
        IF(IFLAG1.EQ.5) GO TO 109
        IFLAG1=IFLAG1+1
        GO TO 101
  109 CONTINUE
        IFLAG1=0
        IF(IFLAG2.EQ.30) GO TO 100
        CALL ZONE(WHD,WCD,THTZ,TCLZ,FCZ,FHZ,WZ,TZONEP,SUMFHZ,
       >SUMFCZ,9,9)
        GO TO 101
  106 CONTINUE
C   DATA FOLLOWS SUBROUTINES
C    FIRST CARD     DELT FOLLOWED BY FINTIM(SECONDS)
C    SECOND CARD    DSETZ FOR 9 ZONES (ZONE SETPOINT DISTUR-
C                   BANCE,F)
C    THIRD CARD    ISETZ FOR 9 ZONES (ZONE SETPOINT,F)
C    FOURTH CARD    QFIX FOR 9 ZONES (SENSIBLE HEAT,BTU/HR)
```

Figure A.1. (Continued)

```
C    FIFTH CARD    TSTART FOR 9 ZONES (INITIAL TEMPERATURE OF
C                  ZONE,F)
C    SIXTH CARD    FZ FOR NINE ZONES (CFM ASSIGNED TO ZONE)
C    SEVENTH CARD   QL FOR 9 ZONES (LATENT HEAT,BTU/HR)
C    EIGHTH CARD   TAUZ FOR 9 ZONES (TIME CONSTANT OF ZONE
C                  DYNAMICS,SECONDS)
C    NINTH CARD    FSUP (SUPPLY FAN AIR FLOW,CFM)
C                  RETURN AND SUPPLY FAN HORSEPOWER
C                  FMIN (MINIMUM AIR DAMPER SUPPLY FLOW,CFM)
C    TENTH CARD    IYEAR (SEASON OF YEAR)
      STOP
      END
```

Figure A.1. (Continued)

```
      SUBROUTINE CLIMAT(TOUT,WOD,IYEAR)
      COMMON/B/ TIME,DELT
C      STATEMENT 100 FOR WINTER
C      STATEMENT 200 FOR SPRING
C      STATEMENT 300 FOR SUMMER
C      STATEMENT 400 FOR FALL
C      TOUT IS OUTSIDE DRY BULB TEMPERATURE.
C      WOD IS CUTSIDE HUMIDITY RATIO IN LBS OF MOISTURE PER
C      POUND OF DRY AIR.  TIME IS IN SECONDS. ** T = 0 IS
C      7./ A.M. ** TIME = 37800 IS 5.30PM.
      GO TO (100,200,300,400), IYEAR
  100 TOUT = 22.0
      IF(TIME.LE.27000.0) TOUT = (8.8889E-4)*TIME - 2.0
      WOD = 0.0018
      IF(TIME.LE.32400.0)  WOD = (2.46914E-8)*TIME + 0.001
      RETURN
  200 TOUT = 62.0
      IF(TIME.LE.25200.0)  TOUT = (1.0318E-3)*TIME + 36.0
      WOD = 0.0058
      IF(TIME.LE.27000.0)  WOD = (1.037037E-7)*TIME + 0.003
      RETURN
  300 TOUT = 87.0
      IF(TIME.LE.27000.0)  TOUT = (9.259E-4)*TIME + 62.0
      WOD = 0.01523
      IF(TIME.LE.30600.0)  WOD = (2.1E-7)*TIME + 0.0088
      RETURN
  400 TOUT = 68.0
      IF(TIME.LE.25200.0)  TOUT = (9.92063E-4)*TIME + 43.0
      WOD = 0.0084
      IF(TIME.LE.30600.0)  WOD = (1.1111E-7)*TIME + 0.005
      RETURN
      END
```

Figure A.2. Subroutine CLIMAT.

```
      SUBROUTINE   WWRTN(FZ,WZ,WRTN)
      COMMON/A/ FRTN,RFANHP,TRFAN,TSFAN,FMIN
      DIMENSION  WZ(10), FZ(10)
C THIS SUBROUTINE CALCULATES THE RETURN AIR HUMIDITY.
C WZ(I) IS THE ZONE HUMIDITY RATIO IN (LBM WATER/LBM AIR)
      WRTNX = 0.0
      DO 81 I = 1,9
      WDUMB = WRTNX + WZ(I)*(FZ(I)-(FZ(I)/38660.0)*FMIN)
   81 WRTNX = WDUMB
      WRTN = WRTNX/FRTN
      RETURN
      END
```

Figure A.3. Subroutine WWRTN.

```
      SUBROUTINE TTRTN(FZ,TZONEP,TRTN)
      COMMON/A/ FRTN,RFANHP,TRFAN,TSFAN,FMIN
      DIMENSION  TZONEP(10), FZ(10)
      TRTNX = 0.0
      DO 82 I = 1, 9
      TDUMB = TRTNX + TZONEP(I)*(FZ(I)-(FZ(I)/38660.0)*FMIN)
   82 TRTNX = TDUMB
      TRTN = (TRTNX/FRTN) + TRFAN
      RETURN
      END
```

Figure A.4. Subroutine TTRTN.

```
      SUBROUTINE DAMPER(PRINT,TRTN,WRTN,WOD,TOUT,EXH,
     >TSUP,WSUP,PDAMP)
      COMMON/A/ FRTN,RFANHP,TRFAN,TSFAN,FMIN
      COMMON/B/ TIME,DELT
      INTEGER PRINT
      REAL KCD,IPRESD,ISETD,ITOUT,LEXH,LASTPS
      DIMENSION   DDUMB(100)
      IF(TIME.NE.0.0) GO TO 101
      JCOUNT=0
C FOR SUMMER MODE, OPMODE=1.0.
C FOR WINTER MODE, OPMODE=0.0.
      OPMODE=0.0
      IF(TOUT.GE.62.0) OPMODE=1.0
      YFLAG = 1.0
      FLAG = 1.0
      TAUVD = 12.0
      LEXH = 1.0
      TAUSD = 5.0
      KCD = -4.5
      IPRESD = 10.2
      LASTPS = IPRESD
      MSD = 3
      AD1 = (DELT)/(DELT + 2.0*TAUVD)
      AD2 = (DELT - 2.0*TAUVD)/(DELT + 2.0*TAUVD)
      BD1 = (DELT)/(DELT + 2.0*TAUSD)
      BD2 = (DELT - 2.0*TAUSD)/(DELT + 2.0*TAUSD)
      XD61 = 0.0
      XMSD1 = 0.0
      XMSD = 0.0
      XD51 = 0.0
      XD41 = 0.0
      DO 18 I = 1,MSD
   18 DDUMB(I) = 0.0
  101 CONTINUE
C   START OF DAMPER CONTROL LOOP
      IF(OPMODE.EQ.1.0) GO TO 28
   99 PDAMP = XD61 + IPRESD
      IF(FLAG.GT.0.5)  GO TO 3
      IF(PDAMP.LE.LASTPS)  GO TO 7
      IF(ZFLAG.EQ.0.0)  GO TO 10
      SAVE = LASTPS
      ZFLAG = 0.0
   10 CALL RIGHT(PDAMP,REXH)
      REXH=FRTN*REXH
      IF(REXH.LT.LEXH)  GO TO 9
      YFLAG = 1.0
      FLAG = 1.0
      GO TO 25
    7 IF(ZFLAG.EQ.1.0)  GO TO 8
      IF(PDAMP.GT.SAVE)  GO TO 9
      ZFLAG = 1.0
```

Figure A.5. Subroutine DAMPER.

```
    8 CALL XLEFT(PDAMP,LEXH)
      LEXH=FRTN*LEXH
    9 EXH = LEXH
      GO TO 27
    3 IF(PDAMP.GE.LASTPS)  GO TO 4
      IF(YFLAG.EQ.0.0)  GO TO 6
      SAVE = LASTPS
      YFLAG = 0.0
    6 CALL XLEFT(PDAMP,LEXH)
      LEXH=FRTN*LEXH
      IF(LEXH.GT.REXH)  GO TO 25
      ZFLAG = 1.0
      FLAG = 0.0
      GO TO 9
    4 IF(YFLAG.EQ.1.0)  GO TO 5
      IF(PDAMP.LE.SAVE)  GO TO 25
      YFLAG = 1.0
    5 CALL RIGHT(PDAMP,REXH)
      REXH=FRTN*REXH
   25 EXH = REXH
   27 LASTPS = PDAMP
      GO TO 29
   28 CONTINUE
      EXH=2000.0
   29 CONTINUE
      FMAX = EXH
      FIN=FMAX+FMIN
      TMIX=((FRTN - EXH)*TRTN + FIN*TOUT)/(FRTN - EXH + FIN)
      WMIX=((FRTN - EXH)*WRTN + FIN*WOD)/(FRTN - EXH + FIN)
      TSUP=TMIX+TSFAN
      WSUP=WMIX
C    ************************************************************
C     FOLLOWING CARD USED TO INPUT DAMPER SETPOINT CHANGE
      DSETD=0.0
C    ************************************************************
      IF(TIME.EQ.0.0)  ISETD = 55.0
      ERD = DSETD + ISETD - TSUP
      XD1 = 0.12*KCD*ERD
      XD2 = XD1 + IPRESD
      XD3 = XD2
      IF(XD3.GT.17.0) XD3 = 17.0
      IF(XD3.LT.0.0)  XD3 = 0.0
      XD4 = XD3 - IPRESD
      XD5 = AD1*XD4 + AD1*XD41 - AD2*XD51
      XD51 = XD5
      XD41 = XD4
      XD6 = BD1*XMSD + BD1*XMSD1 - BD2*XD61
      XD61 = XD6
      XMSD1 = XMSD
      DO 97 I = 1,MSD
   97 DDUMB(MSD+2-I) = DDUMB(MSD+1-I)
```

Figure A.5. (Continued)

```
      DDUMB(1) = XD5
      XMSD = DDUMB(MSD)
      IF(PRINT.EQ.0) GO TO 92
      IF(TIME.EQ.0.0) GO TO 94
      JCOUNT = JCOUNT + 1
      IF(JCOUNT.EQ.5)  GO TO 94
   94 WRITE(3,93) TIME,EXH,TMIX,WMIX,PDAMP
   93 FORMAT(4X,F5.1,8X,F10.1,8X,F7.2,8X,F5.2,8X,F7.2)
      JCOUNT = 0
   92 CONTINUE
      RETURN
      END
```

Figure A.5. (Continued)

```
      SUBROUTINE XLEFT(X,Y)
      DIMENSION ARG(13),VAL(13)
      DATA VAL/2000.0,2050.0,2150.0,2400.0,4200.0,8600.0,
     >11200.0,16000.0,21400.0,24400.0,25600.0,2*26000.0/
      DATA ARG/3.0,4.0,5.0,6.0,7.0,8.0,
     >8.4,9.0,10.0,11.0,12.0,13.0,14.0/
      N=13
      IF(X-ARG(1)) 10,10,20
20    IF(ARG(N)-X) 30,30,40
40    DO 300 J=2,N
      M=J
      IF(X-ARG(J)) 100,200,300
300   CONTINUE
200   Y=VAL(M)
      GO TO 400
C INTERPOLATION
100   X1=ARG(M-1)
      X2=ARG(M)
      X3=X
      Y1=VAL(M-1)
      Y2=VAL(M)
      Y3=Y1+(X3-X1)/(X2-X1)*(Y2-Y1)
      Y=Y3
400   CONTINUE
      GO TO 50
10    Y=2000.0
      GO TO 50
30    Y=26000.0
50    CONTINUE
C NORMALIZED DAMPER CHARACTERISTICS
      Y=Y/26000.0
      RETURN
      END
```

Figure A.6. Subroutine XLEFT.

```
      SUBROUTINE RIGHT(X,Y)
      DIMENSION ARG(12),VAL(12)
      DATA VAL/4*2000.0,2500.0,4500.0,9000.0,
     >16800.0,21700.0,24500.0,2*26000.0/
      DATA ARG/3.0,4.0,5.0,6.0,7.0,8.0,9.0,
     >10.0,11.0,12.0,13.0,14.0/
      N=12
      IF(X-ARG(1)) 10,10,20
20    IF(ARG(N)-X) 30,30,40
40    DO 300 J=2,N
      M=J
      IF(X-ARG(J)) 100,200,300
300   CONTINUE
200   Y=VAL(M)
      GO TO 400
C INTERPOLATION
100   X1=ARG(M-1)
      X2=ARG(M)
      X3=X
      Y1=VAL(M-1)
      Y2=VAL(M)
      Y3=Y1+(X3-X1)/(X2-X1)*(Y2-Y1)
      Y=Y3
400   CONTINUE
      GO TO 50
10    Y=2000.0
      GO TO 50
30    Y=26000.0
50    CONTINUE
C NORMALIZED DAMPER CHARACTERISTICS
      Y=Y/26000.0
      RETURN
      END
```

Figure A.7. Subroutine RIGHT.

```
      SUBROUTINE COLD(PRDEL,PRINT,DTSETC,TDB1,W1,CFM,TCOLD,
     >WCOLD,PERROR)
      COMMON/B/ TIME,DELT
      COMMON/C/ QHOT,QCOLD
      COMMON/E/TW2,TDB2,KCOR,GPM,QWATER,K,DPVLV
      DIMENSION TDB(100),W(100),FILTER(100)
      REAL KCOR,KINTG,K,LAMBDA,M,LTD,LMTD,ITSETC,KTRANS,
     >KCONC,ICOUNT,IPVLVC,KXX
      INTEGER PRINT
C
C
C----------------PROGRAM INITIALIZATION--------------------
C
C
C*******************CONSTANTS*********************************
      IF(TIME.NE.0.0) GO TO 111
C THESE MAY BE SPECIFIED IN MAIN
      DTSETC=0.0
      PRDEL=3.0
C.............................
      SUM=0.0
      NSAMP=30
      QCOLD=0.0
      KCOR=0.00002
      AREA=76.3
      ROWS=8.0
      LAMBDA=1050.0
      CSUBPW=1.0
      RHSAT=100.0
      TW1=43.0
      KCONC=-3.0
      ITSETC=53.0
      IPVLVC=5.0
      KTRANS=0.12
      TAUVC=33.0
      TAUC=11.46
      N=6
      NP1=N+1
      NP2=N+2
      AA=DELT/(DELT+2.0*TAUVC)
      AB=(DELT-2.0*TAUVC)/(DELT+2.0*TAUVC)
      BA=DELT/(DELT+2.0*TAUC)
      BB=(DELT-2.0*TAUC)/(DELT+2.0*TAUC)
      TSTART=TDB1
      WSTART=W1
C************THESE VALUES WILL BE VARIABLES*****************
      TDB11=TSTART
      W11=WSTART
      ICOUNT=0.0
C********INITIALIZATION***********
C INITIAL ESTIMATE OF TDB2.
```

Figure A.8. Subroutine COLD.

```
      TDB2=TSTART-1.0
C      THE PAST VALUES OF W2 ARE ASSUMED TO BE WSTART
      DO 30 I=1,NP2
      TDB(I)=TSTART
      W(I)=WSTART
30    CONTINUE
      TDLAY1=TSTART
      WDLAY1=WSTART
      TCOLD1=TSTART
      WCOLD1=WSTART
      PCONC1=0.0
      DPVLV1=0.0
555   CONTINUE
C
C
C-----------------PROGRAM DYNAMICS-------------------------
C
C
111   CONTINUE
C
C*********LOOP DYNAMICS***************
      TSETC=ITSETC+DTSETC
      TERRC=TSETC-TCOLD1
      PERRC=KTRANS*TERRC
      PCONC=KCONC*PERRC
      IF(PCONC.LT.(0.0-IPVLVC)) PCONC=-IPVLVC
      IF(PCONC.GT.(17.0-IPVLVC)) PCONC=17.0-IPVLVC
      PHOLD=PCONC
      IF(TIME.NE.0.0) GO TO 117
      PCONC=0.0
  117 CONTINUE
      DPVLV=PCONC*AA+PCONC1*AA-DPVLV1*AB
      PCONC1=PCONC
      PCONC=PHOLD
      PVLVC=IPVLVC+DPVLV
      DPVLV1=DPVLV
C FAIR AND FWATER HAVE UNITS OF LBS/HR.
C MAX AIR FLOW IS 171,822 LBS/HR(38,660 CFM);
C MAX WATER FLOW IS 150,000 LBS/HR(300 GPM).
      CALL FLOWS(PVLVC,GPM)
      FWATER=GPM*60.0*(8.0+1.0/3.0)
      FAIR=CFM*60.0/13.5
      IF(W1.NE.W11) GO TO 116
      IF(TDB1.EQ.TDB11) GO TO 115
116   CONTINUE
      M=3.0
      CALL PSYSUN(M,TDB1,TWB1,RH1,W1,H1,DP1)
      TDB11=TDB1
      W11=W1
115   CONTINUE
      HHEAT=0.24+0.46*W1
```

Figure A.8. (Continued)

```
      IF(GPM.LT.60.0) GO TO 120
      XX=((GPM-10.0)/(300.0-10.0))*0.5+
     >((CFM-1933.0)/(38660.0-1933.0))*0.5
      KXX=200.0*XX
      GO TO 121
  120 CONTINUE
      XX=((GPM-10.0)/(300.0-10.0))*0.95+
     >((CFM-1933.0)/(38660.0-1933.0))*0.05
      KXX=400.0*XX-15.0
      IF(KXX.LT.1.0) KXX=1.0
  121 CONTINUE
      IF(CFM.LE.1933.0) KXX=1.0
      IF(GPM.LE.10.0) KXX=1.0
      IF(TIME.GT.29.0) GO TO 70
      NTIME=30.0-TIME
      FILTER(NTIME)=KXX
      SUM=SUM+FILTER(NTIME)
      K=KXX
      GO TO 80
   70 CONTINUE
      SUM=SUM-FILTER(NSAMP)
      DO 60 MM=2,NSAMP
      FILTER(NSAMP+2-MM)=FILTER(NSAMP+1-MM)
   60 CONTINUE
      FILTER(1)=KXX
      SUM=SUM+FILTER(1)
      K=SUM/30.0
   80 CONTINUE
      IF(PRINT.EQ.0) GO TO 113
      IF(TIME.GT.0.0) GO TO 113
      WRITE(3,16) IPVLVC,KCONC,ITSETC
      WRITE(3,2)
      WRITE(3,7)
      WRITE(3,1) M,TDB1,TWB1,RH1,W1,H1,DP1
      WRITE(3,3)
      WRITE(3,17)
113   CONTINUE
114   CONTINUE
C START ITERATIVE LOOP
      D=0.0
      ERPAST=0.0
      L=0
      PERR01=0.0
      TK=0.0
      TKK=0.0
      TDB2MN=TW1
      KCOR=0.00002
      IF(TDB1.LE.TW1) GO TO 690
      IF(GPM.LE.10.0) GO TO 690
      IF(CFM.LE.0.0) GO TO 690
      IF(K.GT.1.0) GO TO 200
```

Figure A.8. (Continued)

```
  690 TDB2=TDB1
      W2=W1
      QAIR=0.0
      QWATER=0.0
      TW2=TW1
      PERROR=0.0
      GO TO 696
200   CONTINUE
      TDB2=TDB2-TK
      IF(TDB2.GE.TDB1) TDB2=0.999999*TDB1
      IF(TDB2.LE.TDB2MN) TDB2=1.000001*TDB2MN
      GO TO 202
  201 CONTINUE
      TDB2=TDB2-TKK
  202 CONTINUE
      M=2.0
      CALL PSYSUN(M,TDB2,TWBSAT,RHSAT,WSAT,HSAT,DPSAT)
      IF(WSAT.GE.W1) GO TO 10
      W2=WSAT
      M=3.0
      CALL PSYSUN(M,TDB2,TWB2,RH2,W2,H2,DP2)
      GO TO 20
10    W2=W1
      M=3.0
      CALL PSYSUN(M,TDB2,TWB2,RH2,W2,H2,DP2)
20    QAIR=FAIR*(HHEAT*(TDB1-TDB2)+LAMBDA*(W1-W2))
C (TW2.LE.TDB1).  SINCE QAIR=QWATER, QAIR MAXIMUM IS:
      QAIRMX=FWATER*CSUBPW*(TDB1-TW1)
      IF(QAIRMX-QAIR) 118,119,119
  118 CONTINUE
      TDB2MN=TDB2
      TKK=-((TDB2MN+TDB1)/2.0-TDB2MN)
      GO TO 201
  119 CONTINUE
      QWATER=QAIR
      TW2=TW1+QWATER/(FWATER*CSUBPW)
      GTD=TDB1-TW2
      LTD=TDB2-TW1
      LMTD=(GTD-LTD)/ALOG(GTD/LTD)
      QDSIGN=K*AREA*ROWS*LMTD
      ERROR=QDSIGN-QWATER
      PERROR=(ERROR/QWATER)*100.0
C
C     ERROR TRAP FOR UNBOUNDED PERROR OSCILLATIONS
      IF(PERROR.GT.0.0) GO TO 400
      IF(PERROR.LT.PERR01) L=L+1
      PERR01=PERROR
      GO TO (1000,2000,3000),L
1000  GO TO 400
2000  GO TO 400
3000  L=0
```

Figure A.8. (Continued)

```
      PERROR1=0.0
      GO TO 100
C
400   AERROR=ABS(PERROR)
      TK=KCOR*ERROR
      D=D+1.0
      IF(D.GT.100.0) GO TO 600
      IF(AERROR.GT.7.5) GO TO 200
600   CONTINUE
  696 CONTINUE
      QCOLD=(QWATER/3600.0)*DELT+QCOLD
C************DELAY*************
      DO 40 J=1,NP1
      TDB(NP2+1-J)=TDB(NP2-J)
      W(NP2+1-J)=W(NP2-J)
40    CONTINUE
      TDB(1)=TDB2
      W(1)=W2
C*************LAG***************
      TDLAY=TDB(NP2)
      WDLAY=W(NP2)
      TCOLD=TDLAY*BA+TDLAY1*BA-TCOLD1*BB
      WCOLD=WDLAY*BA+WDLAY1*BA-WCOLD1*BB
      TCOLD1=TCOLD
      WCOLD1=WCOLD
      TDLAY1=TDLAY
      WDLAY1=WDLAY
666   CONTINUE
C*************TIMING*********************************************
      ICOUNT=ICOUNT+1.0
      DELTIM=ICOUNT*DELT
      IF(PRINT.EQ.0) GO TO 777
      IF(TIME.LE.8.0) GO TO 300
      IF(DELTIM.GE.PRDEL) GO TO  300
      GO TO 444
300   WRITE(3,13) TIME,TDB2,W2,TW2,FWATER,TCOLD,DPVLV,
     >QWATER,PERROR,KCOR,TDB1,W1,FAIR,K
      ICOUNT=0.0
444   GO TO 777
C
C************ERROR TRAP**********************
100   CONTINUE
      TDB2=TDB1-1.0
      KCOR=KCOR*0.90
      GO TO 200
C
C*******************************************
1     FORMAT(1H ,2X,F2.0,3F6.1,2F10.5,F6.1//)
2     FORMAT(1H ,'ENTERING AIR CONDITIONS')
3     FORMAT(1H ,'WATER,AIR CONDITIONS AND % LOAD ERROR')
7     FORMAT(1H ,3X'M',3X'DB',4X'WB',4X'RH',7X'W',8X'H',
```

Figure A.8. (Continued)

```
     >7X'DP')
13    FORMAT(1H ,F8.4,1X,F6.3,1X,F7.5,1X,F6.3,1X,F8.1,1X,
     >F8.5,1X,F7.3,F13.4,F8.3,2X,1PE10.4,2X,0PF8.3,2X,F7.5,
     >2X,F8.0,2X,F5.1)
16    FORMAT(1H 'IPVLVC = ',F4.1,6X'KCONC = ',F6.2,
     >5X'ITSETC = ',F6.2)
17    FORMAT(1H T5,'TIME',T12,'TDB2',T21,'W2',T27,'TW2',T35,
     >'FWATER',T44,'TCOLD',T53,'DPVLV',T63,'QWATER',T73,
     >'PERROR',T83,'KCOR',T96,'TDB1',T106,'W1',T115,'FAIR',
     >T124,'K')
777   CONTINUE
      RETURN
      END
```

Figure A.8. (Continued)

```
      SUBROUTINE FLOWS(PVLVC,GPM)
      DIMENSION PRESS(16),FLOW(16)
      DATA PRESS/4.1,4.4,4.8,5.0,5.4,5.8,6.4,7.0,8.0,9.0,
     >10.0,11.0,12.0,13.0,14.0,15.0/
      DATA FLOW/10.0,25.0,50.0,65.0,85.0,103.0,130.0,155.0,
     >183.0,206.0,230.0,250.0,267.5,285.0,298.0,300.0/
      N=16
      IF(PVLVC-PRESS(1)) 10,10,20
   20 IF(PRESS(N)-PVLVC) 30,30,40
   40 DO 300 J=2,N
      M=J
      IF(PVLVC-PRESS(J)) 100,200,300
  300 CONTINUE
  200 GPM=FLOW(M)
      GO TO 400
C INTERPOLATION
  100 P1=PRESS(M-1)
      GPM=(290.0/10.9)*PVLVC-99.08
      GO TO 50
      P2=PRESS(M)
      P3=PVLVC
      F1=FLOW(M-1)
      F2=FLOW(M)
      F3=F1+((P3-P1)/(P2-P1))*(F2-F1)
      GPM=F3
  400 CONTINUE
      GO TO 50
   10 GPM=10.0
      GO TO 50
   30 GPM=300.0
   50 CONTINUE
      RETURN
      END
```

Figure A.9. Subroutine FLOWS.

```
      SUBROUTINE PSYSUN(M,DB,WB,R,W,H,DP)
      REAL M
C---- FOR M=1.0, INPUT=DB,WB       OUTPUT=R,W,H,DP
C---- FOR M=2.0, INPUT=DB,R        OUTPUT=WB,W,H,DP
C---- FOR M=3.0, INPUT=DB,W        OUTPUT=WB,R,H,DP
C---- FOR M=4.0, INPUT=DB,H        OUTPUT=WB,R,W,DP
C---- FOR M=5.0, INPUT=DB,DP       OUTPUT=WB,R,W,H
      DATA PB,FS/29.921,1.0045/
      IF(M.EQ.1.0) GO TO 10
      IF(M.EQ.2.0) GO TO 20
      IF(M.EQ.3.0) GO TO 30
      IF(M.EQ.4.0) GO TO 40
      IF(M.EQ.5.0) GO TO 50
10    PVP=PV(DB,WB,PB,FS)
      W=0.622*FS*PVP/(PB-FS*PVP)
      R=PVP/PVSF(DB)
      GO TO 15
20    W=WF(DB,R,PB,FS)
      GO TO 25
50    PVP=PVSF(DP)
      W=0.622*FS*PVP/(PB-FS*PVP)
      GO TO 30
40    W=(H-0.24*DB)/(1061.0+0.444*DB)
30    R=RHF(DB,W,PB,FS)
25    WB=WBF(DB,W,PB,FS)
      IF(M-5.0) 15,45,15
15    DP=DPF(DB,W,PB,FS)
      IF(M-4.0) 45,55,45
45    H=0.24*DB+(1061.0+0.444*DB)*W
55    R=R*100
      RETURN
      END
C---- SATURATED VAPOR PRESSURE AT TEMPERATURE DB.....
      FUNCTION PVSF(DB)
      DATA A,B,C/-7.90298,5.02808,-1.3816E-7/
      DATA D,E,F/11.344,8.1328E-3,-3.49149/
      DATA G,H/-9.09718,-3.56654/
      DATA P/0.876793/
      DATA Q/6.0273E-3/
      T=(DB+459.688)/1.8
      IF(T.LT.273.16) GO TO 3
      Z=373.16/T
      S=A*(Z-1.0)+B*ALOG10(Z)+C*(10.0**(D*(1-1.0/Z))-1.0)
      S=S+E*(10.0**(F*(Z-1.0))-1.0)
      GO TO 4
3     Z=273.16/T
      S=G*(Z-1)+H*ALOG10(Z)+P*(1.0-1.0/Z)+ALOG10(Q)
4     PVSF=29.921*10**S
      RETURN
      END
C---- VAPOR PRESSURE AT TEMPERATURES DB AND WB.....
```

Figure A.10. Subroutine PSYSUN.

```
      FUNCTION PV(DB,WB,PB,FS)
      R=0.0
      PVS=PVSF(WB)
      IF(DB.LE.WB) GO TO 4
      WS=0.622*PVS/(PB-PVS)
      IF(WB.GT.32.0) GO TO 2
      PV=PVS-5.704E-4*PB*(DB-WB)/1.8
      GO TO 3
4     PV=PVS
      GO TO 3
2     CDB=(DB-32.0)/1.8
      CWB=(WB-32.0)/1.8
      HL=597.31+0.4409*CDB-CWB
      CH=0.2402+0.4409*WS
      EX=(WS-CH*(CDB-CWB)/HL)/0.622
      PV=PB*(EX/(1.0+EX))
      IF(R.GT.0.0) GO TO 3
      R=PV/PVSF(DB)
      IF(R.GT.0.1) GO TO 3
      WS=0.622*FS*PVS/(PB-FS*PVS)
      GO TO 2
3     RETURN
      END
C---- HUMIDITY RATIO AT TEMPERATURE DB & RELATIVE HUMIDITY R
      FUNCTION WF(DB,R,PB,FS)
      PVS=PVSF(DB)
      WS=0.622*FS*PVS/(PB-FS*PVS)
      R=R*0.01
      DS=R*(PB-FS*PVS)/(PB-R*FS*PVS)
      WF=WS*DS
      RETURN
      END
C---- RELATIVE HUMIDITY AT TEMPERATURE DB & HUMIDITY RATIO W
      FUNCTION RHF(DB,W,PB,FS)
      PVS=PVSF(DB)
      WS=0.622*FS*PVS/(PB-FS*PVS)
      DS=W/WS
      RHF=DS/(1.0-(1.0-DS)*FS*PVS/PB)
      RETURN
      END
C---- WB TEMPERATURE AT TEMPERATURE DB AND HUMIDITY RATIO W
      FUNCTION WBF(DB,W,PB,FS)
      WBF=DB
      PVD=PB*W/((0.622+W)*FS)

11    PVP=PV(DB,WBF,PB,FS)

      IF(PVP-PVD) 20,30,10

10    WBF=WBF-1.0
      GO TO 11
```

Figure A.10. (Continued)

```
20      WBH=WBF+1.0
        PVH=PV(DB,WBH,PB,FS)

        X=(PVD-PVP)/(PVH-PVP)
        WBF=WBH*X+WBF*(1.0-X)
30      RETURN
        END
C---- DP TEMPERATURE AT TEMPERATURE DB AND HUMIDITY RATIO W
        FUNCTION DPF(DB,W,PB,FS)
        DPF=DB
        PVD=PB*W/((0.622+W)*FS)
11      PVS=PVSF(DPF)
        IF(PVS-PVD) 20,30,10
10      DPF=DPF-1.0
        GO TO 11
20      DPH=DPF+1.0
        PVH=PVSF(DPH)
        X=(PVD-PVS)/(PVH-PVS)
        DPF=DPH*X+DPF*(1.0-X)
30      RETURN
        END
```

Figure A.10. (Continued)

```
      SUBROUTINE HOT(PRINT,FLOWH,TOUT,TSFAN,TSUP,WSUP,THOT,
     >WHOT)
      COMMON/B/ TIME,DELT
      COMMON/C/ QHOT,QCOLD
      DIMENSION HDUMB(100)
      REAL KHCC,ISETD,KCH,KH,ISETH
      INTEGER PRINT
C             THOT=TSUP
C             WHOT=WSUP
C             GO TO 16
      IF(TIME.NE.0.0) GO TO 101
      QHOT=0.0
      ISETD=TSUP
      ICOUNT=0
      KHCC = 1.0
      TAUVH = 3.0
      TAUSH = 36.0
      TAUHC = 10.0
      KCH = -0.8
      KH = -17.6
      TADJH = TSUP
      TMAXUP=150.0
      MHS = 26
      TQHOT1 = 0.0
      ERH1 = 0.0
      HSTMD = 0.0
      HSTM11 = 0.0
      HSTM1 = 0.0
      HSUP1 = 0.0
      DHSUP1 = 0.0
      DO 15 I = 1,MHS
   15 HDUMB(I) = 0.0
      THOT1 = TADJH
      AH1 = DELT/(DELT+2.0*TAUVH)
      AH2 = (DELT-2.0*TAUVH)/(DELT+2.0*TAUVH)
      BH1 = (KH*DELT)/(DELT+2.0*TAUSH)
      BH2 = (DELT-2.0*TAUSH)/(DELT+2.0*TAUSH)
      CH1 = (KHCC*DELT)/(DELT+2.0*TAUHC)
      CH2 = (DELT-2.0*TAUHC)/(DELT + 2.0*TAUHC)
  101 CONTINUE
C   HOT DUCT SIMULATION FOLLOWS
      ISETH = 90.0 - 0.25*TOUT
      IF(TOUT.GE.60.0) ISETH=75.0
      IF(TOUT.LE.0.0) ISETH=90.0
      DSETH=0.0
      ERRORH = DSETH + ISETH - THOT1
      ERH=0.12*KCH*ERRORH
      HSTM = AH1*ERH + AH1*ERH1 - AH2*HSTM1
      ERH1 = ERH
      HSTM1 = HSTM
      TQHOT = BH1*HSTMD + BH1*HSTM11 - BH2*TQHOT1
```

Figure A.11. Subroutine HOT.

```
      TQHOT1 = TQHOT
      HSTM11 = HSTMD
      DO 10 I = 1,MHS
   10 HDUMB(MHS+2-I) = HDUMB(MHS+1-I)
      HDUMB(1) = HSTM
      HSTMD = HDUMB(MHS)
      DHSUP = TSUP - ISETD
      HSUP = CH1*DHSUP + CH1*DHSUP1 - CH2*HSUP1
      HSUP1 = HSUP
      DHSUP1 = DHSUP
      ADDHOT=TQHOT+(19000.0/FLOWH)
      DELHOT=HSUP+ADDHOT
      THOT=TSUP+DELHOT
      IF(THOT.LT.TSUP) THOT=TSUP
      IF(THOT.GT.TMAXUP) THOT=TMAXUP
      THOT1 = THOT
      QHOT=(((THOT-TSUP)*FLOWH*1.08)/3600.0)+QHOT
      WHOT=WSUP
C    PROGRAM OUTPUT STATEMENTS FOLLOW
      IF(PRINT.EQ.0) GO TO 16
      IF(TIME.EQ.0.0) GO TO 14
      ICOUNT = ICOUNT + 1
      IF(ICOUNT.EQ.5)  GO TO 14
   14 WRITE(3,20) TIME,THOT
   20 FORMAT(4X,F5.1,8X,F10.5)
      ICOUNT = 0
   16 CONTINUE
      RETURN
      END
```

Figure A.11. (Continued)

```
      SUBROUTINE ZFEED(TAMB,THOT,TCOLD,THTZ,TCLZ)
      COMMON/B/ TIME,DELT
      DATA TAUXH,TAUXC/75.0,130.0/
C       HOT AND COLD DECK DYNAMICS
      TZCC = 0.16*TAMB + 0.84*TCOLD
      TZHH = 0.36*TAMB + 0.64*THOT
      IF(TIME.NE.0.0) GO TO 201
      TZCC1 = TZCC
      TZHH1 = TZHH
      TCLZ1 = TAMB
      THTZ1 = TAMB
      ACD1 = (5.0*DELT)/(5.0*DELT + 2.0*TAUXC)
      ACD2 = (5.0*DELT - 2.0*TAUXC)/(5.0*DELT + 2.0*TAUXC)
      AHD1 = (5.0*DELT)/(5.0*DELT + 2.0*TAUXH)
      AHD2 = (5.0*DELT - 2.0*TAUXH)/(5.0*DELT + 2.0*TAUXH)
  201 CONTINUE
      TCLZ = ACD1*(TZCC + TZCC1) - ACD2*TCLZ1
      THTZ = AHD1*(TZHH + TZHH1) - AHD2*THTZ1
      TZCC1 = TZCC
      TCLZ1 = TCLZ
      TZHH1 = TZHH
      THTZ1 = THTZ
      RETURN
      END
```

Figure A.12. Subroutine ZFEED.

```
      SUBROUTINE ZONE(WHD,WCD,THTZ,TCLZ,FCZ,FHZ,WZ,TZONEP,
     >SUMFHZ,SUMFCZ,N,M)
      DIMENSION  DSETZ(10), ISETZ(10), QFIX(10), TSTART(10),
     >FZ(10)
      DIMENSION QL(10),AZ1(10),AZ2(10)
      DIMENSION  TAUZ(10)
      DIMENSION FHZ(10),FCZ(10),WZ(10)
      DIMENSION  TZONE(10), TZONE1(10), XTS(10), ERZ(10),
     >ZPSI(10)
      DIMENSION XNORM(10), XLIM(10), TMIX(10), TZONEP(10),
     >TCAUL(10)
      DIMENSION TDIST(10), TBUMP(10), TBUMP1(10), TRESP(10),
     >TRESP1(10)
      REAL  ISETZ
      COMMON DSETZ,ISETZ,QFIX,TSTART,FZ,QL,TAUZ,TAMB,TMIX
      COMMON/A/ FRTN,RFANHP,TRFAN,TSFAN,FMIN
      COMMON/B/ TIME,DELT
C   THIS SUBROUTINE SIMULATES THE ZONES.
C    THE FOLLOWING DO LOOP GOES FROM N TO M WHERE N AND M
C    ARE PLACED IN THE ARGUMENT LIST OF THE CALL STATEMENT.
C    N=1 FOR ZONE1.1, N=2 FOR ZONE 1.2, N=3 FOR ZONE 2.1,
C    N=4 FOR ZONE2.2, N=5 FOR ZONE2.3, N=6 FOR ZONE 4.1,
C    N=7 FOR ZONE 4.2, N=8 FOR ZONE 4.3, AND N=9 FOR ZONE
C    3.1.  ZONE 3.1 IS READ ON A SEPARATE CALL SINCE IT USES
C    A DIFFERENT INTEGRATION STEP SIZE.
      IF(TIME.NE.0.0) GO TO 103
      DO 31 I = 1,9
      IF(I.EQ.9) GO TO 33
      AZ1(I) = (30.0*DELT)/(30.0*DELT + 2.0*TAUZ(I))
      AZ2(I) = (30.0*DELT - 2.0*TAUZ(I))/(30.0*DELT +
     >2.0*TAUZ(I))
      GO TO 31
   33 AZ1(I) = (5.0*DELT)/(5.0*DELT + 2.0*TAUZ(I))
      AZ2(I) = (5.0*DELT - 2.0*TAUZ(I))/(5.0*DELT +
     >2.0*TAUZ(I))
   31 CONTINUE
      THTZ=TAMB
      TCLZ=TAMB
  103 CONTINUE
      DO 27 I = N,M
      IF(TIME.EQ.0.0) TZONE1(I) = TSTART(I)
      ERZ(I) = DSETZ(I) + ISETZ(I) - TZONE1(I)
      XTS(I) = -2.5*ERZ(I)
      ZPSI(I) = 7.5 + XTS(I)
      XNORM(I) = (0.2)*(ZPSI(I) - 5.0)
      XLIM(I) = XNORM(I)
      IF(XNORM(I).GT.0.95)  XLIM(I) = 0.95
      IF(XNORM(I).LT.0.05)  XLIM(I) = 0.05
      FCZ(I) = FZ(I)*XLIM(I)
      FHZ(I) = FZ(I) - FCZ(I)
      TMIX(I) = (FHZ(I)*THTZ + FCZ(I)*TCLZ)/FZ(I)
```

Figure A.13. Subroutine ZONE.

```
C CFM*(60 MIN/HR)*(1.0 LBM/13.5 FT**3)=LBM/HR
      WZ(I)=(((FHZ(I)*WHD + FCZ(I)*WCD)*60.0/13.5) +
     >(GL(I)/1050.0))/(FZ(I)*60.0/13.5)
      TCAUL(I) = TMIX(I) - TSTART(I)
C TEMPERATURE RISE=(BTU/HR)/ CFM*(60 MIN/HR)*(1 LBM/
C                   13.5 FT**3)*(0.244 BTU/LBM-F)
C                  =(BTU/HR)/ CFM*1.08
      TDIST(I) = QFIX(I)/(1.08*FZ(I))
      IF(TIME.LT.20.0) TDIST(I)=0.0
      TBUMP(I) = TDIST(I) + TCAUL(I)
      IF(TIME.NE.0.0) GO TO 28
      TBUMP1(I) = 0.0
      TRESP1(I) = 0.0
   28 TRESP(I) = AZ1(I)*(TBUMP(I) + TBUMP1(I))-AZ2(I)*
     >TRESP1(I)
      TBUMP1(I) = TBUMP(I)
      TRESP1(I) = TRESP(I)
C      **** TZONEP IS THE PRESENT ZONE TEMPERATURES
      TZONEP(I) = TZONE1(I)
      TZONE(I) = TSTART(I)+ TRESP(I)
   27 TZONE1(I) = TZONE(I)
      MMN=M-N
      IF(MMN.NE.8) GO TO 102
      SUMFHZ=0.0
      SUMFCZ=0.0
      DO 101 J=1,9
      SUMFHZ=SUMFHZ+FHZ(J)
      SUMFCZ=SUMFCZ+FCZ(J)
  101 CONTINUE
  102 CONTINUE
      RETURN
      END
```

Figure A.13. (Continued)

VITA

David Reed Oglesby was born June 5, 1951 in Milledgeville, Georgia. Shortly afterwards, his family moved to Concord, in east Tennessee. There, he resided with his parents while attending elementary, junior high, and senior high school in the Farragut community.

In June, 1969, he enrolled in the electrical engineering curriculum at the University of Tennessee in Knoxville. He entered the cooperative engineering program in 1970 and worked a total of two years with the Louisville and Nashville Railroad and the Square D Company.

In 1971 Mr. Oglesby became an active member of Circle K, a campus service organization. He presided over this organization throughout the academic year of 1974-75.

During the summer of 1974, he accepted employment in Mt. McKinley National Park, Alaska. Upon receiving his Bachelor of Science degree in electrical engineering in June, 1975, he returned to Mt. McKinley National Park for summer employment.

Mr. Oglesby entered the graduate program in electrical engineering at the University of Tennessee, Knoxville, in September, 1975. Since then he has worked as a research assistant in control systems.

He is married to the former Stephanie Berry of Mt. McKinley National Park, Alaska.